DIRECTIONAL TIME-FREQUENCY ANALYSIS WITH APPLICATIONS

A Dissertation
presented to
the Faculty of the Graduate School
University of Missouri-Columbia

In Partial Fulfillment
of the Requirements for the Degree

Doctor of Philosophy

---

by
CHRISTOPHER SANSING

Dr. Loukas Grafakos, Dissertation Supervisor

MAY 2006

©Copyright by Christopher Sansing 2006
All Rights Reserved

The undersigned, appointed by the Dean of the Graduate School, have examined the dissertation entitled

DIRECTIONAL TIME-FREQUENCY ANALYSIS WITH APPLICATIONS

presented by Christopher Sansing,

a candidate for the degree of Doctor of Philosophy,

and hereby certify that in their opinion it is worthy of acceptance.

_____ (Loukas Grafakos)

_____ (Evan Boote)

_____ (Peter Casazza)

_____ (Marius Mitrea)

_____ (Stephen Montgomery-Smith)

To Allie Rose.

ACKNOWLEDGMENTS

It is impossible to thank, in only a few pages, all the people who have helped this dissertation come to fruition. I will attempt to thank as many as possible and apologize for anyone inadvertently left out.

I would first like to thank my graduate advisor, Loukas Grafakos. Without his support and many mathematical conversations, this research would not be possible. He first introduced me to the pure and applied world of harmonic analysis and I have been hooked ever since. His passion for mathematics and research has pushed me forward and has given me a great example of constantly striving for academic excellence. My advisor also taught a lot of the graduate classes which I attended while in graduate school, including basic preparation courses for the qualifying exams and more advanced courses like harmonic analysis. I can say from a lot of experience that he is an excellent teacher and I owe a lot of my mathematical knowledge to him. Finally, I would like to thank him for all of his advice and the hospitality he has shown to me during my time at the University of Missouri.

There are many other professors I would like to thank for their excellent teaching, which I have benefited greatly from during my graduate education. For some excellent courses and seminars I took part of, I would like to thank Carmen Chicone,

Steve Hofmann, Nigel Kalton, Alexander Koldobsky, Yuri Latushkin, Marius Mitrea, Igor Verbitsky, and Mark Rudelson. I would also like to thank my other dissertation committee members: Pete Casazza, Marius Mitrea, Stephen Montgomery-Smith, and Evan Boote; who have been very supportive and helpful during my time preparing this work. I would like to especially thank Pete Casazza for many discussions which I have benefited from. He was an excellent source for many questions on frame theory and different mathematical applications. We also had many fruitful discussions about the teaching of mathematics in general. Another person to which I owe thanks is Yuri Latushkin who was the Director of Graduate Studies when I started graduate school and has been a source of excellent advice. He also introduced me to the annual TULKA internet seminar which I took part of and learned a lot from. Special thanks are also due to Loukas Grafakos and Nigel Kalton for financial support during my summers here. I would also like to collectively thank the mathematics department at the University of Missouri for the hospitality shown to me and the chance to pursue my graduate education here. There are many special people in this department including Sandi Athanassiou, Julie Aston, Brenda Cook, Kimberly Dostoglou, and Jessica White who have been amazing in their help by answering my many questions and offering their support. Thanks are also due to some of the other graduate students who I enjoyed spending my time with here. Ryan, Geoff, Joe, and Pierre have helped me a lot in their explanation of different mathematical concepts and have also been good friends and helped make my time at the mathematics department quite enjoyable.

A special thanks also goes out to the current and past mathematics faculty at the Mississippi University for Women. Dorothy Kerzel, Jane Wenstrom, Shaochen Yang, and my undergraduate advisor G. Beate Zimmer (now at Texas A&M University, Corpus Christi) are excellent mathematicians and helped push me forward into my graduate career. They provided an undergraduate mathematical education for me that served to be a core part of my knowledge in graduate school. Also, I would like to thank Bharat Soni, Roy Koomullil, Yung Choo, and Herb Schilling for their role as assistants and mentors during my internships at the Engineering Research Center in Starkville, MS and at the NASA Glenn Research Center in Cleveland, OH where I was able to hone a lot of application skills including those used in this dissertation.

I would like to thank my wife, Lara, for her support during the (sometimes stressful) time I was completing my doctoral work. She has been the greatest blessing of my life and my own personal support staff when I needed her. Without her, I would not have been able to accomplish the things I have. I would also like to thank my family for their prayers and support during these last five years. My parents, Mike and Donna Sansing, and my sister, Traci Sansing Baird, have been a special blessing and have always supported me in all that I did.

An extra special thanks to all the friends we have made while living here in Columbia. I believe they also deserve credit for being there when Lara and I needed them and giving us much joy while we were in graduate school. Thank you Shawn, Chrissy, Jonathan, Amanda, Brian T., Karis, Brian K., Elizabeth, Shannon, Dani, Glenn, Sybil, Brian L., Somer, Aaron, Tara, Troy, Dorcas, Joe, Barbi and their

families for being our friends, now, and in the future. I would also like to thank Amanda Gurney for allowing me to use some of her artwork in the applications chapters of this dissertation.

Finally, I would like to thank God for the extra special gift my wife and I received on December 28, 2005 at 9:27 pm. Allie Rose has been a blessing to our family and I am glad she came into this world during our time in Columbia. It is to her that this dissertation is dedicated.

Contents

List of Figures

DIRECTIONAL TIME-FREQUENCY ANALYSIS WITH APPLICATIONS

Christopher Sansing

Dr. Loukas Grafakos, Dissertation Supervisor

ABSTRACT

The purpose of this dissertation is to introduce a new directionally-sensitive time-frequency representation of a function. It is shown that we may break up a function (or signal) into individual time-frequency-direction pieces. A certain coefficient ($\langle f, G_{m,t,u} \rangle$) will allow one to see "how much" frequency is in the function (i.e. signal, image, etc.) in a certain time interval, and also in a certain direction. This has been done using wavelets (ridgelets) and this dissertation introduces a similar concept using time-frequency (Gabor) elements. For such elements, a Parseval formula and a continous frame-type representation together with boundedness properties of a semi-discrete frame operator are obtained. New spaces of functions are also presented which are tailored to fit our time-frequency-direction analysis. Applications relating to image processing and medical imaging are also presented along with development of some algorithms.

"So where does this leave the philosophers, the scholars, and the world's brilliant debaters? God has made them all look foolish and has shown their wisdom to be useless nonsense. Since God in his wisdom saw to it that the world would never find him through human wisdom, he has used our foolish preaching to save all who believe."

Paul's letter to the Corinthians [1]

[1] 1 Corinthians 1:20-21, New Living Translation

Introduction

The idea behind this work was born from two different concepts that blended together in a very natural and useful way. Those two concepts are the Radon transform and time-frequency analysis.

The Radon transform, named after Johann Radon, originated in his classical 1917 paper [49] entitled *Über die Bestimmung von Funktionen durch ihre Integralwerte längs gewisser Mannigfaltigkeiten.* This translates to *On the determination of functions from their integrals along certain manifolds*, and a good translation of this paper into english can be found in [18].

The Radon transform is the collection of integrals of a function over all hyperplanes. Radon proved in two and three dimensions that a function satisfying certain regularity conditions can be completely determined from its integrals over all hyperplanes. Specifically for $n = 2$, it was shown that

$$f(x, y) = -\frac{1}{\pi} \int_0^\infty \frac{dF_{(x,y)}(q)}{q},$$

where

$$F_{(x,y)}(q) = \frac{1}{2\pi} \int_0^{2\pi} F(x\cos(u) + y\sin(u) + q, u)du,$$

and $F(p, u)$ is a line integral of f over the line perpendicular to the direction u and distance p from the origin. This collection of line (or hyperplane for $n \neq 2$) integrals

is what has been called the Radon transform. It is usually denoted in the literature as

$$R_u f(p) = \int_{u \cdot x = p} f(x) dx.$$

Extensions to higher dimensions have been studied in [36] and the Radon transform has been utilized in some important applications over recent decades. One such example is computerized tomography where an object's internal components can be studied non-invasively through the use of x-ray technology. Here the x-rays act as collections of "line" integrals and a discrete Radon transform is inverted giving the actual density of the interior of the object at (theoretically) any point. There are, of course, many other obstacles such as noise and discretization of the problem to consider so that the theory can be implemented on a digtal computer. Besides computerized tomography [44], the Radon transform is used in many other medical imaging modalities [45],[55] and in areas such as astronomy, electron microscopy, optics, seismic activity, and general image processing with more applications being developed even now [42],[48],[52].

The Radon transform is a very interesting and remarkable operator. While it is fairly transparent and seemingly elementary in nature, its uses and relations to other areas of mathematics [29] and science allow it to transcend to a classical transform which has been studied for almost a century now and is still a topic which receives a lot of research and interest.

Time-frequency analysis is a theory that allows one to investigate simultaneous time and frequency information of a function or "signal" [9],[14],[22],[32]. This corre-

sponds to information about a function f and its Fourier transform $\widehat{f}$. The analysis here is restricted by the *Heisenberg uncertainty principle* which states it is actually impossible to "know" the exact frequency of a signal at a specific instant. Heisenberg stated it in the following way in his famous uncertainty paper [35], "The more precisely the position is determined, the less precisely the momentum is known in this instant, and vice versa."

One of the main tools of time-frequency analysis is the short-time Fourier transform which allows one to obtain localized information of time and frequency of a function. It is related to the classical Fourier transform in the following manner:

$$V_g f(x,\omega) = \int_{\mathbb{R}^n} f(t)\overline{g(t-x)}e^{-2\pi i t\cdot\omega}dt$$

for $x, \omega \in \mathbb{R}^n$, where g is a function of essential compact support. This is essentially the Fourier transform of a small piece of the function f, hence the name *short-time* Fourier transform.

The short-time Fourier transform can itself be broken up into the main building block of time-frequency analysis, *modulation* and *translation*, given by

$$T_x h(t) = h(t-x), \qquad M_\omega h(t) = e^{2\pi i\omega\cdot t}h(t).$$

Time-frequency analysis is a very useful and applicable theory which has found its use in signal processing and other scienctific aspects of time and frequency. Some of the main results are that a suitable function (or signal) can be broken into time-frequency components (or coefficients) and can then be reconstructed using these components. Many applications of Fourier analysis in the real world are based on

decomposing functions into components and "putting them back together."

Now we get to the purpose of this research, and that is to combine these two well-developed concepts of the Radon transform and time-frequency analysis to create a new time-frequency-direction analysis which uses the directional sensitivity of the Radon transform along with time-frequency localization to generalize the concept of time-frequency analysis to account for direction. In short, it provides a way to localize information in time, frequency, and direction. Instead of simply asking "how much" frequency there is in a signal at a certain time, we are now going to ask "how much" of a certain frequency there is in a signal at a certain time (or point in space) *along a certain direction or hyperplane.*

This work is divided into three parts. The first part gives a brief introduction to several of the topics that are essential to understanding the later results. It consists of chapters on the Radon transform, time-frequency analysis, and frame theory. All of these concepts were crucial in forming the ideas and later results of this research.

The second part includes the new results of this work. Chapter 3 contains the initial idea to apply a time-frequency representation to the Radon transform of a functions at different directions. Here is where we first mention the concept of the *Gabor ridge function* given by

$$g_{m,t,u}(x) = e^{2\pi i m(u\cdot x - t)} g(u \cdot x - t).$$

These functions will form the building block of the time-frequency-direction analysis presented here. One thing proven in this work is that one can reconstruct something related to the original function using a continuous representation involving the

Gabor ridge functions:

$$\mathcal{B}(f) = C_{g,\psi} \int_{\mathbb{S}^{n-1}} \int_{\mathbb{R}} \int_{\mathbb{R}} \langle f, g_{m,t,u} \rangle \psi_{m,t,u} dm dt du.$$

Chapter 4 includes an alternate representation utilizing certain weights that actually allow us to reproduce the original function in a similar way:

$$f = C_{g,\psi} \int_{\mathbb{S}^{n-1}} \int_{\mathbb{R}} \int_{\mathbb{R}} \langle f, G_{m,t,u} \rangle \Psi_{m,t,u} dm dt du.$$

Parseval-type formulas and orthogonality relationships are also obtained. Next the continuous theory is viewed in a way which can be implemented and applied in a discrete setting.

This leads us to Chapter 5, where a semi-discrete reproduction formula is produced. We also view some of the analysis involved in the discretization such as apodizing functions, analysis and reconstruction operators, and a representation formula. This will allow us to show how these representations might be used in an algorithm of some kind.

Finally, in Chapter 6, new classes of functions are presented which are shown to be appropriate function classes to study our time-frequency-direction analysis. They are built from the modulation spaces $M^{p,q}$ of time-frequency analsyis and have a representation which is built from the perspective of time-frequency-direction analysis.

$$\|f\|_{G_s^{p,q,r}} = \left(\int_{\mathbb{S}^{n-1}} \|(\widehat{R_u f} \widehat{\omega_s})^\vee\|_{M^{p,q}}^r du \right)^{1/r},$$

where ω_s is some weight to be later determined.

It is shown that these function spaces are closely related to other classical functions

spaces and that we may extend many of our properties of time-frequency-direction analysis to these spaces as they are very natural for this type of analysis.

The last part of this work consists of chapters on algorithm development, image processing, and medical imaging. These chapters go into some of the applications that have already been found for this type of analysis.

Part I

Preliminaries

Chapter 1

Radon Transform

In this chapter, the Radon transform will be presented and some of its properties will be reviewed as they will be useful in later parts of this work. For an introduction to the Radon transform along with more of its properties, one may consult [36], [44], [18].

The Radon transform has many applications in different areas including image processing, medical imaging (which will be mentioned in a later section), and in other areas of mathematics and applied sciences.

The Radon transform was presented in two and three dimensions in the original work of Johann Radon in 1917 [49]. It was later generalized and also studied in a discrete form (Hough transform [27]).

Some of the aspects that will be used and studied in this work are the inversion of the Radon transform along with some of its properties and applications to computerized tomography.

1.1 Definition of the Radon Transform

There are many different representations of the Radon Transform. For the purposes of this work, we will use the following definition (for an explanation of the Schwartz class of functions, please see Appendix A.1.1):

Definition 1.1.1 *Let $f \in L^1(\mathbb{R}^n)$. If $u \in \mathbb{S}^{n-1}$ and $s \in \mathbb{R}$, then the Radon transform of f is given by*

$$Rf(u,s) = \int_{x \cdot u = s} f(x)dx \tag{1.1}$$

or, equivalently

$$Rf(u,s) = \int_{\mathbb{R}^n} f(x)\delta(s - x \cdot u)dx. \tag{1.2}$$

In (1.2), δ denotes the Dirac delta distribution (see Appendix A.2.1). This can be regarded as a "function" given by the following for $x \in \mathbb{R}$:

$$\begin{aligned} \delta(0) &= \infty, \\ \delta(x) &= 0 \qquad \forall x \neq 0, \\ \int_{\mathbb{R}} \delta(x)dx &= 1. \end{aligned}$$

The Radon transform is the integral of f (or collection of integrals) over the hyperplane(s) perpendicular to u with signed distance s from the origin. We will usually write the Radon transform with dependence on u implied and dependence of s emphasized as follows:

$$R_u f(s) = Rf(u,s).$$

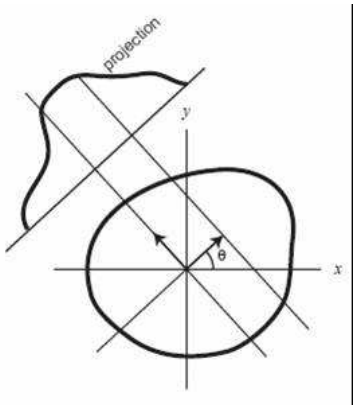

Figure 1.1: Radon Transform

In the case of $n = 2$, the Radon transform is a "collection" of all line integrals of the function f. For a fixed direction u, $R_u f(s)$ is the integral of f over the line perpendicular to u, s units from the origin (see Figure 1.1).

The Radon transform gets its name from Johann Radon, who in 1917 studied this transform and was interested in how to invert it [49]. He wanted to know how to reconstruct a function f from these hyperplane integrals. He succeeded and several decades later his work became extremely useful in many applied settings such as medical imaging. The Radon transform is also seen in many scientific texts, both pure and applied, and its usefulness is becoming more apparent [5].

One property of the Radon transform is that it is an even function defined on the unit cylinder ($\mathcal{Z} = \mathbb{S}^{n-1} \times \mathbb{R}$). That is, $R_{-u} f(-s) = R_u f(s)$. This is because the hyperplane perpendicular to direction u with signed distance s from the origin and the hyperplane perpendicular to direction $-u$ with signed distance $-s$ from the origin are the same hyperplane. Here we are using the convention that $-u$ is the vector in

the opposite direction of u.

The Radon transform may be extended to a homogeneous function of degree -1. This is easily seen from the fact that the δ distribution is homogeneous of degree -1 (when defined on $\mathbb{R}$). This means, for $t \in \mathbb{R}, t \neq 0$:

$$\begin{aligned} Rf(tu, ts) &= \int_{\mathbb{R}^n} f(x)\delta(ts - x \cdot tu)dx \\ &= |t|^{-1} \int_{\mathbb{R}^n} f(x)\delta(s - x \cdot u)dx \\ &= |t|^{-1} Rf(u, s). \end{aligned}$$

Another interesting property is that the Radon transform preserves a convolution,

$$R_u(f * g) = R_u(f) * R_u(g),$$

a fact that can be easily checked.

1.2 Inverting the Radon Transform

Inversion of the Radon transform will play an important role in this work. Radon originally inverted the transform for $n = 2, 3$ and extensive work has been accomplished since that time. Algorithms for computer implementation have been created and other inversion techniques have been invented. Inversion of the Radon transform involves reconstructing a function f given the Radon transform of f for values on the cylinder. The reasons for inversion are for both theory (inversion is always a question to ask) and application (computerized tomography, image processing, etc.).

1.2.1 An Initial Guess

An initial, heuristic guess at inverting the Radon transform might be to simply integrate, over the sphere, the Radon transform evaluated at $u \cdot x$ since these are the hyperplanes (perpendicular to u) which intersect with the point x. So, we want to integrate over all hyperplanes (lines if $n = 2$) which contain the point x. We will call this new transform R^*. This will be another operator which takes functions defined on $\mathcal{Z}$ to functions defined on $\mathbb{R}^n$:

$$R^* g(x) = \int_{\mathbb{S}^{n-1}} g(u, u \cdot x) du.$$

Here g is a function defined on $\mathcal{Z}$ and $R^* f$ is called the "back-projection of g." Then our initial guess for inversion is $R^*(R_u f)$.

$$R^*(R_u f)(x) = \int_{\mathbb{S}^{n-1}} R_u f(u \cdot x) du.$$

While this is an interesting choice (and a useful transform we will use later), it is not equal to $f(x)$. We will now see that what one actually gets is a convolution of $f(x)$ with $|x|^{-1}$.

For the following statements we are assuming $f \in \mathcal{S}(\mathbb{R}^n)$, the Schwartz class of infinitely differentiable, rapidly decreasing functions.

Lemma 1.2.1 *With R and R^* defined as above and $f \in \mathcal{S}(\mathbb{R}^n)$, we have the following calculation:*

$$R^*(R_u f) = |\mathbb{S}^{n-2}|(|x|^{-1} * f).$$

Proof :

Here we give the simple proof from Natterer [44].

$$\begin{aligned} R^*(R_u f)(x) &= \int_{\mathbb{S}^{n-1}} R_u f(x \cdot u) du \\ &= \int_{\mathbb{S}^{n-1}} \int_{u^\perp} f((x \cdot u)u + y) dy du \\ &= \int_{\mathbb{S}^{n-1}} \int_{u^\perp} f(x + y) dy du, \end{aligned}$$

since $x - (x \cdot u)u \in u^\perp$.

For the rest of the proof we will need the following lemma which we will prove after this theorem is shown:

Lemma 1.2.2 *For a function $f \in \mathcal{S}(\mathbb{R}^n)$ and $n \geq 2$,*

$$\int_{\mathbb{S}^{n-1}} \int_{u^\perp} f(x + y) dy du = |\mathbb{S}^{n-2}| \int_{\mathbb{R}^n} |y|^{-1} f(x + y) dy$$

So,

$$\begin{aligned} R^*(R_u f)(x) &= |\mathbb{S}^{n-2}| \int_{\mathbb{R}^n} |x - y|^{-1} f(y) dy \\ &= |\mathbb{S}^{n-2}| \left(|x|^{-1} * f \right). \end{aligned}$$

□

Proof of Lemma 1.2.2:

$$\int_{\mathbb{S}^{n-1}} \int_{u^\perp} f(x + y) dy du = \int_{\mathbb{S}^{n-1}} \int_{e_1{}^\perp} f(x + \rho_u(y)) dy du$$

where ρ_u is the rotation which takes u to $e_1 = (1, 0, \ldots, 0)$ by taking the shortest path over a great circle (if $u = -e_1$ this is not unique, but any path over a great circle

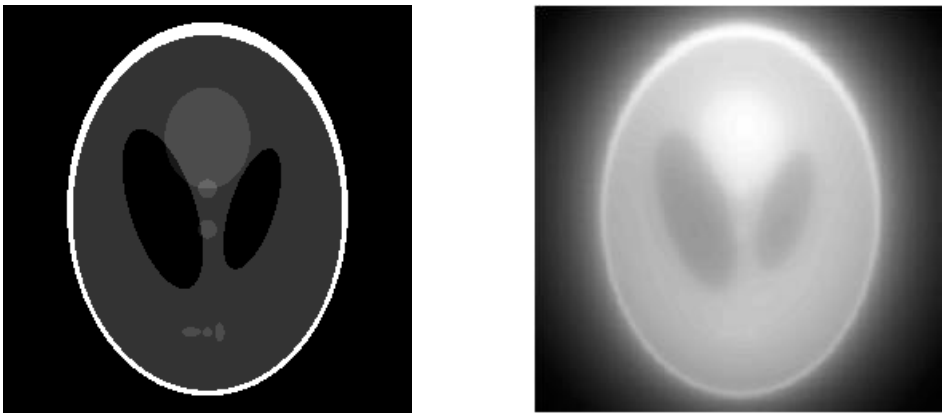

Figure 1.2: Two Phantom Images: The first is f and the second is $f * |x|^{-1}$.

may be chosen). Switching to polar coordinates ($y = r\omega, \omega \in \mathbb{S}^{n-1} \cap e_1^{\perp}$) gives us

$$\begin{aligned} &= \int_0^{\infty} r^{n-2} \int_{\mathbb{S}^{n-1}\cap e_1^{\perp}} \int_{\mathbb{S}^{n-1}} f(x + r\rho_u(\omega)) du d\omega dr \\ &= \int_{\mathbb{S}^{n-1}\cap e_1^{\perp}} \int_0^{\infty} r^{n-2} \int_{\mathbb{S}^{n-1}} f(x + r\rho_u(\omega)) du dr d\omega \\ &= |\mathbb{S}^{n-2}| \int_{\mathbb{R}^n} |y|^{-1} f(x+y) dy. \end{aligned}$$

since when u ranges over $\mathbb{S}^{n-1}$ for a fixed ω, $\rho_u(\omega)$ covers uniquely $\mathbb{S}^{n-1}$. We also used the fact that $\mathbb{S}^{n-1} \cap e_1^{\perp}$ is isomorphic to $\mathbb{S}^{n-2}$. □

Consider an image which will be represented as a function defined of $\mathbb{R}^2$. The back projection of the Radon transform of this function would not produce the original image f, but a blurry version of it (see Figure 1.2).

Our new transform R^* is actually the *adjoint* or *dual operator* of R. This means we have the following relationship:

$$\int_{\mathbb{S}^{n-1}} \int_{\mathbb{R}} R_u f(s) g(s,u) ds du = \int_{\mathbb{R}^n} f(x) R^* g(x) dx,$$

where $f \in \mathcal{S}(\mathbb{R}^n)$ and $g \in \mathcal{S}(\mathcal{Z})$.

Proof :

$$\begin{aligned}
\int_{\mathbb{R}^n} f(x)R^*g(x)dx &= \int_{\mathbb{R}^n} f(x)\left(\int_{\mathbb{S}^{n-1}} g(u, x\cdot u)du\right)dx \\
&= \int_{\mathbb{R}^n} f(x)\left(\int_{\mathbb{S}^{n-1}}\int_{\mathbb{R}} g(u,s)\delta(s-x\cdot u)dsdu\right)dx \\
&= \int_{\mathbb{S}^{n-1}}\int_{\mathbb{R}}\int_{\mathbb{R}^n} f(x)\delta(s-x\cdot u)g(s,u)dxdsdu \\
&= \int_{\mathbb{S}^{n-1}}\int_{\mathbb{R}} R_u f(s)g(s,u)dsdu.
\end{aligned}$$

□

Originally, the blurry aspect was fixed by using a *"de-blurring" filter*. For our purposes, a filter applied to f is simply some function convolved with f in a well-defined manner. This filtering concept led to what is the true inversion formula (reproduces f at every $x \in \mathbb{R}^n$) and it was noted that the filtering could be done before or after the back-projection, which leads us to the next section.

1.2.2 True Inversion

As was seen, simple back-projection of the Radon transform is not enough to reproduce f. Now, a true inversion formula will be presented. Notice that R^* still plays an important role, but we need something extra called a *filter*. For this reason, the true inversion formula is often call the *filtered back-projection*.

Before the inversion formula is presented, a very useful theorem is needed. In the theorem below we use the usual convention for the Fourier transform of the Radon transform where we consider a one-dimensional Fourier transform (see Ap-

pendix A.1.2) of the variable in $\mathbb{R}$.

$$\widehat{R_u f}(\sigma) = \int_{\mathbb{R}} R_u f(s) e^{-2\pi i s\sigma} ds.$$

Theorem 1.2.3 (Fourier Slice Theorem) *Let $f \in L^1(\mathbb{R}^n)$. Then the n-dimensional Fourier transform of the function is related to the 1-dimensional Fourier transform of its Radon transform by*

$$\widehat{R_u f}(\sigma) = \widehat{f}(\sigma u).$$

Proof :

$$\widehat{R_u f}(\sigma) = \int_{\mathbb{R}} R_u f(s) e^{-2\pi i s\sigma} ds = \int_{\mathbb{R}} e^{-2\pi i s\sigma} \int_{u^\perp} f(su + y) dy ds.$$

Now, making a change of variables ($x = su + y$), we have $s = u \cdot x$ and $dx = dyds$ leaving

$$\widehat{R_u f}(\sigma) = \int_{\mathbb{R}^n} f(x) e^{-2\pi i \sigma u \cdot x} dx = \widehat{f}(\sigma u).$$

□

So, this theorem says that if we take a central slice of the Fourier transform of our function f, then it will be equal to the Fourier transform of $R_u f$ in the direction u that the slice was taken.

One way to view Theorem 1.2.3 is that if we take the Fourier transform of the Radon transform for every direction $u \in \mathbb{S}^{n-1}$, we can "build" the Fourier transform of our function f.

We may now prove the actual inversion formula.

Theorem 1.2.4 (Inversion Forumula) *Let $f \in \mathcal{S}(\mathbb{R}^n)$. Then the following inversion formula holds:*

$$f(x) = \frac{1}{2}\int_{\mathbb{S}^{n-1}} (\widehat{R_u f}(\xi)|\xi|^{n-1})^{\vee}(u \cdot x)du.$$

Proof :

We first express f using the Fourier transform and then convert to polar coordinates and apply Theorem 1.2.3 to obtain

$$\begin{aligned} f(x) &= \int_{\mathbb{R}^n} \widehat{f}(\xi)e^{2\pi i x\cdot\xi}d\xi \\ &= \int_{\mathbb{S}^{n-1}}\int_0^{\infty} \widehat{f}(ru)e^{2\pi i x\cdot u}|r|^{n-1}drdu \\ &= \int_{\mathbb{S}^{n-1}}\int_0^{\infty} \widehat{R_u f}(r)e^{2\pi i x\cdot u}|r|^{n-1}drdu. \end{aligned}$$

Finally, since the $\widehat{R_u f}$ is even (a simple consequence of the eveness of $R_u f$), we get the result intended:

$$\begin{aligned} f(x) &= \frac{1}{2}\int_{\mathbb{S}^{n-1}}\int_{-\infty}^{+\infty} \widehat{R_u f}(r)e^{2\pi i x\cdot u}|r|^{n-1}drdu \\ &= \frac{1}{2}\int_{\mathbb{S}^{n-1}} (\widehat{R_u f}(\xi)|\xi|^{n-1})^{\vee}(u \cdot x)du. \end{aligned}$$

□

1.3 Medical Imaging: An Application

One of the many applications of the Radon transform is in the area of medical imaging. A brief overview of the transform's usefulness in computerized tomography (CT) will

be presented here, but the transform is used is many more advanced medical imaging modalities (MRI, PET, etc.)

It was Radon who first showed that a function (or density) could be reconstructed from infinitely many projections. It was not until the 1960's and 70's that scientists first realized this transform of Radon could be used to study, without intrusion, the inside of the human body. Olendorf developed the first prototype CT scanner in 1961 and Hounsfield developed the first clinical CT scanner in 1972, helping him win a joint Nobel prize in medicine with Cormack for their work in CT [20].

1.3.1 Computerized Tomography

The idea of computerized tomography ($\tau\acute{o}\mu$os is the Greek work for slice) is to consider a 2D cross section or "slice" of an object and try to visualize it by sending x-rays through it at different directions and measuring the intensity of the x-ray as it exits the other side. From this data, one can easily approximate the Radon transform, albeit discretely, and using the inversion formula works towards an algorithm that will give back the density.

In a clinical setting, x-rays are sent through a patient and the ratio of intensities of the x-rays before and after they are sent through the patient are collected.

Suppose we consider the *attenuation coefficient* $\mu(x)$, for $x \in \mathbb{R}^2$, of a slice of an object at the point x. The attenuation coefficient is simply the "density" of the object at at certain point (i.e. it is how much x-ray is absorbed when an x-ray of a certain frequency passes through it).

It has been shown [20] that x-ray beam intensity traveling through a material of

attenuation μ_0 decreases according to the equation

$$I = I_0 e^{-\mu_0 x},$$

where I is the observed intensity of a x-ray after it passes through a distance x, and μ the attenuation of the material.

Assuming the beam is traveling along a line l, through material with an attenuation depending on position $\mu(x)$, then we have

$$\frac{I}{I_0} = exp\left[-\int_l \mu(x)ds\right]$$

or,

$$-\log\left(\frac{I}{I_0}\right) = \int_l \mu(x)ds.$$

Therefore, if we have a continuous collection of x-ray intensities (i.e. all lines l along directions $u \in [0, \pi)$), we have the values of the Radon transform of μ and may invert it to find μ at any point $x \in \mathbb{R}^2$ (see Figure 1.3).

So, what is the attenuation in terms of the patient? It is the density of the different tissues in the body. They are a measure of the amount of x-ray intensity absorbed by a certain tissue. These are often expressed in *Hounsfield units* which are normalized with respect to water and given by

$$H_{tissue} = \frac{\mu_{tissue} - \mu_{water}}{\mu_{water}} \cdot 1000.$$

Below is a table of some attenuation coefficients of different tissues in the body where we are assuming an x-ray of 100 keV(kiloelectron volts) since the attenuation actually depends on the energy of the x-ray.

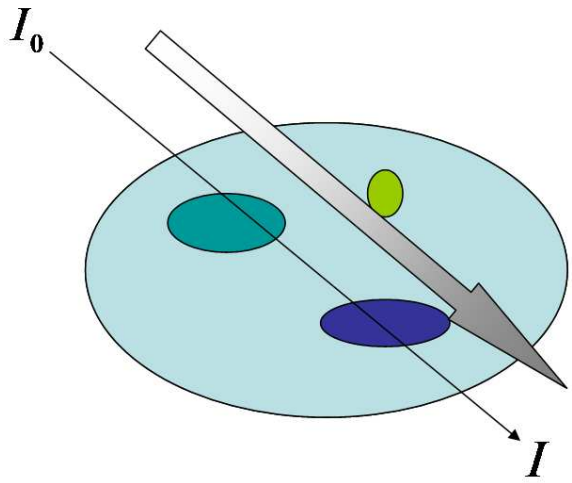

Figure 1.3: Example of an x-ray through different tissues (attenuation values).

Material	**Attenuation Coefficient**
Water	0
Air	-1000
Bone	1086
Blood	53
Fat	-61
Brain white/gray	-4
Muscle	41
Soft Tissue	51

So, once all of this data is collected, we may use our filtered back-projection formula to recover μ, which, in the clinical setting, when visualized, will give an image of the inside of a patients body.

There are obvious problems with this. The main one is that it is physically impossible to collect all the data we need (a continuous collection). Also, there are certain convergence issues and quantization errors that arise. For this reason the filtered back-projection formula will need to be replaced with a discrete approximation

algorithm.

1.3.2 Filtered Back-projection Implementation

In practice, we can only obtain values of the Radon transform of μ on a discrete set of lines. Once the values of the Radon transform on a discrete set are known, one needs to implement an algorithm to approximate μ. This has been achieved and very robust algorithms are now used in modern CT machines. We will now discuss briefly how this can be accomplished. For a more detailed explanation, one may consult [2].

We will assume first that f has compact support. This is a normal assumption that makes sense in the case of CT. For a function $f \in \mathcal{S}(\mathbb{R}^2)$, our filtered back-projection formula becomes

$$f(x) = \frac{1}{2}\int_0^{\pi} (\widehat{R_u f}(\xi)|\xi|)^{\vee}(x \cdot u)du.$$

Working towards a discretization of the above formula, the operators for back-projection and filtering are considered separately. We define the discrete filtering operator as follows using a discrete convolution ($*^d$).

$$R_{u_j} f *^d \omega(s) = \sum_{l=-q}^{q} \omega(s - s_l) R_{u_j} f(s_l),$$

where we are assuming to know the values of the Radon transform at the discrete set of pairs (u_j, s_l), where $l = -q, \ldots, q$, $j = 1, \ldots, p$, where $u_j \in S^1$ and $s_l = hl$, $h = \frac{1}{q}$.

Instead of using $|\xi|$ for our filter, we will apply a different filter in our algorithm for reasons of convergence and noise. Basically our filter will be $\widehat{\omega}(\xi) = |\xi|\widehat{\phi}(\xi)$, where $\widehat{\phi}(\xi)$ is a low-pass filter such that $0 \leq \widehat{\phi} \leq 1$ and $\widehat{\phi}(\xi) = 0$ for $|\xi| \geq a$.

The function ϕ is called an *apodization function* and it will play an important

role later in this work. This function is crucial for our algorithms to be properly implemented. Some example of apodizing or apodization functions commonly used are listed in the following chart:

Name	**Filter**
Band-limited	$\widehat{\phi}(\xi) = \chi_{[-a,a]}(\xi)$
Shepp-Logan	$\widehat{\phi}(\xi) = \frac{1}{2}\frac{\sin(\frac{\pi\xi}{2a})}{\frac{\pi\xi}{2a}}$
Hann	$\widehat{\phi}(\xi) = 1 + \cos(\frac{\pi\xi}{a})$
Hamming	$\widehat{\phi}(\xi) = \alpha + (1-\alpha)\cos(\frac{\pi\xi}{a})$

The next step is to discretize the back-projection operator. This is done using a Riemann sum:

$$\int_0^\pi g(x \cdot u, u)du \approx \sum_{j=1}^{p} g(x \cdot u_j, u_j),$$

where we may get as close the function as we want by summing over more and more projections. There are many more technical details necessary to form a working algorithm. These details will be brought up when necessary.

Some examples of a *phantom* reconstructed from different numbers of projections are shown in Figure 1.4. The first image (top left), is the original image. This is a classical image used in studying algorithms for medical imaging. It represents a slice of the human head, with the inner ellipses being part of the brain. Basically, each ellipse is given some attenuation value and then we use a computer to implement the algorithm by taking integrals over a discrete set of lines and using the filtered back-projection in the way described in this section. The other images are of the reconstructions of the data using 10, 25, 50, and 320 projections (or directions). The last image on the second row is the error of the 320 projection approximation. Finally, the last image is what the projection data looks like. This is a graph of the Radon

transform (320 projections) data where the horizontal axis is the affine parameter s and the vertical axis is the angular variable u.

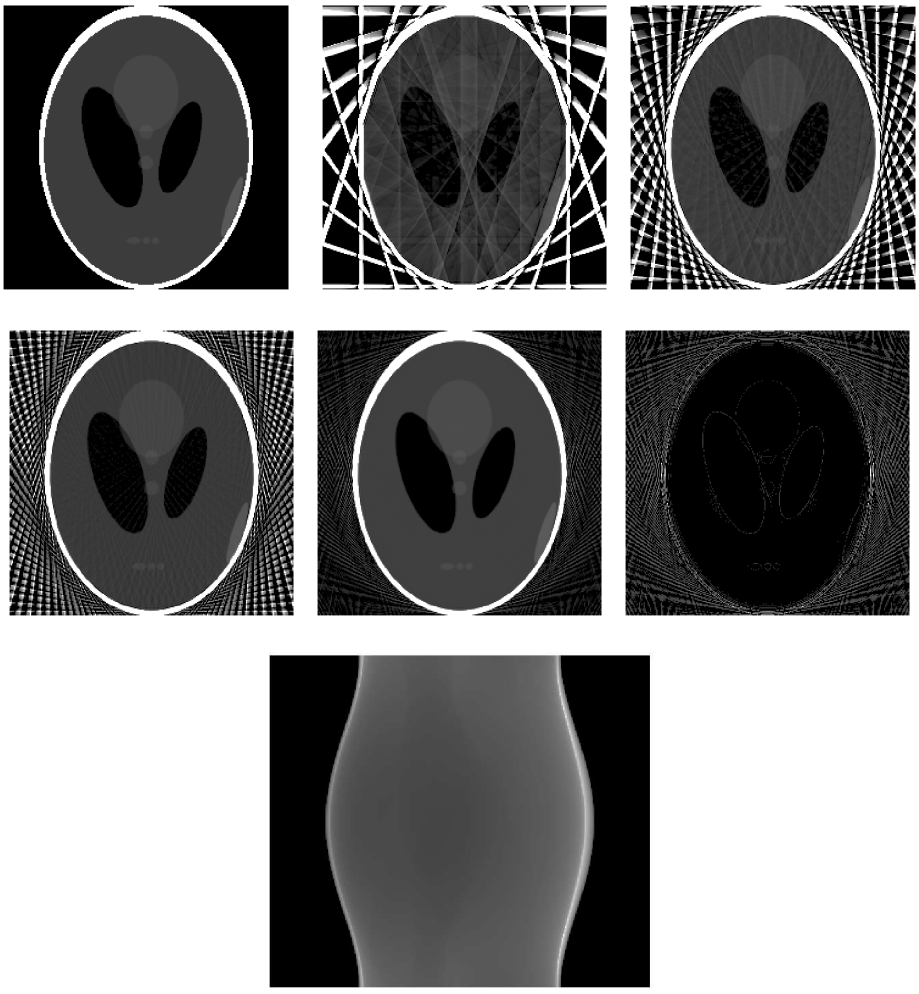

Figure 1.4: Original phantom with reconstruction using 10,25,50, and 320 projections. The last figure on the second row is the error of the 320 projection approximation. The final figure is a plot of Radon transform data for the 320 projection case.

Chapter 2

Frame Theory and Time-Frequency Analysis

Time-frequency analysis is a very interesting and applicable field of mathematics. It has close ties to frame theory, harmonic analysis, physics, and many other related fields. The general idea is that one can study a function or "signal" with fine details in both space and frequency. The ever-present force working against this is, of course, the uncertainty principle of Heisenberg [35]. There are very ingenious ways, however, to overcome this obstacle and derive as much information as possible from a signal.

The first section of this chapter will be a brief introduction of frame theory introducing all the necessary properties that will be used later and that are necessary to understand the next sections on time-frequency analysis and Gabor frames.

For a comprehensive and well-written reference of time-frequency analysis, see [32]. Also, an extensive survey of frame theory was accomplished by Casazza [10].

2.1 Frame Theory

A frame is an extension of the concept of an orthonormal basis to an overdetermined system. The idea is that if we consider the ℓ^2 norm of the *frame coefficients* $\langle f, e_j \rangle$, it is comparable to the norm of the function f. The concept is solidified by the following definition:

Definition 2.1.1 (Frame) *A sequence* $\{e_j : j \in J\}$ *in a separable Hilbert space* $\mathcal{H}$ *is called a frame if there exists* $A, B > 0$ *such that for all* $f \in \mathcal{H}$

$$A\|f\|^2 \leq \sum_{j \in J} |\langle f, e_j \rangle|^2 \leq B\|f\|^2,$$

where $\|\cdot\|$ *is* $\|\cdot\|_{\mathcal{H}}$.

The constants A, B in the above definition are called *frame bounds*. If $A = B$, then $\{e_j\}$ forms what is called a *tight frame*.

Definition 2.1.2 (Frame Operator) *We will also define the frame operator* S *on* $\mathcal{H}$ *by*

$$Sf = \sum_{j \in J} \langle f, e_j \rangle e_j.$$

Some of the important properties of S, which we will state without proof, are the following (for proof, see [32]):

(i) S maps $\mathcal{H}$ onto $\mathcal{H}$ and is a positive invertible operator satisfying

$$AI_{\mathcal{H}} \leq S \leq BI_{\mathcal{H}},$$

and

$$B^{-1}I_{\mathcal{H}} \leq S^{-1} \leq A^{-1}I_{\mathcal{H}}.$$

(ii) The frame operator S is self-adjoint

(iii) The optimal frame bounds are $B = \|S\|_{op}$ and $A = \|S^{-1}\|_{op}^{-1}$ where $\|\cdot\|_{op}$ is the *operator norm* of S.

We now want to look at a very important part of frame theory and that is the ability to reconstruct a function from is frame coefficients. First, we need to understand in what sense $\sum_{j\in J} c_j e_j$ converges to a function $f \in \mathcal{H}$.

Lemma 2.1.3 *Let $\{e_j\}$ be a frame for $\mathcal{H}$. Suppose $f = \sum_{j\in J} c_j e_j$ for some sequence $\{c_j\} \in l^2(J)$, then for every $\epsilon > 0$ there exist a finite subset $F(\epsilon) \subseteq J$ such that*

$$\|f - \sum_{j\in G} c_j e_j\| < \epsilon$$

for all finite subsets $G \supseteq F$ and we say that the series $\sum_{j\in J} c_j e_j$ converges unconditionally to $f \in \mathcal{H}$.

For a proof of this lemma, see [32].

We now present the following classical theorem concerning the reconstruction of a function f from the frame coefficients.

Theorem 2.1.4 *If $\{e_j\}$ is a frame with frame bounds $A, B > 0$, then $\{S^{-1}e_j\}$ is a frame with frame bounds $B^{-1}, A^{-1} > 0$, which we will call the dual frame. Also, every $f \in \mathcal{H}$ has non-orthogonal expansions*

$$f = \sum_{j\in J} \langle f, S^{-1}e_j\rangle e_j$$

and

$$f = \sum_{j\in J} \langle f, e_j\rangle S^{-1}e_j,$$

where both sums converge unconditionally in $\mathcal{H}$.

For a detailed proof of the previous theorem, one may consult [32].

The inverse frame operator S^{-1} also has a simple coefficient expansion given by

$$S^{-1}f = \sum_{j\in J} \langle f, S^{-1}e_j\rangle S^{-1}e_j.$$

This implies S^{-1} is the frame operator with respect to the dual frame $\{S^{-1}e_j\}$.

2.2 Time-Frequency Analysis

Time-frequency analysis allows us to see how much of a certain frequency there is at a certain time (or point in space) in our function or *signal*. Only certain aspects of it will be presented in this section. The opponent of time-frequency analysis, the uncertainty principle, will be presented first. Following this, the short-time Fourier transform will be defined and the question of inversion will be answered.

2.2.1 The Uncertainty Principle

The uncertainty principle (due to Heisenberg [35]) basically says that one cannot know both the position and velocity of a moving particle at the same instant. In the context of $L^2(\mathbb{R})$, this may be expressed in a theorem.

Theorem 2.2.1 (Uncertainty Principle, Heisenberg [35]) *If* $f \in L^2(\mathbb{R})$, *and* $a, b \in \mathbb{R}$, *then*

$$\|(x-a)f\|_2 \|(\xi - b)\widehat{f}\|_2 \geq \frac{1}{4\pi}\|f\|_2^2.$$

An uncertainty principle on $\mathbb{R}^n$ was produced by Donoho and Stark [19]. For a presentation of this principle one needs the concept of a function being ϵ-*concentrated*.

Definition 2.2.2 *A function $f \in L^2(\mathbb{R}^n)$ is ϵ-concentrated on a measurable set $D \subseteq \mathbb{R}^n$, if*

$$\left(\int_{D^c} |f(x)|^2 dx\right)^{1/2} \leq \epsilon \|f\|_2.$$

Theorem 2.2.3 (Donoho, Stark [19]) *Assume $f \in L^2(\mathbb{R}^n), f \neq 0$, is ϵ_1-concentrated on $D \subseteq \mathbb{R}^n$ and $\widehat{f}$ is ϵ_2-concentrated on $E \subseteq \mathbb{R}^n$. Then,*

$$|D||E| \geq (1 - \epsilon_1 - \epsilon_2)^2.$$

2.2.2 Short-time Fourier Transform

One of the main tools we have in our possession to find frequency information about a function or signal is the Fourier transform. Applying the Fourier transform to a function for which it is well defined will give you a new function which describes "how much" of a certain frequency component is in the function. The main disadvantage of this is that it describes how much of that component there is in the complete function, not a part of the function restricted to a certain time (or space) interval. The Fourier transform is global in nature and the goal of this section is to present ways that have been studied to determine how much frequency there is in a function at a certain time, which as we saw in the previous section is not possible in the most literal sense. So, one naturally moves to the next best thing and that is a new transform which give frequency information for, not a specific instant in time, but a small interval of time. Small in the sense that the uncertainty principle is not violated (i.e. not to small).

With this in mind, the following clever invention is introduced:

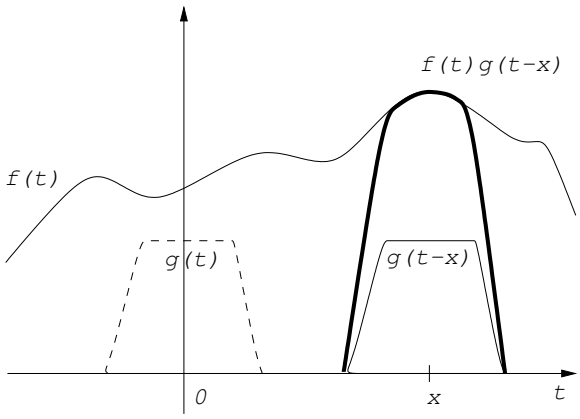

Figure 2.1: Short-time Fourier Transform

Definition 2.2.4 (Short-time Fourier Transform) *Let g be some non-zero function (called a window function). Then the short-time Fourier transform (STFT) of a function f with respect to the window g is given by*

$$V_g f(x,\xi) = \int_{\mathbb{R}^n} f(t)\overline{g(t-x)}e^{-2\pi i t\cdot\xi}dt, \quad \textit{for } x,\xi \in \mathbb{R}^n. \tag{2.1}$$

In the above definition g simply acts like a cut-off function (although one usually takes some smooth window function). Therefore, the STFT is simply the Fourier transform of a truncated version of f. We restrict f to an interval of time (using g) and then take the Fourier transform of that restriction. This can be done with g translated wherever one wants which is why there are two variables in the definition of the STFT, one for the position of g and the other is the normal frequency variable of the Fourier transform (see Figure 2.1).

Another way to write the STFT is to use modulation and tranlation operators. They are defined as follows:

$$T_x f(t) = f(t-x) \tag{2.2}$$

and

$$M_\xi f(t) = e^{2\pi i \xi t} f(t). \tag{2.3}$$

Then the STFT can simply be written in the following way:

$$V_g f(x, \xi) = \langle f, M_\xi T_x g \rangle. \tag{2.4}$$

Some properties of the STFT will now be presented leading up to the next section where they will be discretized giving the general concept of a Gabor frame.

One important property of the STFT is the orthogonality property. We present it here without detailed proof (it is a simple application of Parseval's formula and Fubini's theorem).

Theorem 2.2.5 (Orthogonality [32]) *Let $f_1, f_2, g_1, g_2 \in L^2(\mathbb{R}^n)$. Then*

$$\langle V_{g_1} f_1, V_{g_2} f_2 \rangle = \langle f_1, f_2 \rangle \overline{\langle g_1, g_2 \rangle}. \tag{2.5}$$

where the first inner product above is on $L^2(\mathbb{R}^{2n})$.

This leads to the following corollary relating the L^2 norms of the STFT and the functions f and g.

Corollary 2.2.6 *Let $f, g \in L^2(\mathbb{R}^n)$, then*

$$\|V_g f\|_2 = \|f\|_2 \|g\|_2.$$

Finally, an important formula which allows inversion of the STFT to reconstruct the function f will be presented. It is now a simple corollary of Theorem 2.2.5.

Corollary 2.2.7 (Inversion formula for the STFT) *Suppose $g, \psi \in L^2(\mathbb{R}^n)$ and $\langle g, \psi \rangle \neq 0$. Then for all $f \in L^2(\mathbb{R}^n)$, we have*

$$f = \frac{1}{\langle g, \psi \rangle} \int_{\mathbb{R}^n} \int_{\mathbb{R}^n} V_g f(x, \xi) M_\xi T_x \psi d\xi dx. \tag{2.6}$$

2.3 Gabor Frames

In the previous section we developed a continuous reproduction from time-frequency elements which were time-frequency shifts of a non-zero window function. In this section, we present an introduction to Gabor frames which utilizes the previous information on frame theory and time-frequency analysis.

Consider the set of time-frequency shifts with a non-zero window function $g \in L^2(\mathbb{R}^n)$ and lattice parameters $\alpha, \beta > 0$

$$\{T_{\alpha k} M_{\beta n} g : k, n \in \mathbb{Z}^n\}.$$

We call this a *Gabor system* $G_{g,\alpha,\beta}$. If G is a frame for $L^2(\mathbb{R}^n)$, it is called a *Gabor frame* or *Weyl-Heisenberg frame*. The Gabor frame operator is then given by

$$Sf = \sum_{k,n \in \mathbb{Z}^n} \sum \langle f, T_{\alpha k} M_{\beta n} g \rangle T_{\alpha k} M_{\beta n} g.$$

Theorem 2.3.1 (Walnut [57]) *If $G_{g,\alpha,\beta}$ is a frame for $L^2(\mathbb{R}^n)$, then there exists a dual window $\psi \in L^2(\mathbb{R}^n)$, such that the dual frame of $G_{g,\alpha,\beta}$ is $G_{\psi,\alpha,\beta}$. As a consequence, every $f \in L^2(\mathbb{R}^n)$ can be expressed as*

$$\begin{aligned} f &= \sum_{k,n \in \mathbb{Z}^n} \sum \langle f, T_{\alpha k} M_{\beta n} g \rangle T_{\alpha k} M_{\beta n} \psi \\ &= \sum_{k,n \in \mathbb{Z}^n} \sum \langle f, T_{\alpha k} M_{\beta n} \psi \rangle T_{\alpha k} M_{\beta n} g \end{aligned}$$

with unconditional convergence in $L^2(\mathbb{R}^n)$.

We also have the following norm equivalences:

$$A\|f\|_2^2 \leq \sum_{k,n\in\mathbb{Z}^n}\sum |\langle f, T_{\alpha k}M_{\beta n}g\rangle|^2 \leq B\|f\|_2^2,$$

$$B^{-1}\|f\|_2^2 \leq \sum_{k,n\in\mathbb{Z}^n}\sum |\langle f, T_{\alpha k}M_{\beta n}\psi\rangle|^2 \leq A^{-1}\|f\|_2^2.$$

For proofs of the above statements, please refer to [32]. This dual window ψ is just another window function which is obtained from g in the following manner.

Corollary 2.3.2 *If* $G_{g,\alpha,\beta}$ *is a frame for* $L^2(\mathbb{R}^n)$ *with dual window* $\psi = S^{-1}g \in L^2(\mathbb{R}^n)$, *then the inverse frame operator is given by*

$$S^{-1}f = \sum_{k,n\in\mathbb{Z}^n}\sum \langle f, T_{\alpha k}M_{\beta n}\psi\rangle T_{\alpha k}M_{\beta n}\psi.$$

2.3.1 Boundedness of the Frame Operator

In the continuous setting, we saw that one could produce a reproduction formula with any L^2-functions g and ψ. This is due to the vastness of information achieved from a continuous formula. When we look at the discrete case, we will see that only certain window functions will give us a reproduction formula.

First, we need to define the Wiener space of functions.

Definition 2.3.3 *A function* $g \in L^\infty(\mathbb{R}^n)$ *belongs to the Wiener space* W *if*

$$\|g\|_W = \sum_{n\in\mathbb{Z}^n} \operatorname*{ess\,sup}_{x\in[0,1]^n} |g(x+n)| < \infty.$$

There is another classical result which is often called *Walnut's representation* which is a different way to express the Gabor frame operator. From this follows the boundedness of the Gabor frame operator from L^p to L^p [57].

Before this is presented, we need to define the *correlation function* of the pair (g, ψ) by

$$G_j(x) = \sum_{k \in \mathbb{Z}^n} \overline{g}(x - \frac{j}{\beta} - \alpha k)\psi(x - \alpha k),$$

for $n \in \mathbb{Z}^n$.

Theorem 2.3.4 (Walnut's Representation [57]) *Let $g, \psi \in W(\mathbb{R}^n)$ and let $\alpha, \beta > 0$. Then the operator*

$$Sf = \sum_{k,j \in \mathbb{Z}^n} \sum \langle f, T_{\alpha k} M_{\beta n} g \rangle T_{\alpha k} M_{\beta n} \psi$$

can be written as

$$Sf = \beta^{-n} \sum_{j \in \mathbb{Z}^n} G_j \cdot T_{\frac{j}{\beta}} f.$$

Also, S is bounded on all L^p-spaces, $1 \leq p \leq \infty$ with operator norm

$$\|S\|_{L^p \to L^p} \leq 2^n \left(\frac{1}{\alpha} + 1\right)^n \left(\frac{1}{\beta} + 1\right)^n \|g\|_W \|\psi\|_W.$$

We extend the above result to boundedness on L^p for $0 < p < 1$. For this, we will need slightly stronger restrictions on the window and dual functions g, ψ. First we will need a lemma which we will state here without proof. For a proof, see [32].

Lemma 2.3.5 *If $g, \psi \in W(\mathbb{R}^n)$, then $G_n \in L^\infty(\mathbb{R}^n)$, and*

$$\|G_j\|_\infty \leq \left(\frac{1}{\alpha} + 1\right)^n \|T_{\frac{j}{\beta}} \overline{g} \cdot \psi\|_W. \tag{2.7}$$

Theorem 2.3.6 (Walnut's Representation for $0 < p < 1$) *Let $g, \psi \in W$ such that $\|g\|_{W(p)}$ and $\|\psi\|_{W(p)}$ are finite, where*

$$\|f\|_{W(p)}^p = \sum_{k\in\mathbb{Z}^n} \|f \cdot T_k \chi_{[0,1]^n}\|_\infty^p.$$

Then the frame operator Sf (as in the previous theorem) is bounded on L^p spaces for $0 < p < 1$.

Proof :

For $0 < p < 1$, we have the following variant of the triangle inequality:

$$\|f + g\|_p^p \leq (\|f\|_p^p + \|g\|_p^p).$$

So, starting with Walnut's representation, we have

$$\begin{aligned}
\|Sf\|_p^p &\leq \beta^{-np} \left(\sum_{j\in\mathbb{Z}^n} \|G_j \cdot T_{\frac{j}{\beta}} f\|_p^p \right) \\
&\leq \beta^{-np} \sum_{j\in\mathbb{Z}^n} \|G_j\|_\infty^p \|T_{\frac{j}{\beta}} f\|_p^p \\
&\leq \beta^{-np} \left(\sum_{j\in\mathbb{Z}^n} \|G_j\|_\infty^p \right) \|f\|_p^p.
\end{aligned}$$

Now the question is when is $\sum_{j\in\mathbb{Z}^n} \|G_j\|_\infty^p < \infty$?

From Lemma 2.3.5,

$$\|G_j\|_\infty \leq \left(\frac{1}{\alpha} + 1\right)^n \|T_{\frac{j}{\beta}} \overline{g} \cdot \psi\|_W,$$

$$\|G_j\|_\infty^p \leq \left(\frac{1}{\alpha} + 1\right)^{np} \|T_{\frac{j}{\beta}} \overline{g} \cdot \psi\|_W^p,$$

$$\sum_{j\in\mathbb{Z}^n} \|G_j\|_\infty^p \le \left(\frac{1}{\alpha}+1\right)^{np} \sum_{j\in\mathbb{Z}^n} \|T_{\frac{j}{\beta}}\overline{g}\cdot\psi\|_W^p$$

$$= \left(\frac{1}{\alpha}+1\right)^{np} \sum_{j\in\mathbb{Z}^n} \left(\sum_{k\in\mathbb{Z}^n} \|(T_{\frac{j}{\beta}}\overline{g}\cdot T_k\chi_{[0,1]^n})\cdot(\psi\cdot T_k\chi_{[0,1]^n})\|_\infty^p \right)$$

$$\le \left(\frac{1}{\alpha}+1\right)^{np} \sum_{k\in\mathbb{Z}^n} \left(\sum_{j\in\mathbb{Z}^n} \|T_{\frac{j}{\beta}}\overline{g}\cdot T_k\chi_{[0,1]^n}\|_\infty^p \right) \|\psi\cdot T_k\chi_{[0,1]^n}\|_\infty^p.$$

From a simple counting argument (see [32], page 112) we have

$$\sum_{j\in\mathbb{Z}^n} \|T_{\frac{j}{\beta}}\overline{g}\cdot T_k\chi_{[0,1]^n}\|_\infty^p \le (2\beta+2)^{np} \sum_{l\in\mathbb{Z}^n} \|g\cdot T_l\chi_{[0,1]^n}\|_\infty^p.$$

So, this finally imples that

$$\|Sf\|_p^p \le \beta^{-np}\left(\frac{1}{\alpha}+1\right)^{np}(2\beta+2)^{np}\|g\|_{W(p)}^p\|\psi\|_{W(p)}^p.$$

□

2.3.2 Existence

A theorem on the existence of Gabor frames by Walnut is presented.

Theorem 2.3.7 (Walnut [57]) *Let $g \in W(\mathbb{R}^n)$ and $\alpha > 0$ be chosen such that for constants $a, b > 0$*

$$a \le \sum_{k\in\mathbb{Z}^n} |g(x-\alpha k)|^2 \le b < \infty \quad a.e. \tag{2.8}$$

Then there exists a value $\beta_0 > 0$ such that $G_{g,\alpha,\beta}$ is a Gabor frame for all $\beta \le \beta_0$.

This theorem basically says that if g is any function from the Wiener class and $\alpha, \beta > 0$ are "small enough," then we have a Gabor frame for $L^2(\mathbb{R}^n)$ using our window function g in an appropriate way. The proof involves the correlation functions along with some of their properties.

Example 2.3.1 If $g \in L^\infty([0,1]^n)$ and $\alpha, \beta \leq 1$, then the frame operator S is simply given by

$$Sf(x) = \left(\beta^{-n} \sum_{k \in \mathbb{Z}^n} |g(x - \alpha k)|^2 \right) f(x).$$

This can been seen by simply considering Walnut's representation (Theorem 2.3.4) and evaluating what the correlation functions (G_j) would be in this case.

In the above example all of the things we discussed in this section apply in an obvious fashion. For example, $\mathcal{G}(g, \alpha, \beta)$ will be a frame with frame bounds $\beta^{-n}a$ and $\beta^{-n}b$ where

$$a \leq \sum_{k \in \mathbb{Z}^n} |g(x - \alpha k)|^2 \leq b \ \ a.e.$$

Also, $\mathcal{G}(g, \alpha, \beta)$ is a tight frame if and only if $\sum_{k \in \mathbb{Z}^n} |g(x - \alpha k)|^2$ is constant almost everywhere.

Part II

Results

Chapter 3

Initial Idea

The initial idea was to create a certain directional time-frequency representation. In this direction, we took a basic Gabor-like element and introduced a new parameter that accounted for "direction." This turned out to be a useful continuous representation, but not the "right one" in the sense that it does not reproduce the original function f, but another function closely related to f which we have seen in the first chapter. This initial chapter of results describes the work at this initial stage.

The next chapter presents the necessary work to establish a true continuous representation formula and generalize time-frequency analysis to include a directional parameter. Our goal is to create an analogy between elements of time-frequency analysis and a new time-frequency-direction analysis. To do this, we take the concepts of the Radon transform and classical time-frequency analysis and combine them to form the new theory which lends itself to many applications to be presented in part three of this work.

3.1 Gabor Ridge Functions

We begin by introducing a concept that will be fundamental in this work. We take a time-frequency element (see chapter 2) and add to it a sense of directional sensitivity by evaluating it at the point $u \cdot x$, where x is an element of $\mathbb{R}^n$ and u is some direction from $\mathbb{S}^{n-1}$.

Definition 3.1.1 (Gabor Ridge Function) *Let $g(x) \in \mathcal{S}(\mathbb{R})$ be some real-valued (non-zero) window function. We construct a Gabor element on $\mathbb{R}$ with g in the following way:*

$$g^{m,t}(s) := e^{2\pi i m(s-t)} g(s-t), \qquad \text{for } s,t,m \in \mathbb{R}.$$

Then we call the following function a Gabor ridge function.

$$g_{m,t,u}(x) := g^{m,t}(u \cdot x), \text{for } x \in \mathbb{R}^n, \tag{3.1}$$

where $u \in \mathbb{S}^{n-1}$ and $m, t \in \mathbb{R}$.

These functions are constant along the direction $u^{\perp}$ and modulate in a Gabor (time-frequency) manner in the direction u (see Figure 3.1).

In the rest of this work, we will use the following definition for the inner product of two functions $f, h \in L^2(\mathbb{R}^n)$ (or two functions for which the following integral is defined):

$$\langle f, h \rangle = \int_{\mathbb{R}^n} f\overline{h}\, dx.$$

The general question of this theory is what information are we actually collecting when we calculate $\langle f, g_{m,t,u} \rangle$ and also what can we do with this information. While

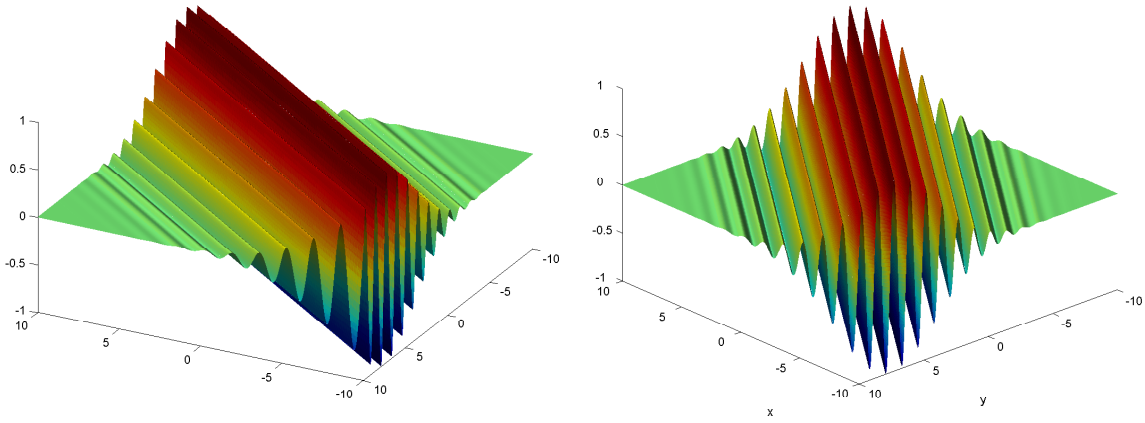

Figure 3.1: Gabor Ridge Functions

this will be explained in more detail later, a brief idea should be presented.

Given a certain $g_{m,t,u}$ for specific m, t and u, and a function f for which $\langle f, g_{m,t,u} \rangle$ is defined, what we collect is actually directional time-frequency information. Consider the case of f and g defined for $x \in \mathbb{R}^2$ (this corresponds to the visualization provided by Figure 3.1). When we pair f and $g_{m,t,u}$ we pick up time frequency information of f in the direction of u because of the directional modulations of $g_{m,t,u}$ and the parameters m and t control the modulations and translations of the classical time-frequency theory. It is important to note here that $g_{m,t,u} \notin L^2(\mathbb{R}^n)$, so we need to be careful about where our function f is defined. It should be noted, however, that if we consider our function f as a function on $L^2(\Omega)$, where Ω is some compact set in $\mathbb{R}^n$, the Radon transform and inverse Radon transform are well-defined, making this another good space to work with.

The first idea was to see if f was equal to $\int_{\mathbb{S}^{n-1}} \int_{\mathbb{R}} \int_{\mathbb{R}} \langle f, g_{m,t,u} \rangle \psi_{m,t,u} dm dt du$ (with du being the Lebesgue measure on $\mathbb{S}^{n-1}$) for any functions $g, \psi \in \mathcal{S}(\mathbb{R}^n)$. This is

actually not the case. We get something close to the original function, the back-projection of the Radon transform of f as was defined in the first chapter. For the rest of this work du will stand in place of $\mu_n du$ for the spherical integration.

Theorem 3.1.2 *Let $f \in L^1(\mathbb{R}^n)$. Given any other functions $g, \psi \in \mathcal{S}(\mathbb{R})$, we have the following:*

$$\mathcal{B}(f) = R^*(R_u f) = \frac{1}{\langle g, \psi \rangle} \int_{\mathbb{S}^{n-1}} \int_{\mathbb{R}} \int_{\mathbb{R}} \langle f, g_{m,t,u} \rangle \psi_{m,t,u} dm dt du. \tag{3.2}$$

Before this is proved, a lemma is needed concerning the relationship of the Radon transform with our representation.

Lemma 3.1.3 *With f, g defined as in Theorem 3.1.2 , we have the following equality:*

$$\langle f, g_{m,t,u} \rangle = \langle R_u f, g^{m,t} \rangle.$$

Proof :

First fix a direction $u \in \mathbb{S}^{n-1}$. Then

$$\begin{aligned}
\langle f, g_{m,t,u} \rangle &= \int_{\mathbb{R}^n} f(x) e^{-2\pi i m(u \cdot x - t)} \overline{g(u \cdot x - t)} dx \\
&= \int_{\mathbb{R}} \left(\int_{u \cdot x = s} f(x) e^{-2\pi i m(u \cdot x - t)} \overline{g(u \cdot x - t)} dx \right) ds \\
&= \int_{\mathbb{R}} e^{-2\pi i m(s-t)} \overline{g(s-t)} \left(\int_{u \cdot x = s} f(x) dx \right) ds \\
&= \int_{\mathbb{R}} R_u f(s) \overline{g^{m,t}(s)} ds \\
&= \langle R_u f, g^{m,t} \rangle.
\end{aligned}$$

which is well-defined since $R_u f \in L^1(\mathbb{R})$ ($f \in L^1(\mathbb{R}^n)$), and $g \in \mathcal{S}(\mathbb{R})$.

$$\int_{\mathbb{R}} |R_u f(s)| ds \leq \int_{\mathbb{R}^n} |f(x)| dx.$$

□

The previous lemma is of course valid for functions f, g, and ψ in a much more general sense. The proof only requires restrictions of the functions so that appropriate integrals converge and manipulations may be made.

This lemma is interesting because is shows the natural appearance of the Radon transform into this directionally sensitive ridge function. We did not force it in by definition, it just arose from the fact that our Gabor ridge function depends upon $u \in \mathbb{S}^{n-1}$.

Now Theorem 3.1.2 may be proved.

Proof :

We continue as follows, noting that $\langle R_u f, g^{m,t} \rangle = \langle f, g_{m,t,u} \rangle$ by the previous lemma:

$$\begin{aligned}
&\int_{\mathbb{S}^{n-1}} \int_{\mathbb{R}} \int_{\mathbb{R}} \langle f, g_{m,t,u} \rangle \psi_{m,t,u} dm dt du \\
&= \int_{\mathbb{S}^{n-1}} \int_{\mathbb{R}} \int_{\mathbb{R}} \langle R_u f, g^{m,t} \rangle \psi_{m,t,u} dm dt du \\
&= \int_{\mathbb{S}^{n-1}} \int_{\mathbb{R}} \int_{\mathbb{R}} \left(\int_{\mathbb{R}} \widehat{R_u f}(\sigma) \overline{\widehat{g^{m,t}}(\sigma)} d\sigma \right) e^{2\pi i m(u \cdot x - t)} \psi(u \cdot x - t) du dm dt \\
&= \int_{\mathbb{S}^{n-1}} \int_{\mathbb{R}} \int_{\mathbb{R}} \int_{\mathbb{R}} \widehat{R_u f}(\sigma) \overline{\widehat{g}(\sigma - m)} e^{2\pi i \sigma t} e^{2\pi i m(u \cdot x - t)} \psi(u \cdot x - t) d\sigma du dm dt.
\end{aligned}$$

where we used that

$$\langle h, k \rangle = \langle \widehat{h}, \widehat{k} \rangle$$

if $h \in L^1(\mathbb{R})$ and $k \in \mathcal{S}(\mathbb{R})$ and the fact that $\widehat{g^{m,t}}(\sigma) = \widehat{g}(\sigma - m) e^{-2\pi i \sigma t}$ by the properties of modulations and translation acting under the Fourier transform.

Next, a change of variables ($\sigma - m \to m$) is made leaving us with,

$$\int_{\mathbb{S}^{n-1}} \int_{\mathbb{R}} \int_{\mathbb{R}} \widehat{R_u f}(\sigma) \overline{\widehat{g}(m)} e^{2\pi i \sigma t} e^{2\pi i (\sigma - m)(u \cdot x - t)} \psi(u \cdot x - t) d\sigma du dm dt.$$

Combining the exponentials yields

$$\int_{\mathbb{S}^{n-1}} \int_{\mathbb{R}} \int_{\mathbb{R}} \widehat{R_u f}(\sigma) \overline{\widehat{g}(m)} e^{2\pi i \sigma u \cdot x} e^{-2\pi i m u \cdot x} e^{2\pi i m t} \psi(u \cdot x - t) d\sigma du dm dt.$$

Next we integrate over m, noting that $\int \overline{\widehat{g}(m)} e^{2\pi i m (t - u \cdot x)} dm = \overline{g(u \cdot x - t)}$.

$$\int_{\mathbb{R}} \int_{\mathbb{S}^{n-1}} \int_{\mathbb{R}} \widehat{R_u f}(\sigma) \overline{g(u \cdot x - t)} e^{2\pi i \sigma u \cdot x} \psi(u \cdot x - t) d\sigma du dt.$$

Finally, we integrate over the translation variable t and recognize the inverse Fourier transform of the Radon transform at the point $u \cdot x$:

$$\begin{aligned} & \langle \psi, g \rangle \int_{\mathbb{S}^{n-1}} \int_{\mathbb{R}} \widehat{R_u f}(\sigma) e^{2\pi i \sigma u \cdot x} d\sigma du. \\ = \; & \langle \psi, g \rangle \int_{\mathbb{S}^{n-1}} R_u f(u \cdot x) du \\ = \; & \langle \psi, g \rangle \mathcal{B}(f), \end{aligned}$$

where the above integral converges absolutely since $f \in L^1(\mathbb{R}^n)$:

$$\begin{aligned} & \int_{\mathbb{S}^{n-1}} \int_{\mathbb{R}} |\widehat{R_u f}(\sigma)| d\sigma du \\ \leq \; & \int_{\mathbb{S}^{n-1}} \int_{|\sigma| \leq 1} |\widehat{f}(\sigma u)| d\sigma du + \int_{\mathbb{S}^{n-1}} \int_{|\sigma| > 1} |\widehat{f}(\sigma u)| |\sigma|^{n-1} d\sigma du \\ \leq \; & C_n \|f\|_{L^1} + \|f\|_{L^1(|x|>1)} \end{aligned}$$

since $\|\widehat{f}\,\|_{L^\infty} \leq \|f\|_{L^1}$.

□

So this means we have a reconstruction formula for the backprojection of f which we saw in the first chapter is f convolved with a certain weight. We will present an

example using this formula to show a visualization of the results. To do this a discrete algorithm was necessary. This algorithm will be presented later in this work.

Consider the image presented in Figure 3.2. We reconstructed the image by breaking into time-frequency-direction components as discussed in this section and putting them back together. What you see is a blurry version of the original image, just as we suspect from the backprojection of the Radon transform of the image.

3.2 A Parseval Formula

The next step was to get some type of Parseval formula even though we don't yet have a true reproduction formula. This idea is to get some sense of (L^2) energy conservation of our transform. We will now see what we actually get when we look at $\int_{\mathbb{S}^{n-1}} \int_{\mathbb{R}} \int_{\mathbb{R}} |\langle f, g_{m,t,u}\rangle|^2 dm dt du$.

$$\begin{aligned} \langle f, g_{m,t,u}\rangle &= \langle R_u f, g^{m,t}\rangle \\ &= \int_{\mathbb{R}} R_u f(s) e^{-2\pi i m(s-t)} \overline{g(s-t)} ds \\ &= (R_u f * \widetilde{\overline{g^{-m,0}}})(t) \end{aligned}$$

where $\widetilde{g}(x) = g(-x)$.

Before we continue notice that the function shown above is in $L^2(\mathbb{R})$ by Young's inequality,

$$\|R_u f * \widetilde{\overline{g^{-m,0}}}\|_2 \leq \|R_u f\|_1 \|\widetilde{\overline{g^{-m,0}}}\|_2$$

where $R_u f \in L^1(\mathbb{R})$ since $f \in L^1(\mathbb{R}^n)$.

Figure 3.2: Example Reconstruction: The top picture is the original and the bottom picture is the reconstructed version using the methods of this chapter which reconstrusts the back-projection of $R_u f$ instead of f. This reconstruction is inadequate and will be improved in the next chapter.

So, we now have

$$\begin{aligned}
\int_{\mathbb{S}^{n-1}}\int_{\mathbb{R}}\int_{\mathbb{R}} |\langle f, g_{m,t,u}\rangle|^2 dmdtdu &= \int_{\mathbb{S}^{n-1}}\int_{\mathbb{R}}\int_{\mathbb{R}} |(R_u f * \widetilde{\overline{g^{-m,0}}})(t)|^2 dudmdt \\
&= \int_{\mathbb{R}}\int_{\mathbb{S}^{n-1}} \|R_u f * \widetilde{\overline{g^{-m,0}}}\|_2^2 dudm \\
&= \int_{\mathbb{R}}\int_{\mathbb{S}^{n-1}} \|(R_u f * \widetilde{\overline{g^{-m,0}}})\widehat{\ }\|_2^2 dudm \\
&= \int_{\mathbb{R}}\int_{\mathbb{R}}\int_{\mathbb{S}^{n-1}} |(R_u f * \widetilde{\overline{g^{-m,0}}})\widehat{\ }(\xi)|^2 dudmd\xi \\
&= \int_{\mathbb{R}}\int_{\mathbb{R}}\int_{\mathbb{S}^{n-1}} |\widehat{f}(\xi u)|^2 |\widehat{\overline{g}}(\xi+m)|^2 dudmd\xi \\
&= \|g\|_2^2 \int_{\mathbb{R}}\int_{\mathbb{S}^{n-1}} |\widehat{f}(\xi u)|^2 dud\xi.
\end{aligned}$$

where we used our previous result to work with a function of the variable t. We then used Parseval's formula and integrated over the variable m.

So, we don't get $\|f\|_2^2$, but we get something that we should expect because of what our "reproduction formula" gave us.

$$\begin{aligned}
\|g\|_2^2 \int_{\mathbb{R}}\int_{\mathbb{S}^{n-1}} |\widehat{f}(\xi u)|^2 dud\xi &= 2\int_0^\infty \int_{\mathbb{S}^{n-1}} |\widehat{f}(\xi u)|^2 dud\xi \\
&= 2\int_0^\infty \int_{\mathbb{S}^{n-1}} |\widehat{f}(\xi u)|^2 |\xi|^{n-1} du \frac{d\xi}{|\xi|^{n-1}}.
\end{aligned}$$

Now, by a change of variables ($y = \xi u$) we have,

$$\begin{aligned}
& 2\int_{\mathbb{R}^n} |\widehat{f}(y)|^2 \frac{dy}{|y|^{n-1}} \\
= \; & 2c(n) \int_{\mathbb{R}^n} \left| \left(f * \frac{1}{|x|} \right)\widehat{\ }(y) \right|^2 dy \\
= \; & 2c(n) \left\| f * \frac{1}{|x|} \right\|_2^2 \quad (n \geq 2),
\end{aligned}$$

which is a multiple of the L^2 norm of the back-projection of the Radon transform which we obtained from the continuous representation formula.

Here, the constant $c(n) = \frac{\Gamma(\frac{n-1}{2})}{\pi^{\frac{n-1}{2}}}$ arises from the definition of $\widehat{|x|^z}$ as a distribution (see Appendix A.2.2).

3.3 Concluding Remarks

This first initial guess left a few things to be desired to get the type of representation we were looking for. We wanted some type of directional Gabor element that would allow us to break up our function, analyze it, and reconstruct it in an appropriate way. We do have a hope for this because being able to reconstruct the backprojection of the function essentially tells us we have "enough" information to do the actual reconstruction of f. We know this from the Radon inversion formula mentioned in the first chapter.

Also, we have seen already how to work with the Radon transform and if one looks closely it can already be seen exactly why we don't reconstruct f and why we will need something called "weighted Gabor ridge functions."

It should be noted that this chapter and the next extend the theory that was first mentioned [56]. This paper is a nice precursor to both Gabor ridge functions and the ridgelet analysis developed by Candes and Donoho.

The next chapter will be similar to this one with the exception that we use our knowledge of Radon inversion to alter our Gabor ridge functions in an appropriate way.

Chapter 4

A Continuous Transform

What we saw in the last chapter is that more is required to reproduce a function f in the way we are attempting. A hint should be that the original inversion of the Radon transform (which our representation is closely related to) required a *filtered* form of back-projection. Following this idea, we define a more suitable class of Gabor ridge functions. We then apply these new ridge functions in the same fashion as before and the theory that we were originally interested in comes to fruition.

4.1 Weighted Gabor Ridge Functions

Again we start with a definition to solidify notation. It is technically incorrect to continue to use the term Gabor in reference to our function as we are about to make them more involved than just a simple time-frequency element. However, as will be seen, the functions are still essentially time-frequency elements and Gabor theory will play a crucial role in the development.

In what follows we will use the operator $D_\alpha f$, which is a form of differential

operator (for $\alpha > 0$) given by

$$D_\alpha f = (\widehat{f}(\xi)|\xi|^\alpha)^\vee.$$

Definition 4.1.1 (Weighted Gabor Ridge Function) *Let $g(x) \in \mathcal{S}(\mathbb{R})$ be some real-valued (non-zero) window function. We define the $g^{m,t}$'s and $g_{m,t,u}$'s as before:*

$$g^{m,t}(s) := e^{2\pi i m(s-t)} g(s-t), \quad \textit{for } s \in \mathbb{R},$$

$$g_{m,t,u}(x) = e^{2\pi i m((u\cdot x)-t)} g((u\cdot x)-t), \quad \textit{for } x \in \mathbb{R}^n.$$

Now, we introduce weighted functions (denoted by upper case letters):

$$G^{m,t}(s) := D_{\frac{n-1}{2}}(g^{m,t})(s) = \left(\widehat{g^{m,t}}(\sigma)|\sigma|^{\frac{n-1}{2}}\right)^\vee(s), \quad \textit{for } s \in \mathbb{R}, \tag{4.1}$$

We also define

$$G_{m,t,u}(x) := G^{m,t}(u\cdot x), \quad \textit{for } x \in \mathbb{R}^n. \tag{4.2}$$

It would be interesting and useful to determine the Fourier transform of our $G_{m,t,u}$'s. We calculate this and present it in the following theorem.

Theorem 4.1.2 (Fourier transform of $G_{m,t,u}$) *The Fourier transform of $G_{m,t,u}$ on $\mathbb{R}^n$ is as follows:*

$$\widehat{G_{m,t,u}}(\xi) = \widehat{g}(u\cdot\xi - m)e^{-2\pi i(u\cdot\xi)t}|u\cdot\xi|^{\frac{n-1}{2}}\delta(\xi - (u\cdot\xi)u)$$

Proof :

For this proof, we will prove the more general statement that for any function h on

$\mathbb{R}$ for which the one-dimensional Fourier transform is well-defined, when extended to $\mathbb{R}^n$ in the following way:

$$H(x) = h(u \cdot x)$$

has an n-dimensional Fourier transform which is a distribution and is given by

$$\widehat{H}(\xi) = \widehat{h}(u \cdot \xi)\delta(\xi - (u \cdot \xi)u).$$

$$\begin{aligned} \widehat{H}(\xi) &= \int_{\mathbb{R}^n} h(u \cdot x) e^{-2\pi i x \cdot \xi} dx \\ &= \int_{\mathbb{R}} \dots \int_{\mathbb{R}} h(u \cdot x) e^{-2\pi i x_1 \cdot \xi_1} e^{-2\pi i x_2 \cdot \xi_2} \dots e^{-2\pi i x_n \cdot \xi_n} dx_1 dx_2 \dots dx_n \end{aligned}$$

where we have divided $\mathbb{R}^n$ into n variables ranging over $\mathbb{R}$ by writing x as the part of x in the u direction and the other $n-1$ directions that make up the orthogonal complement of u:

$$x = (x \cdot u)u + x', \quad x' \in u^{\perp},$$

$$\xi = (\xi \cdot u)u + \xi', \quad \xi' \in u^{\perp}.$$

Then we have that $u \cdot x = x_1$ and we arrive at the result:

$$\begin{aligned} & \int_{\mathbb{R}^{n-1}} \int_{\mathbb{R}} h(x_1) e^{-2\pi i (x_1(\xi \cdot u) + x' \cdot \xi')} dx_1 dx' \\ = \ & \widehat{h}(u \cdot \xi)\delta(\xi') \\ = \ & \widehat{h}(u \cdot \xi)\delta(\xi - (u \cdot \xi)u) \end{aligned}$$

where $\xi - (u \cdot \xi)u$ is the part of ξ corresponding to $u^{\perp}$.

Now set $h(s) = G^{m,t}(s)$ and we arrive at the result of this theorem. $\square$

This Fourier transform truly shows the one-dimensional nature of the Gabor ridge functions. The Fourier transform corresponds to the one-dimensional Fourier transform of $G^{m,t}$ and is projected onto the line in the direction of u by the delta distribution.

It turns out the extra weight applied to the Gabor ridge functions works perfectly to reconstruct the function f instead of the back-projection. This weight corresponds to the filter in the filtered back-projection that we saw in the first chapter concerning the inversion of the Radon transform.

The next theorem is the backbone of our generalized theory in that it shows reconstruction from directional Gabor elements is possible and later we will see how to do this in a discrete sense. From this theorem we will extend other concepts of classical time-frequency analysis.

Theorem 4.1.3 (Continuous Representation) *Given a function $f \in L^1(\mathbb{R}^n)$ such that $\widehat{f} \in L^1(\mathbb{R}^n)$, and $G_{m,t,u}, \Psi_{m,t,u}$ defined by (4.2), we have*

$$f(x) = C_{g,\psi} \int_{\mathbb{S}^{n-1}} \int_{\mathbb{R}} \int_{\mathbb{R}} \langle f, G_{m,t,u} \rangle \Psi_{m,t,u} dm dt du. \tag{4.3}$$

Proof :

Starting with the right-hand side of (4.3) and using Lemma (3.1.3), we have

$$\int_{\mathbb{S}^{n-1}} \int_{\mathbb{R}} \int_{\mathbb{R}} \langle f, G_{m,t,u} \rangle \Psi_{m,t,u} dm dt du = \int_{\mathbb{S}^{n-1}} \int_{\mathbb{R}} \int_{\mathbb{R}} \langle R_u f, G^{m,t} \rangle \Psi_{m,t,u} dm dt du$$

where the inner product is well-defined since $R_u f \in L^1(\mathbb{R})$ and $G^{m,t} \in L^\infty(\mathbb{R})$ since

$\|G^{m,t}\|_\infty \leq \|\widehat{G^{m,t}}\|_1$. So, we may use Plancherel's formula to arrive at

$$\begin{aligned}
&\int_{\mathbb{S}^{n-1}} \int_{\mathbb{R}} \int_{\mathbb{R}} \langle \widehat{R_u f}, \widehat{G^{m,t}} \rangle \Psi_{m,t,u} dm dt du \\
= &\int_{\mathbb{S}^{n-1}} \int_{\mathbb{R}} \int_{\mathbb{R}} \left(\int_{\mathbb{R}} \widehat{R_u f}(\sigma) \overline{\widehat{g^{m,t}}(\sigma)} |\sigma|^{\frac{n-1}{2}} d\sigma \right) \Psi^{m,t}(u \cdot x) dm dt du.
\end{aligned}$$

Noting that $\overline{\widehat{g^{m,t}}(\sigma)} = e^{2\pi i t \sigma} \overline{\widehat{g}(\sigma - m)}$, we are left with

$$\int_{\mathbb{S}^{n-1}} \int_{\mathbb{R}} \int_{\mathbb{R}} \int_{\mathbb{R}} \widehat{R_u f}(\sigma) e^{2\pi i t \sigma} \overline{\widehat{g}(\sigma - m)} |\sigma|^{\frac{n-1}{2}} (\widehat{\psi^{m,t}}(s) |s|^{\frac{n-1}{2}})^\vee (u \cdot x) d\sigma dm du dt.$$

We expand out the inverse Fourier transform, which yields

$$\begin{aligned}
&\int_{\mathbb{S}^{n-1}} \int_{\mathbb{R}} \int_{\mathbb{R}} \int_{\mathbb{R}} \widehat{R_u f}(\sigma) e^{2\pi i t \sigma} \overline{\widehat{g}(\sigma - m)} |\sigma|^{\frac{n-1}{2}} \\
&\qquad \left(\int_{\mathbb{R}} e^{2\pi i (u \cdot x) \eta} \widehat{\psi}(\eta - m) e^{-2\pi i \eta t} |\eta|^{\frac{n-1}{2}} d\eta \right) d\sigma dm dt du.
\end{aligned}$$

Noting that the translation variable t only appears in the exponentials terms, we combine exponentials and integrate in t.

$$\begin{aligned}
&\int_{\mathbb{S}^{n-1}} \int_{\mathbb{R}} \int_{\mathbb{R}} \int_{\mathbb{R}} \widehat{R_u f}(\sigma) \overline{\widehat{g}(\sigma - m)} |\sigma|^{\frac{n-1}{2}} \\
&\qquad \left(\int_{\mathbb{R}} e^{2\pi i (u \cdot x) \eta} \widehat{\psi}(\eta - m) |\eta|^{\frac{n-1}{2}} d\eta \right) e^{2\pi i t (\sigma - \eta)} d\sigma dm dt du. \\
= &\int_{\mathbb{S}^{n-1}} \int_{\mathbb{R}} \int_{\mathbb{R}} \int_{\mathbb{R}} \widehat{R_u f}(\sigma) \overline{\widehat{g}(\sigma - m)} |\sigma|^{\frac{n-1}{2}} \\
&\qquad e^{2\pi i (u \cdot x) \eta} \widehat{\psi}(\eta - m) |\eta|^{\frac{n-1}{2}} \delta(\sigma - \eta) d\eta d\sigma dm du.
\end{aligned}$$

where δ is the Dirac delta distribution.

Now we integrate over the η variable noting that $\int_{\mathbb{R}} f(x) \delta(x - a) dx = f(a)$.

$$\int_{\mathbb{S}^{n-1}} \int_{\mathbb{R}} \int_{\mathbb{R}} \widehat{R_u f}(\sigma) \overline{\widehat{g}(\sigma - m)} |\sigma|^{\frac{n-1}{2}} e^{2\pi i (u \cdot x) \sigma} \widehat{\psi}(\sigma - m) |\sigma|^{\frac{n-1}{2}} d\sigma dm du.$$

$$= \int_{\mathbb{S}^{n-1}} \int_{\mathbb{R}} \int_{\mathbb{R}} \widehat{R_u f}(\sigma) |\sigma|^{n-1} e^{2\pi i (u\cdot x)\sigma} \overline{\widehat{g}(\sigma - m)} \widehat{\psi}(\sigma - m) d\sigma dm du.$$

Integrating over m yields

$$\langle g, \psi \rangle \int_{\mathbb{S}^{n-1}} \int_{\mathbb{R}} \widehat{R_u f}(\sigma) |\sigma|^{n-1} e^{2\pi i (u\cdot x)\sigma} d\sigma du.$$

$$= \langle g, \psi \rangle \int_{\mathbb{S}^{n-1}} \int_{\mathbb{R}} \widehat{f}(\sigma u) |\sigma|^{n-1} e^{2\pi i (u\cdot x)\sigma} d\sigma du.$$

by the Fourier slice theorem (Theorem 1.2.3). Now we can divide the integral above into two integrals over the cylinder as follows:

$$\langle g, \psi \rangle \int_{\mathbb{S}^{n-1}} \int_{\mathbb{R}} \widehat{f}(\sigma u) |\sigma|^{n-1} e^{2\pi i (u\cdot x)\sigma} d\sigma du$$

$$= \langle g, \psi \rangle \left(\int_{\mathbb{S}^{n-1}} \int_0^\infty \widehat{f}(\sigma u) |\sigma|^{n-1} e^{2\pi i (u\cdot x)\sigma} d\sigma du + \int_{\mathbb{S}^{n-1}} \int_{-\infty}^0 \widehat{f}(\sigma u) |\sigma|^{n-1} e^{2\pi i (u\cdot x)\sigma} d\sigma du \right).$$

We make a change of variables in the second integral ($\sigma \to -\sigma$, $u \to -u$) leaving us with

$$2\langle g, \psi \rangle \int_{\mathbb{S}^{n-1}} \int_0^\infty \widehat{f}(\sigma u) |\sigma|^{n-1} e^{2\pi i (u\cdot x)\sigma} d\sigma du.$$

By a change of variables ($k = \sigma u$), we arrive at

$$2\langle g, \psi \rangle \int_{\mathbb{R}^n} \widehat{f}(k) e^{2\pi i x\cdot k} dk = 2\langle g, \tilde{\psi} \rangle f(x).$$

□

4.2 True Reconstruction Example

Using the same image example from the previous chapter, we will now attempt to reproduce the image using our reconstruction formula. As mentioned earlier, we have

to use an algorithm to produce the results and currently we do not have a discrete form of the representation. We will look at this in the next chapter and later construct an algorithm from this. Currently, we are just previewing some of the results which will be explained more later.

We will begin the the same example picture (see Figure 4.1) and attempt to reconstruct it using a discrete version of our continuous representation which we have just developed. As should be expected, we reproduce f (actually an approximation) as intended.

4.3 Another Parseval Formula

As should be expected, we can can show that a Parseval type of formula exists. We will prove that $\|f\|_2^2 = C_g \int_{\mathbb{S}^{n-1}} \int_{\mathbb{R}} \int_{\mathbb{R}} |\langle f, G_{m,t,u} \rangle|^2 dmdtdu$ for any function $g \in \mathcal{S}(\mathbb{R})$. This provides us the (L^2) energy conservation that we would expect. Before we do this, a lemma is needed.

Lemma 4.3.1 *Given a function $f \in L^1 \cap L^2(\mathbb{R}^n)$, we have that*

$$D_{\frac{n-1}{2}}(R_u f) \in L^2(\mathbb{R})$$

for almost every $u \in \mathbb{S}^{n-1}$.

Proof :

$$\|f\|_2^2 \;=\; \int_{\mathbb{R}^n} |\widehat{f}(\xi)|^2 d\xi$$

Figure 4.1: True Reconstruction: The top picture is the original and the bottom picture is the reconstructed version using the methods of this chapter.

$$
\begin{aligned}
&= \int_{\mathbb{S}^{n-1}} \int_0^\infty |\widehat{R_u f}(\sigma)|\sigma|^{\frac{n-1}{2}}|^2 d\sigma du \\
&= \frac{1}{2} \int_{\mathbb{S}^{n-1}} \int_{\mathbb{R}} |D_{\frac{n-1}{2}}(R_u f)|^2 ds du.
\end{aligned}
$$

since $R_u f$ is even. It follows that for almost every $u \in \mathbb{S}^{n-1}$, $D_{\frac{n-1}{2}}(R_u f) \in L^2(\mathbb{R})$.

□

Theorem 4.3.2 (Parseval Formula) *For $f \in L^1 \cap L^2(\mathbb{R}^n)$ and $g \in \mathcal{S}(\mathbb{R}^n)$ we have the following equality:*

$$
\|f\|_2^2 = (2\|g\|_2^2)^{-1} \int_{\mathbb{S}^{n-1}} \int_{\mathbb{R}} \int_{\mathbb{R}} |\langle f, G_{m,t,u} \rangle|^2 dm dt du \tag{4.4}
$$

We start with a necessary lemma.

Lemma 4.3.3 *Given $f \in L^1 \cap L^2(\mathbb{R}^n)$ and $g \in \mathcal{S}(\mathbb{R})$ we have the following equality:*

$$
\begin{aligned}
\langle f, G_{m,t,u} \rangle &= (R_u f * D_{\frac{n-1}{2}}(\overline{g^{m,0}}))(t) \\
&= (D_{\frac{n-1}{2}}(R_u f) * \overline{g^{m,0}})(t) \\
&= D_{\frac{n-1}{2}}(R_u f * \overline{g^{m,0}})(t).
\end{aligned}
$$

Proof :

$$
\begin{aligned}
\langle R_u f, G^{m,t} \rangle &= \int_{\mathbb{R}} R_u f(s) \overline{(D_{\frac{n-1}{2}}(g^{m,t}))(s)} ds \\
&= \int_{\mathbb{R}} R_u f(s) \left(\int_{\mathbb{R}} e^{-2\pi i s y} \overline{\widehat{g}(y-m)} e^{2\pi i y t} |y|^{\frac{n-1}{2}} dy \right) ds \\
&= \int_{\mathbb{R}} \widehat{R_u f}(y) \overline{\widehat{g}(y-m)} e^{2\pi i y t} |y|^{\frac{n-1}{2}} dy \\
&= R_u f * D_{\frac{n-1}{2}}(\overline{g^{m,0}}))(t).
\end{aligned}
$$

□

We may now prove Theorem 4.3.2.

Proof :

By Lemma 4.3.3, let $h := (D_{\frac{n-1}{2}}(R_u f) * \overline{g^{m,0}})(t) = \langle f, G_{m,t,u}\rangle$ be a function of the translation variable t. Then by Lemma 4.3.1 and an application of Young's inequality $h \in L^2(\mathbb{R})$, for almost every $u \in \mathbb{S}^{n-1}$, we have

$$\|h\|_2 \leq \|D_{\frac{n-1}{2}}(R_u f)\|_2 \|\overline{g^{m,0}}\|_1.$$

Then

$$\begin{aligned}
\int_{\mathbb{S}^{n-1}}\int_{\mathbb{R}}\int_{\mathbb{R}} |\langle f, G_{m,t,u}\rangle|^2 dmdtdu &= \int_{\mathbb{S}^{n-1}}\int_{\mathbb{R}}\int_{\mathbb{R}} |h(t)|^2 dmdtdu \\
&= \int_{\mathbb{S}^{n-1}}\int_{\mathbb{R}} \|h\|_2^2 dmdu \\
&= \int_{\mathbb{S}^{n-1}}\int_{\mathbb{R}} \|\widehat{h}\|_2^2 dmdu \\
&= \int_{\mathbb{S}^{n-1}}\int_{\mathbb{R}}\int_{\mathbb{R}} |\widehat{h}(\sigma)|^2 d\sigma dmdu \\
&= \int_{\mathbb{S}^{n-1}}\int_{\mathbb{R}}\int_{\mathbb{R}} |\widehat{f}(\sigma u)|^2 |\sigma|^{n-1} |\widehat{\overline{g}}(\sigma - m)|^2 d\sigma dmdu.
\end{aligned}$$

where we have used Theorem 1.2.3.

Integrating over m yields,

$$\|g\|_2^2 \int_{\mathbb{R}}\int_{\mathbb{S}^{n-1}} |\widehat{f}(\sigma u)|^2 |\sigma|^{n-1} dud\sigma.$$

By change of variables ($k = \sigma u$),

$$2\|g\|_2^2 \int_{\mathbb{R}^n} |\widehat{f}(k)|^2 dk = 2\|g\|_2^2 \|f\|_2^2.$$

where the constant 2 comes again from dividing the integral over $\mathbb{R}$ into two integrals and changing variables as in Theorem 4.1.3.

It should be noted we are requiring f to be in L^1 so that $|\langle f, G_{m,t,u}\rangle|$ is finite.

$$\langle \widehat{f}, \widehat{G_{m,t,u}} \rangle = \int_{\mathbb{R}^n} \widehat{f}(\xi)\overline{\widehat{g}(u\cdot\xi - m)}e^{2\pi i(u\cdot\xi)t}|u\cdot\xi|^{\frac{n-1}{2}}\delta(\xi - (u\cdot\xi)u)d\xi$$

$$= \int_{\mathbb{R}} \widehat{f}(\lambda u)\overline{\widehat{g}(\lambda - m)}e^{2\pi i(\lambda)t}|\lambda|^{\frac{n-1}{2}}d\lambda$$

which is finite if $\widehat{f} \in L^\infty(\mathbb{R}^n)$ ($f \in L^1(\mathbb{R}^n)$) since $\overline{\widehat{g}(\lambda - m)}e^{2\pi i(\lambda)t}|\lambda|^{\frac{n-1}{2}} \in L^1(\mathbb{R})$.

□

4.4 Orthogonality Relation

From what we already know about our $G_{m,t,u}$'s, we can extend our Parseval formula to a more general statement. The following theorem on orthogonality shows that our transform possesses properties similar to those of the ordinary Fourier transform and the short-time Fourier transform.

For example, there is a linear transformation $\mathcal{G}$ which when restricted to functions in $L^1(\mathbb{R}^n)$ is defined as follows:

$$\mathcal{G}(f)(m,t,u) = \langle f, G_{m,t,u}\rangle.$$

Then we want to show that $\langle f, h\rangle = \int_{\mathbb{S}^{n-1}}\int_{\mathbb{R}}\int_{\mathbb{R}} \mathcal{G}(f)(m,t,u)\mathcal{G}(h)(m,t,u)dmdtdu$.

This can be achieved with a simple polarization argument. We will, however, present a proof which is slightly more illustrative and specific to this example.

Theorem 4.4.1 (Orthogonality Relation) *Given two function $f, h \in L^1 \cap L^2(\mathbb{R}^n)$*

and a window function $g \in \mathcal{S}(\mathbb{R})$, we have

$$2\langle f, h\rangle = \int \mathcal{G}(f)(m,t,u)\mathcal{G}(h)(m,t,u)dmdtdu. \tag{4.5}$$

Proof :

By Theorem 4.3.3 we have,

$$\begin{aligned}
& \int_{\mathbb{S}^{n-1}} \int_{\mathbb{R}} \int_{\mathbb{R}} \langle f, G_{m,t,u}\rangle \langle h, G_{m,t,u}\rangle dmdtdu \\
= & \int_{\mathbb{S}^{n-1}} \int_{\mathbb{R}} \int_{\mathbb{R}} \langle D_{\frac{n-1}{2}}(R_u f) * \overline{g^{m,0}}, D_{\frac{n-1}{2}}(R_u h) * \overline{g^{m,0}}\rangle dtdmdu \\
= & \int_{\mathbb{S}^{n-1}} \int_{\mathbb{R}} \int_{\mathbb{R}} \langle (D_{\frac{n-1}{2}}((R_u f) * \overline{g^{-m,0}})\widehat{\ }, D_{\frac{n-1}{2}}(R_u h) * \overline{g^{-m,0}})\widehat{\ }\rangle dtdmdu \\
= & \int_{\mathbb{S}^{n-1}} \int_{\mathbb{R}} \int_{\mathbb{R}} \widehat{f}(\xi u)\overline{\widehat{h}(\xi u)}|\xi|^{n-1}|\widehat{\overline{g}}(\xi + m)|^2 d\xi dmdu
\end{aligned}$$

Integrating over m yields

$$\|g\|_2^2 \int_{\mathbb{S}^{n-1}} \int_{\mathbb{R}} \widehat{f}(\xi u)\overline{\widehat{h}(\xi u)}|\xi|^{n-1} dud\xi.$$

By a change of variables ($k = \xi u$) and dividing our integral over $\mathbb{R}$ into two integrals, we have

$$\begin{aligned}
& 2\int_{\mathbb{R}^n} \widehat{f}(k)\overline{\widehat{h}(k)}dk \\
= & \ 2\langle f, h\rangle.
\end{aligned}$$

. □

With this extended parseval relation in hand we can easily see how this implies the original Parseval relation and the actual reproduction formula. We can just consider

$$\left\langle \int_{\mathbb{S}^{n-1}} \int_{\mathbb{R}} \int_{\mathbb{R}} \langle f, G_{m,t,u}\rangle G_{m,t,u} dmdtdu, h \right\rangle.$$

This is equal to

$$\int_{\mathbb{S}^{n-1}} \int_{\mathbb{R}} \int_{\mathbb{R}} \langle f, G_{m,t,u} \rangle \langle h, G_{m,t,u} \rangle dmdtdu.$$

Of course, the last expression is equal to $\langle f, h \rangle$, by our extended Parseval. So, we have

$$f = C_g \int_{\mathbb{S}^{n-1}} \int_{\mathbb{R}} \int_{\mathbb{R}} \langle f, G_{m,t,u} \rangle G_{m,t,u} dmdtdu.$$

4.5 Comparison

It is interesting to note the similarities and differences of our new time-frequency-direction analysis with that of standard time-frequency analysis. The new analysis actually coincides with standard time-frequency analysis for $n = 1$. This can be seen by noting that $\mathbb{S}^0$ just contains $\{-1, 1\}$. Therefore our new analysis gives us

$$\int_{S^0} \int_{\mathbb{R}} \int_{\mathbb{R}} \langle f, G_{m,t,u} \rangle \Psi_{m,t,u} dmdtdu = 2 \int_{\mathbb{R}} \int_{\mathbb{R}} \langle f, g^{m,t} \rangle \psi^{m,t} dmdt = \frac{2}{\langle g, \psi \rangle} f.$$

This is because the integral over $\mathbb{S}^0$ is just a sum of two integrals corresponding to x and $-x$ and the differential operator that was important in the reconstruction is now just $D_0 = I$.

Now, if we consider $n = 2$, for example, we see where the new analysis gives us something different than the standard time-frequency analysis. Our new theory gives us

$$f = \frac{2}{\langle g, \psi \rangle} \int_{S^1} \int_{\mathbb{R}} \int_{\mathbb{R}} \langle f, G_{m,t,u} \rangle \Psi_{m,t,u} dmdtdu,$$

while the standard analysis gives us

$$f = \frac{1}{\langle g, \psi \rangle} \int_{\mathbb{R}} \int_{\mathbb{R}} \langle f, g_2^{m,t} \rangle \psi_2^{m,t} dmdt,$$

where g_2, ψ_2 are window functions defined on $\mathbb{R}^2$. As we can see, our new analysis localizes time and frequency along a certain direction, while the standard analysis localizes time and freqency at a certain point in $\mathbb{R}^2$.

4.6 Concluding Remarks

We have now established a theory for representation of certain functions as a continuous collection of time-frequency-direction elements. Along with this theory comes the naturally related statements like a parseval equality and orthogonality relations. Now that we have a general theory, we may attempt to see how to discretize the continuous theory (next chapter) and address some of the analysis issues. We also want to be able to apply this theory to some problems and to do this we need algorithms and ideas of stability in our discrete reconstruction.

The next two chapters will discuss how to discretize this theory and present some new functional spaces which are useful in the analysis of time, frequency, and direction.

Finally, in the last part of this dissertation, we will look at certain applications using our algorithms to be presented.

Chapter 5

A Semi-Discrete Reproduction Formula

We will now show how the continuous reproduction formula can be turned into a semi-discrete one. By this, we mean a discretization in the modulation and translation variables while leaving the integral over the sphere. Later we will show this is sufficient because when we transform this into an algorithm we will simply need to add up over "enough" directions to get as close to f as we want. The purpose in using a semi-discrete formula is simply for theoretical reasons (i.e. we want to reproduce f exactly instead of an approximation.).

5.1 Utilizing Gabor Frame Theory

We want to utilize our classical time-frequency analysis and frame theory from the second chapter to prove our results involving a discretization of the reproduction formula.

We move immediately to the main theorem of this chapter.

Theorem 5.1.1 (Semi-discrete Reproduction) *There exist $g, \psi \in \mathcal{S}(\mathbb{R})$ such that for all $f \in L^1 \cap L^2(\mathbb{R}^n)$, there exist $\alpha, \beta > 0$ such that:*

$$A\|f\|_2^2 \leq \int_{\mathbb{S}^{n-1}} \sum_{m\in\mathbb{Z}} \sum_{t\in\mathbb{Z}} |\langle f, G_{\alpha m,\beta t,u}\rangle|^2 du \leq B\|f\|_2^2$$

where A, B depend on the choice of g, α, and β. (It is possible that $A = B$.) Also,

$$f = \frac{1}{2} \int_{\mathbb{S}^{n-1}} \sum_{m\in\mathbb{Z}} \sum_{t\in\mathbb{Z}} \langle f, G_{\beta m,\alpha t,u}\rangle \Psi_{\beta m,\alpha t,u} du.$$

Proof :

First note that we may move the weight from the Gabor element to the Radon tranform of f.

$$\langle f, G_{m,t,u}\rangle = \langle R_u f, G^{m,t}\rangle = \langle D_{\frac{n-1}{2}}(R_u f), g^{m,t}\rangle.$$

Now this just becomes a standard pairing of an element of $L^2(\mathbb{R})$ (Lemma 4.3.1) with a Gabor element and there is a general theory to work with this. First of all, let us define the Wiener class of functions.

Definition 5.1.2 *The function g belongs to the Wiener class W if*

$$\|g\|_W = \sum_{n\in\mathbb{Z}} \text{ess sup}_{x\in[0,1]} |g(x+n)| < \infty.$$

Now, it is already known [32] that if α and β are "small enough", and $g \in W(\mathbb{R})$, we have a Gabor frame for $L^2(\mathbb{R})$. For example, if g is some Gaussian function in $L^2(\mathbb{R})$, then there exist $\alpha, \beta > 0$ (with the conditions of Theorem 2.3.1), such that we have the following for almost every $u \in \mathbb{S}^{n-1}$:

$$A\|D_{\frac{n-1}{2}}(R_u f)\|_2^2 \leq \sum_{m\in\mathbb{Z}} \sum_{t\in\mathbb{Z}} |\langle D_{\frac{n-1}{2}}(R_u f), g^{\alpha m,\beta t}\rangle|^2 \leq B\|D_{\frac{n-1}{2}}(R_u f)\|_2^2$$

where A and B depend upon the choice of g, α, and β. (It is possible that $A = B$).

Now, notice the following:

$$\begin{aligned} \|D_{\frac{n-1}{2}}(R_u f)\|_2^2 &= \int_{\mathbb{R}} |\widehat{R_u f}(\xi)|\xi|^{\frac{n-1}{2}}|^2 d\xi \\ &= \int_{\mathbb{R}} |\widehat{R_u f}(\xi)|^2 |\xi|^{n-1} d\xi \\ &= \int_{\mathbb{R}} |\widehat{f}(\xi u)|^2 |\xi|^{n-1} d\xi. \end{aligned}$$

And we know that $\int_{\mathbb{S}^{n-1}} \int_{\mathbb{R}} |\widehat{f}(\xi u)|^2 |\xi|^{n-1} d\xi du = 2\|f\|_2^2$.

So,

$$2A\|f\|_2^2 \leq \int_{\mathbb{S}^{n-1}} \sum_{m\in\mathbb{Z}} \sum_{t\in\mathbb{Z}} |\langle f, G_{\alpha m,\beta t,u}\rangle|^2 du \leq 2B\|f\|_2^2.$$

Now, the question is what does this imply concerning the reproduction of f over a semi-discrete set of parameters? For this we will need to apply the results of frame theory, specifically, the properties of Gabor (or Weyl-Heisenberg) frames.

Using Theorem 2.1.4, since we have the frame relationship above and Lemma 4.3.1, we can then produce the following reproduction formula for almost every $u \in \mathbb{S}^{n-1}$:

$$D_{\frac{n-1}{2}}(R_u f) = \sum_{m\in\mathbb{Z}} \sum_{t\in\mathbb{Z}} \langle D_{\frac{n-1}{2}}(R_u f), g^{\alpha m,\beta t}\rangle \psi^{\alpha m,\beta t}$$

where ψ is the dual function of g.

We may now apply our differential operator to both sides of the equation which gives us

$$D_{n-1}(R_u f) = D_{\frac{n-1}{2}} D_{\frac{n-1}{2}}(R_u f) = \sum_{m\in\mathbb{Z}} \sum_{t\in\mathbb{Z}} \langle D_{\frac{n-1}{2}}(R_u f), g^{\alpha m,\beta t}\rangle D_{\frac{n-1}{2}}(\psi^{\alpha m,\beta t})$$

And we know that if we evaluate the left hand side of the equation at the point $u \cdot x$ and integrate over the sphere we get f, since this is the filtered back projection inversion for the Radon transform.

$$f = \frac{1}{2} \int_{\mathbb{S}^{n-1}} \sum_{m \in \mathbb{Z}} \sum_{t \in \mathbb{Z}} \langle D_{\frac{n-1}{2}}(R_u f), g^{\alpha m, \beta t} \rangle D_{\frac{n-1}{2}}(\psi^{\alpha m, \beta t})(u \cdot x) du.$$

So,

$$f = \frac{1}{2} \int_{\mathbb{S}^{n-1}} \sum_{m \in \mathbb{Z}} \sum_{t \in \mathbb{Z}} \langle f, G_{\alpha m, \beta t, u} \rangle \Psi_{\alpha m, \beta t, u}.$$

□

5.2 Apodizing Functions

As we saw in the case of inverting the Radon transform for applications, it is sometimes necessary to use an apodizing function to have a stable and implementable method of reconstruction. So, we consider a new weight η defined in the following way:

Definition 5.2.1 (Apodizing Weight) *We define a new weight by its Fourier transform:*

$$\widehat{\eta}(\xi) = |\xi|^{\frac{n-1}{2}} \widehat{A}(\xi), \tag{5.1}$$

where $\widehat{A}(\xi)$ is a function with certain decay properties like the ones in Table 1.3.2.

Now, we can consider a new reconstruction in the following way.

Definition 5.2.2 (Apodized Reconstruction) *Consider f, g, ψ as defined in the*

previous theorem. Then we define a new reconstruction using our weight η by

$$S^{\eta}_{g,\psi} f = \int_{\mathbb{S}^{n-1}} \sum_{m\in\mathbb{Z}} \sum_{t\in\mathbb{Z}} \langle f, G^{\eta}_{m,t,u}\rangle \Psi^{\eta}_{m,t,u} du \tag{5.2}$$

where $G^{\eta}_{m,t,u} = (g^{m,t} * \eta)(u \cdot x)$.

This is closer to the actual reconstruction that will be implemented when algorithms are introduced. This form of reconstruction does not reproduce f exactly, but an approximation.

As an example, we will construct an apodized reconstruction formula using a similar weight as was used in [44], although others suffice.

Example 5.2.1 (Apodization Example) We will attempt to choose a weight A so that $S^w f$ approximates $f * \delta = f$. In other words we want to choose a weight A_b so that as b tends to ∞,

$$S^w f \to f * \delta.$$

In our example we will choose η_b such that

$$\widehat{\eta_b}(\xi) = |\xi|^{\frac{n-1}{2}} \widehat{A_b}(\xi)$$

where

$$\widehat{A_b}(\xi) = \widehat{A}\left(\frac{|\xi|}{b}\right),$$

where $0 \le \widehat{A} \le 1$ and $\widehat{A}(\sigma) = 0$ for $\sigma \ge 1$ and $\widehat{A}$ is smooth.

We will use the standard low-pass filter where $\widehat{A}(\sigma) = 1$ for all $\sigma \le 1$.

In this example we have

$$S^{\eta} f \;=\; \int_{\mathbb{S}^{n-1}} \sum_{m\in\mathbb{Z}} \sum_{t\in\mathbb{Z}} \langle f, G^{\eta}_{m,t,u}\rangle \Psi^{\eta}_{m,t,u} du$$

$$
\begin{aligned}
&= \int_{\mathbb{S}^{n-1}} R_u f * \eta_b(u \cdot x) du \\
&= \int_{\mathbb{S}^{n-1}} (R_u(f * R^*(A_b))\widehat{\ } | \cdot |^{n-1})^\vee (u \cdot x) du \\
&= f * R^*(A_b).
\end{aligned}
$$

The function $R^*(A_b)$ has been calculated [44] and is equal to a certain Bessel function of the first kind. Specifically,

$$R^*(A_b)(x) = b^n \frac{J_{n/2}(b|x|)}{(b|x|)^{n/2}},$$

where $J_k(x)$ denotes the Bessel function of the first kind of order k. Hence $R^*(A_b) \to \delta$ as $b \to \infty$.

5.3 Analysis

In this section, we will look at some of the basic and more advanced ideas involved in the analysis of our newly constructed time-frequency-direction atoms.

5.3.1 Analysis and Reconstruction Operators

We will begin with some general aspects of frame theory and see how our weighted Gabor frames relate. First, we will define the *analysis* and *reconstruction* operators.

Definition 5.3.1 *The analysis (or coefficient) operator is given by*

$$\mathcal{C}_g(f) = \{\langle f, G_{m,t,u} \rangle : m \in \mathbb{Z}, t \in \mathbb{Z}, u \in \mathbb{S}^{n-1}\}. \tag{5.3}$$

The analysis operator acting on a function $f \in L^1(\mathbb{R}^n)$ produces a semi-discrete sequence.

Definition 5.3.2 *The synthesis operator is given by*

$$\mathcal{D}_\psi(\{c_{m,t,u}\}) = \int_{\mathbb{S}^{n-1}} \sum_{m\in\mathbb{Z}} \sum_{t\in\mathbb{Z}} c_{m,t,u}\Psi_{m,t,u}du. \tag{5.4}$$

The synthesis operator takes a semi-discrete sequence $c_{m,t,u}$ and produces a function defined on $\mathbb{R}^n$.

Proposition 5.3.3 *The operators $\mathcal{C}$ and $\mathcal{D}$ are adjoint to each other.*

Proof :

$$\begin{aligned}
\langle \mathcal{C}_g^*(\{c_{m,t,u}\}), f\rangle &= \langle \{c_{m,t,u}\}, \mathcal{C}_g(f)\rangle \\
&= \int_{\mathbb{S}^{n-1}} \sum_{m\in\mathbb{Z}} \sum_{t\in\mathbb{Z}} c_{m,t,u}\overline{\langle f, \Psi_{m,t,u}\rangle}du \\
&= \left\langle \int_{\mathbb{S}^{n-1}} \sum_{m\in\mathbb{Z}} \sum_{t\in\mathbb{Z}} c_{m,t,u}\Psi_{m,t,u}, f \right\rangle \\
&= \langle \mathcal{D}_\psi(g), f\rangle.
\end{aligned}$$

□

These operators are the building blocks of what we will call our *Gabor ridge frame operator* which is defined in the following way.

Definition 5.3.4 (Gabor ridge frame operator) *Given a function $f \in L^1(\mathbb{R}^n)$ and functions $g, \psi \in \mathcal{S}(\mathbb{R})$, we call*

$$S_{g,\psi}f = \mathcal{D}_\psi(\mathcal{C}_g(f)) = \int_{\mathbb{S}^{n-1}} \sum_{t\in\mathbb{Z}} \sum_{m\in\mathbb{Z}} \langle f, G_{m,t,u}\rangle \Psi_{m,t,u}du$$

the Gabor ridge frame operator.

This operator will play a role in our decomposition for algorithms in the next chapter.

5.3.2 Representation Formula and Half-filtered Operators

In the general Gabor theory there is a nice representation formula due to Walnut which allows for more analysis and give a different perspective of the problem. A representation formula for our semi-discrete frame is desired. Before continuing we need to define the notion of *half-filtered* operators.

Definition 5.3.5 (Half-filtered Radon Transform) *We define the half-filtered Radon transform as an operator taking functions from $L^1(\mathbb{R}^n)$ and producing a function defined on $\mathbb{S}^{n-1} \times \mathbb{R}$ in the following way:*

$$\mathcal{R}f = D_{\frac{n-1}{2}}(Rf(u,\cdot))(t) = D_{\frac{n-1}{2}}(Rf)(u,t) \tag{5.5}$$

where the convolution is taken with respect to the affine parameter of the Radon transform.

Definition 5.3.6 (Half-filtered Back-projection Operator) *We define the half-filtered back-projection operator taking functions from $\mathbb{S}^{n-1} \times \mathbb{R}$ to functions on $\mathbb{R}^n$ in the following way:*

$$\mathcal{R}^* g = \int_{\mathbb{S}^{n-1}} D_{\frac{n-1}{2}}(g(u,\cdot))(u \cdot x)du. \tag{5.6}$$

Now we can consider our time-frequency-direction analysis in a different manner by breaking it up into different smaller operators to analyze.

Theorem 5.3.7 (Representation Formula) *The semi-discrete Gabor ridge frame operator*

$$S_{g,\psi}f = \int_{\mathbb{S}^{n-1}} \sum_m \sum_t \langle f, G_{m,t,u}\rangle \Psi_{m,t,u} du \tag{5.7}$$

can be written as

$$S_{g,\psi}f = \mathcal{R}^* Q f, \tag{5.8}$$

where

$$Qf = \sum_r G_r(s) \mathcal{R}f(s-r) \tag{5.9}$$

and

$$G_r(s) = \sum_t \psi(s-t)\overline{g(s-r-t)} \tag{5.10}$$

is the standard correlation function of general Gabor theory mentioned in the second chapter.

Proof :

We start with noting that proving this theorem simply requires us to establish that

$$Qf = \sum_{m\in\mathbb{Z}} \sum_{t\in\mathbb{Z}} \langle f, G_{m,t,u}\rangle \psi^{m,t}. \tag{5.11}$$

This is because it can easily be seen that if the previous statement is true, then

$$\mathcal{R}^* Q f = \int_{\mathbb{S}^{n-1}} \sum_{m\in\mathbb{Z}} \sum_{t\in\mathbb{Z}} \langle f, G_{m,t,u}\rangle \Psi_{m,t,u} du,$$

thus proving the theorem.

So, to prove (5.11), we start with the left hand side,

$$\sum_{r\in\mathbb{Z}} G_r(s) \mathcal{R}f(s-r)$$

$$
\begin{aligned}
&= \sum_{r\in\mathbb{Z}}\sum_{t\in\mathbb{Z}} \psi(s-t)\overline{g(s-r-t)} \int_{\mathbb{R}} e^{2\pi i(s-r)\sigma}\widehat{R_u f}(\sigma)|\sigma|^{\frac{n-1}{2}}d\sigma \\
&= \sum_{r\in\mathbb{Z}}\sum_{t\in\mathbb{Z}} \psi(s-t)\overline{g(s-r-t)} \int_{\mathbb{R}} e^{2\pi is\sigma}e^{-2\pi ir\sigma}\widehat{R_u f}(\sigma)|\sigma|^{\frac{n-1}{2}}du \\
&= \sum_{m\in\mathbb{Z}}\sum_{t\in\mathbb{Z}} \psi(s-t)\widehat{\overline{g}}(\sigma-m)e^{-2\pi i(s-t)(\sigma-m)} \int_{\mathbb{R}} e^{2\pi is\sigma}\widehat{R_u f}(\sigma)|\sigma|^{\frac{n-1}{2}}du.
\end{aligned}
$$

where we are using that

$$
\sum_{r\in\mathbb{Z}} \overline{g(s-r-t)}e^{-2\pi ir\sigma} = \sum_{m\in\mathbb{Z}} \overline{\widehat{g}(\sigma-m)}e^{-2\pi i(s-t)(\sigma-m)}
$$

by the Poisson summation formula [30]. Simplifying the last line of the previous calculation leads to

$$
\begin{aligned}
&\sum_{m\in\mathbb{Z}}\sum_{t\in\mathbb{Z}} \int_{\mathbb{R}} \psi(s-t)\overline{\widehat{g}(\sigma-m)}e^{2\pi ism}e^{2\pi it\sigma}e^{-2\pi itm}\widehat{R_u f}(\sigma)|\sigma|^{\frac{n-1}{2}}d\sigma \\
&= \sum_{m\in\mathbb{Z}}\sum_{t\in\mathbb{Z}} \left(\int_{\mathbb{R}} \widehat{R_u f}(\sigma)\overline{\widehat{g}(\sigma-m)}e^{2\pi it\sigma}|\sigma|^{\frac{n-1}{2}}d\sigma\right)\psi(s-t)e^{2\pi im(s-t)} \\
&= \sum_{m\in\mathbb{Z}}\sum_{t\in\mathbb{Z}} \langle f, G_{m,t,u}\rangle\psi^{m,t}.
\end{aligned}
$$

□

These new operators are very natural to study because they form an isometry on L^2 in that $[\mathcal{R}f, \mathcal{R}h] = \langle f, h\rangle$ for functions $f, h \in L^1 \cap L^2(\mathbb{R}^n)$. This is a simple calculation and is closely related to the orthogonality relation of chapter four.

$$
\begin{aligned}
[\mathcal{R}f, \mathcal{R}h] &= [D_{\frac{n-1}{2}}(R_u f), D_{\frac{n-1}{2}}(R_u f)] \\
&= [R_u f, D_{n-1}(R_u h)] \\
&= \langle f, R^*(D_{n-1}(R_u h))\rangle \\
&= \langle f, h\rangle.
\end{aligned}
$$

5.4 Concluding Remarks

In this chapter we have extended our continuous theory to a semi-discrete one. Using the classical time-frequency (Gabor) analysis, a semi-discrete reproduction formula was presented along with the new concept of an apodizing reproduction which will be implemented in the algorithms and applications later (where the spherical integral will finally need to be discretized).

Analysis and reconstruction operators analogous to classical one were presented and several properties were shown to extend to the time-frequency-direction analysis.

The concept of half-filtered operators (which form an isometry) was produced and a representation theorem (comparable to Walnut's [57]) was shown.

Chapter 6

The Functional Spaces $G_S^{p,q,r}$

We will now look at some new functional spaces that measure the quantitative properties of Gabor ridge functions. These spaces are built from the knowledge of our reproduction formula and semi-discrete frame properties of our weighted Gabor ridge functions. They are the functional spaces that naturally lend themselves to time-frequency-direction analysis. They are built from the basic modulation spaces which naturally lend themselves to time-frequency analysis. We will also see that these spaces are rich in substance and not simply constructed spaces with sparse elements.

The motivation behind finding functional spaces where everything is well-behaved is based on the fact that functions in very nice spaces do not always act well under the Radon transform. For example, consider the following function in $L^2(\mathbb{R}^n)$:

$$f(x) = (2 + |x|)^{-\frac{n}{2}} (\log(2 + |x|))^{-1}$$

The Radon transform of f is infinity everywhere (for all $u \in \mathbb{S}^{n-1}$ and all $s \in \mathbb{R}$).

There has been some recent work on what spaces f should be in so that the Radon transform is well-defined. A newer result by Madych [40] shows that if $f \in L^p(\mathbb{R}^2)$ for some p satisfying $\frac{4}{3} < p < 2$, then the Radon transform exists almost everywhere

and the Radon inversion formula exists almost everywhere.

We will start with a brief overview of *modulation spaces* as the later sections will use these spaces.

6.1 Modulation Spaces

We will now look at a certain class of functions which, with its norm, attempts to measure the size of the time and frequency components of the short-time Fourier transform in a standard way. This is another classical theory of time-frequency analysis and we follow closely [32] for the brief overview.

6.1.1 Definition of Modulation Spaces

We will start with a definition of a mixed norm L^p space.

Definition 6.1.1 (Definition of $L^q(L^p)$) *Let $1 \leq p, q < \infty$. Then the mixed-norm space $L^q(L^p)(\mathbb{R}^{2n})$ contains all measurable functions on $\mathbb{R}^{2n}$, such that the norm*

$$\|F\|_{L^q(L^p)} = \left(\int_{\mathbb{R}^n} \left(\int_{\mathbb{R}^n} |F(x,\omega)|^p dx \right)^{q/p} d\omega \right)^{1/q} < \infty$$

If either p or q equal ∞, then the norm is replaced by the essential supremum giving,

$$\|F\|_{L^q(L^\infty)} = \left(\int_{\mathbb{R}^n} \left(\operatorname*{ess\,sup}_{x \in \mathbb{R}^n} |F(x,\omega)| dx \right)^{q} d\omega \right)^{1/q} < \infty$$

and

$$\|F\|_{L^\infty(L^p)} = \operatorname*{ess\,sup}_{\omega \in \mathbb{R}^n} \left(\int_{\mathbb{R}^n} |F(x,\omega)|^p dx \right)^{1/p} < \infty$$

It is also easy to extend this to sequences on $\mathbb{Z}^{2n}$.

Definition 6.1.2 (Discrete mixed-norm spaces $\ell^q(\ell^p)$) *$\ell^q(\ell^p)$ contains all sequences $(a_{jk})_{j,k\in\mathbb{Z}^n}$ of $\mathbb{C}$ such that the norm*

$$\|a_{jk}\|_{\ell^{p,q}} = \left(\sum_{j\in\mathbb{Z}^n}\left(\sum_{j\in\mathbb{Z}^n}|a_{jk}|^p\right)^{q/p}\right)^{1/q} < \infty$$

Now as we begin to venture into the time-frequency aspect of these spaces we will start by defining a generalization of something we have seen before, that being the Wiener class of functions.

Definition 6.1.3 ($W(L^{p,q})$) *Let F be a measurable function on $\mathbb{R}^{2n}$. Consider the following sequence*

$$a_{jk} = \operatorname*{ess\,sup}_{x,\omega\in[0,1]^n} |F(x+j,\omega+k)|.$$

Then if this sequence belongs to $\ell^{p,q}$, we say the function F belongs to $W(L^{p,q})$ with the norm

$$\|F\|_{W(L^{p,q})} = \|a\|_{\ell^q(\ell^p)}.$$

The previous "Wiener class" we have seen can now be identified as $W(L^{1,1})$.

We are now ready to actually define what we mean by a modulation space.

Definition 6.1.4 (Modulation Spaces $M^{p,q}$) *For a fixed non-zero window $g \in \mathcal{S}(\mathbb{R}^n)$ and $1 \le p,q \le \infty$, the modulation space $M^{p,q}$ contains all tempered distributions $f \in S'(\mathbb{R}^n)$ such that the short-time Fourier transform of f, $V_g f \in L^q(L^p)$. The norm on $M^{p,q}$ is*

$$\|f\|_{M^{p,q}} = \|V_g f\|_{L^q(L^p)}.$$

Let's take a closer look at how this norm operates. Expanding out $\|f\|_{M^{p,q}}$ gives us

$$\left(\int_{\mathbb{R}^n}\left(\int_{\mathbb{R}^n}|\langle f,g^{m,t}\rangle|^p dm\right)^{q/p}dt\right)^{1/q}<\infty.$$

This norm calculates the measure of the time and frequency components of our function f. Consider the space $M^2 := (M^{2,2})$. Our norm on this space is

$$\left(\int_{\mathbb{R}^n}\int_{\mathbb{R}^n}|\langle f,g^{m,t}\rangle|^2 dmdt\right)^{1/2}.$$

From general time-frequency analysis we know that $\|f\|_{M^2} = \|g\|_{L^2}\|f\|_{L^2}$ for $f,g \in L^2(\mathbb{R}^n)$. So, for any $g \in \mathcal{S}(\mathbb{R})$, we have that the functional space M^2 is the space L^2.

Finally, we may also define the discrete version of $M^{p,q}$ and call it $m^{p,q}$ given by the following norm:

$$\|f\|_{m^{p,q}} = \left(\sum_{m\in\mathbb{Z}^n}\left(\sum_{t\in\mathbb{Z}^n}|V_g f(m,t)|^p\right)^{q/p}\right)^{1/q}<\infty$$

6.1.2 Properties of Modulation Spaces

We will now look at some important properties of modulation spaces which we will use in the later sections.

Proposition 6.1.5 *Below is a list of properties known for modulation spaces which can be easily verified.*

(a) $M^{p,q}(\mathbb{R}^n)$ *is a Banach space for* $1 \le p,q \le \infty$.

(b) $M^{p,q}$ *is invariant under time-frequency shifts and* $\|T_x M_\omega f\|_{M^{p,q}} \le C\|f\|_{M^{p,q}}$.

(c) If $p = q$, *then* M^p *is invariant under the Fourier transform.*

Theorem 6.1.6 *If $g \in M^1$ and $f \in M^{p,q}$, then $V_g f \in W(L^{p,q})$ and*

$$\|V_g f\|_{W(L^{p,q})} \leq C \|V_g g\|_{W(L^1)} \|f\|_{M^{p,q}}. \tag{6.1}$$

Theorem 6.1.7 *If $f \in W(L^{p,q})$ is continuous, then for all $\alpha, \beta > 0$, $f|_{\alpha\mathbb{Z}^n \times \beta\mathbb{Z}^n}$ (the restriction of f to the grid $\alpha\mathbb{Z}^n \times \beta\mathbb{Z}^n$) is in $\ell^{p,q}$, and*

$$\|f|_{\alpha\mathbb{Z}^n \times \beta\mathbb{Z}^n}\|_{\ell^{p,q}} \leq C_{\alpha,\beta} \|f\|_{W(L^{p,q})}.$$

Theorem 6.1.8 *If $g_{m,t,u} \in M^1$ then $V_g f \in W(L^1)$.*

We can also see what the dual modulation spaces are as a consequence os duality with mixed-norm $L^{p,q}$ spaces.

Proposition 6.1.9 (Duality of Modulation Spaces) *If $1 \leq p, q \leq \infty$, then $(M^{p,q})^* = M^{p',q'}$ under the duality*

$$\langle f, h \rangle = \int \int_{\mathbb{R}^{2n}} V_g f(y) \overline{V_g h(y)} dy$$

for $f \in M^{p,q}$ and $h \in M^{p',q'}$, where $1/p + 1/p' = 1$ and $1/q + 1/q' = 1$.

For a proof of these theorems and properties, we refer the reader to [32].

6.2 Definition of the Spaces $G_s^{p,q,r}$

We will start with a definition of the spaces.

Definition 6.2.1 (The Functional Space $G_s^{p,q,r}$) *For a given function $f \in L^1(\mathbb{R}^n)$, we say $f \in G_s^{p,q,r}$ if the following norm is finite:*

$$\|f\|_{G_s^{p,q,r}} = \left(\int_{\mathbb{S}^{n-1}} \|(\widehat{R_u f} \widehat{\omega_s})^\vee\|_{M^{p,q}}^r du \right)^{1/r},$$

where $\omega_s = (|\xi|^{\frac{n-1}{2}}(1+|\xi|^2)^{\frac{s}{2}})^\vee$ *and* $\omega = \omega_0$.

We will also define a semi-discrete version of this space which we will denote by $g^{p,q,r}$, not to be confused with the window function g.

Definition 6.2.2 *We say that a semi-discrete sequence* $\{c_{m,t,u}\}_{m,t,u}$ *defined on* $\mathbb{S}^{n-1} \times \mathbb{Z} \times \mathbb{Z}$ *we say it belongs to* $g^{p,q,r}$ *if the following norm is finite:*

$$\|\{c_{m,t,u}\}\|_{g^{p,q,r}} = \left(\int_{\mathbb{S}^{n-1}} \|\{c_{m,t,u}\}\|^r_{\ell^q(\ell^p)} du \right)^{1/r}.$$

The idea is that these functional spaces are the type of functional spaces that are specifically tuned to our weighted Gabor ridge function expansions. Analogous to the way modulation spaces are the "right" function spaces for the mathematical analysis of time-frequency theory, these new functional spaces are the "right" functional spaces for time-frequency-direction theory.

6.3 Relation to other Functional Spaces

As with the modulation spaces we will denote $G^{p,q,r}_s$ by just G^p_s when $p = q = r$ and by G^p when $p = q = r$ and $s = 0$.

Proposition 6.3.1 *Let* $f \in L^1 \cap L^2(\mathbb{R}^n)$ *and* $g \in \mathcal{S}(\mathbb{R})$, *then* $\|f\|_{G^2} = \|g\|_{L^2}\|f\|_{L^2}$

Proof :

Recall that $\widehat{\omega}(\xi) = |\xi|^{\frac{n-1}{2}}$.

$$\|f\|^2_{G^2} = \int_{\mathbb{S}^{n-1}} \|(\widehat{R_u f}\widehat{\omega})^\vee\|^2_{M_2} du$$

$$
\begin{aligned}
&= \int_{\mathbb{S}^{n-1}} \int_{\mathbb{R}} \int_{\mathbb{R}} |V_g((\widehat{R_u f \widehat{\omega}})^\vee)|^2 dmdtdu \\
&= \int_{\mathbb{S}^{n-1}} \int_{\mathbb{R}} \int_{\mathbb{R}} |\langle f, G_{m,t,u} \rangle|^2 dmdtdu \\
&= \|g\|_{L^2}^2 \|f\|_{L^2}^2
\end{aligned}
$$

with the last statement justified by Theorem 4.3.2 and the fact that

$$V_g(h) = \langle f, g^{m,t} \rangle.$$

□

This very easy proposition is a catalyst for the next two sections of this chapter which proves the boundedness of our semi-discrete frame operator

$$S_{g,\psi} f = \int_{\mathbb{S}^{n-1}} \sum_{m \in \mathbb{Z}} \sum_{t \in \mathbb{Z}} \langle f, G_{\alpha m, \beta t, u} \Psi_{\alpha m, \beta t, u} \rangle du$$

on the spaces $G^{p,q,r}$.

Theorem 6.3.2 *The functional space G_s^2 is the classical Sobolev space H^s.*

Proof :

$$
\begin{aligned}
\|f\|_{G_s^2}^2 &= \int_{\mathbb{S}^{n-1}} \|(\widehat{R_u f \widehat{\omega_s}})^\vee\|_{M_2}^2 du \\
&= \int_{\mathbb{S}^{n-1}} \int_{\mathbb{R}} \int_{\mathbb{R}} |V_g((\widehat{R_u f \widehat{\omega_s}})^\vee)|^2 dmdtdu \\
&= \int_{\mathbb{S}^{n-1}} \int_{\mathbb{R}} \int_{\mathbb{R}} |\langle (\widehat{R_u f \widehat{\omega_s}})^\vee, g^{m,t} \rangle|^2 dmdtdu \\
&= \int_{\mathbb{S}^{n-1}} \|(\widehat{R_u f \widehat{\omega_s}})^\vee\|_{L^2}^2 du \\
&= \int_{\mathbb{S}^{n-1}} \int_{\mathbb{R}} |\widehat{f}(\sigma u)|^2 |\sigma|^{n-1} (1 + |\sigma|^2)^s d\sigma du
\end{aligned}
$$

$$
\begin{aligned}
&= 2\int_{\mathbb{R}^n} |\widehat{f}(z)|^2(1+|z|^2)^s dz \\
&= 2\|f\|^2_{H^s}.
\end{aligned}
$$

□

6.4 Boundedness of the Frame Operator on the Spaces $G^{p,q,r}$

The most interesting and useful aspect of these new functional spaces for us is the fact that our semi-discrete frame operator is bounded on these spaces. This section will show how we prove this along with showing how natural it is to work with these spaces when working with our time-frequency-direction analysis.

Let us start by recalling some definitions involving the analysis and synthesis operators of S.

$$\mathcal{C}_g(f) = \langle f, G_{m,t,u}\rangle.$$

$$\mathcal{D}_\psi(\{c_{m,t,u}\}) = \int_{\mathbb{S}^{n-1}} \sum_{m\in\mathbb{Z}} \sum_{t\in\mathbb{Z}} c_{m,t,u}\Psi_{m,t,u} du.$$

We can now look at our frame operator Sf as $\mathcal{D}_\psi\mathcal{C}_g f$. This is convenient as we can prove boundedness results for both $\mathcal{C}$ and $\mathcal{D}$.

Theorem 6.4.1 (Boundedness of $\mathcal{C}_g$) *If $g \in M^1$, then $\mathcal{C}_g$ is bounded from $G^{p,q,r}$ into $g^{p,q,r}$ for $1 \le p,q,r \le \infty$, and lattice parameters $\alpha, \beta > 0$ such that*

$$\|\mathcal{C}_g\|_{op} \le C(\alpha,\beta)\|V_g g\|_{W(L^1)}$$

independently of p and q.

Proof :

By Theorem 6.1.6, $V_g((\widehat{R_u f}\widehat{\omega})^\vee) \in W(L^{p,q})$ for $g \in M^1$ and $(\widehat{R_u f}\widehat{\omega})^\vee \in M^{p,q}$. $V_g((\widehat{R_u f}\widehat{\omega})^\vee)$ is continuous and $|\mathcal{C}_g f(m,t)| = |V_g((\widehat{R_u f}\widehat{\omega})^\vee)(\alpha m, \beta t)|$, so by Theorem 6.1.7 and (6.1)

$$\begin{aligned}
\|\mathcal{C}_g(f)\|^r_{g^{p,q,r}} &= \int_{\mathbb{S}^{n-1}} \|\mathcal{C}_g f\|^r_{\ell^{p,q}} du \\
&= \int_{\mathbb{S}^{n-1}} \|V_g((\widehat{R_u f}\widehat{\omega})^\vee)|_{\alpha\mathbb{Z}^n \times \beta\mathbb{Z}^n}\|^r_{\ell^{p,q}} du \\
&\leq C_{\alpha,\beta} \int_{\mathbb{S}^{n-1}} \|V_g((\widehat{R_u f}\widehat{\omega})^\vee)\|^r_{W(L^{p,q})} du \\
&\leq C_{\alpha,\beta} \|V_g g\|^r_{L^1} \int_{\mathbb{S}^{n-1}} \|(\widehat{R_u f}\widehat{\omega})^\vee\|^r_{M^{p,q}} du \\
&= C_{\alpha,\beta} \|V_g g\|^r_{L^1} \|f\|^r_{G^{p,q,r}}.
\end{aligned}$$

□

So we see that $\mathcal{C}_g$ acts very naturally on the space $G^{p,q,r}$ and maps functions of this class into semi-discrete sequences in the space $g^{p,q,r}$. We will now prove a similar boundedness property for $\mathcal{D}_\psi$.

We first need another theorem which we will state without proof. For a nice proof of the following theorem, one may refer to [32].

Theorem 6.4.2 *For a fixed window $g_0 \in M^1$, the short-time Fourier transform,*

$$V_{g_0}(\mathcal{D}_g(\{c_{m,t}\})) = V_{g_0}\left(\sum_{m\in\mathbb{Z}} \sum_{t\in\mathbb{Z}} \{c_{m,t}\} g^{m,t}\right),$$

is in $L^{p,q}(\mathbb{R}^{2n})$ and

$$\|V_{g_0}(\sum_{m\in\mathbb{Z}} \sum_{t\in\mathbb{Z}} \{c_{m,t}\} g^{m,t})\|_{L^{p,q}} \leq C \|V_g g\|_{W(L^1)} \|\{c_{m,t}\}\|_{\ell^{p,q}}.$$

Theorem 6.4.3 (Boundedness of $\mathcal{D}_\psi$) *If $g \in M^1$, then $\mathcal{D}_\psi$ is bounded from $g^{p,q,r}$ into $G^{p,q,r}$ for $1 \leq p, q, r \leq \infty$ with the following norm estimate*

$$\|\mathcal{D}_g\|_{op} \leq \|V_{g_0} g_0\|_{W(L^1)}.$$

Proof :

Consider a semi-discrete sequence $\{c_{m,t,u}\}$.

$$\|\mathcal{D}_\psi c_{m,t,u}\|^r_{G^{p,q,r}} = \int_{\mathbb{S}^{n-1}} \|((R_u(D_\psi c_{m,t,u}))\widehat{\ } \widehat{\omega})^\vee \|^r_{M^{p,q}} du$$

Now, we need to understand what $R_u(\mathcal{D}_\psi c_{m,t,u})$ is actually equal to. Let us expand the synthesis operator.

$$\begin{aligned}
\mathcal{D}_\psi(c_{m,t,u}) &= \int_{\mathbb{S}^{n-1}} \sum_{m\in\mathbb{Z}} \sum_{t\in\mathbb{Z}} c_{m,t,u} \Psi_{m,t,u} du \\
&= \int_{\mathbb{S}^{n-1}} \sum_{m\in\mathbb{Z}} \sum_{t\in\mathbb{Z}} c_{m,t,u} D_{\frac{n-1}{2}}(\psi^{m,t})(u \cdot x) du \\
&= \int_{\mathbb{S}^{n-1}} \sum_{m\in\mathbb{Z}} \sum_{t\in\mathbb{Z}} c_{m,t,u} D_{\frac{n-1}{2}}(\psi^{m,t}) * \omega * \omega^*(u \cdot x) du
\end{aligned}$$

where ω^* is chosen such that $\omega * \omega^* \equiv \delta$. This can be done by choosing ω^* such that $\widehat{\omega^*}(\sigma) = |\sigma|^{\frac{1-n}{2}}$. Then,

$$D_\psi c = \mathcal{B}\left(\sum_{m\in\mathbb{Z}} \sum_{t\in\mathbb{Z}} c_{m,t,u} \psi^{m,t} * \omega^*\right).$$

So,

$$\begin{aligned}
D_{\frac{n-1}{2}}(R_u(D_\psi c)) &= D_{\frac{n-1}{2}}\left(R_u \mathcal{B}\left(\sum_m \sum_t c_{m,t,u} \psi^{m,t} * \omega^*\right)\right) \\
&= \sum_{m\in\mathbb{Z}} \sum_{t\in\mathbb{Z}} c_{m,t,u} D_{\frac{n-1}{2}}(\psi^{m,t}) * \omega^* \\
&= \sum_{m\in\mathbb{Z}} \sum_{t\in\mathbb{Z}} c_{m,t,u} \psi^{m,t}.
\end{aligned}$$

where we are justified in viewing this as a convolution because ω^* looks like $|s|^{\frac{n-3}{2}}$ near 0 (for $n \geq 2$), as is therefore locally integrable. Finally, by Theorem 6.4.2 we have the following:

$$\begin{aligned}
\|D_\psi c_{m,t,u}\|^r_{G^{p,q,r}} &= \int_{\mathbb{S}^{n-1}} \|D_{\frac{n-1}{2}}(R_u(D_\psi c_{m,t,u}))\|^r_{M^{p,q}} du \\
&= \int_{\mathbb{S}^{n-1}} \|\sum_{m\in\mathbb{Z}}\sum_{t\in\mathbb{Z}} \psi^{m,t}\|^r_{M^{p,q}} du \\
&= \int_{\mathbb{S}^{n-1}} \left\| V_{g_0}\left(\sum_{m\in\mathbb{Z}}\sum_{t\in\mathbb{Z}} c_{m,t,u}\psi^{m,t}\right)\right\|^r_{L^q(L^p)} du \\
&\leq \|V_{g_0}g_0\|_{W(L^1)} \int_{\mathbb{S}^{n-1}} \|c_{m,t,u}\|^r_{\ell^q(\ell^p)} du \\
&= \|V_{g_0}g_0\|_{W(L^1)} \|c_{m,t,u}\|^r_{g^{p,q,r}}.
\end{aligned}$$

□

We may now finish with the main statement of this section which is a simple corollary of the Theorem 6.4.1 and Theorem 6.4.3.

Corollary 6.4.4 (Boundedness of $S_{g,\psi} = \mathcal{D}_\psi \mathcal{C}_g$) *If $g, \psi \in M^1$ such that $V_g((\widehat{R_u f}\widehat{\omega})^\vee) \in M^{p,q}$, then our semi-discrete frame is bounded on $G^{p,q,r}$ for all $1 \leq p, q, r \leq \infty$ and $\alpha, \beta > 0$ with the following norm estimate:*

$$\|S_{g,\psi}\|_{op} \leq C(\alpha,\beta)\|V_g g\|_{W(L^1)}\|V_\psi \psi\|_{W(L^1)},$$

independent of $p, q,$ and r.

6.5 Characterization of $G^{p,q,r}$

We also have a corollary which extends the concept of our frame from $L^1 \cap L^2$ to $G^{p,q,r}$, by characterizing these spaces using our weighted Gabor ridge functions, similar to

[28].

Corollary 6.5.1 *Assume $g, \psi \in M^1$ such that $S_{g,\psi} = I$ on $L^1 \cap L^2(\mathbb{R}^n)$. Then*

$$\begin{aligned} f &= \int_{\mathbb{S}^{n-1}} \sum_{m\in\mathbb{Z}} \sum_{t\in\mathbb{Z}} \langle f, G_{m,t,u}\rangle \Psi_{m,t,u} du \\ &= \int_{\mathbb{S}^{n-1}} \sum_{m\in\mathbb{Z}} \sum_{t\in\mathbb{Z}} \langle f, \Psi_{m,t,u}\rangle G_{m,t,u} du \end{aligned}$$

with unconditional convergence in $G^{p,q,r}$ if $p, q, r < \infty$. Also, there are constants $A, B > 0$ such that for all $f \in G^{p,q,r}$

$$A\|f\|_{G^{p,q,r}} \leq \left(\int_{\mathbb{S}^{n-1}} \left(\sum_{m\in\mathbb{Z}} \left(\sum_{t\in\mathbb{Z}} |\langle f, G_{m,t,u}\rangle|^p \right)^{q/p} \right)^{r/q} du \right)^{1/r} \leq B\|f\|_{G^{p,q,r}}.$$

Proof :

We have seen that both the coefficient and synthesis operators are bounded on $G^{p,q,r}$ and $g^{p,q,r}$, we know that $f = \mathcal{D}_\psi \mathcal{C}_g f$ hold for all $f \in G^{p,q,r}$. The norm equivalence is all just a coincidence of our norm estimates for $\mathcal{C}$ and $\mathcal{D}$.

$$\begin{aligned} \|f\|_{G^{p,q,r}} &= \|\mathcal{D}_\psi \mathcal{C}_g f\|_{G^{p,q,r}} \leq \|\mathcal{D}_\psi\|_{op} \|\mathcal{C}_g\|_{g^{p,q,r}} \\ &\leq \|\mathcal{D}_\psi\|_{op} \|\mathcal{C}_g\|_{op} \|f\|_{G^{p,q,r}}. \end{aligned}$$

Note: we can choose $A = \|\mathcal{D}_\psi\|_{op}^{-1}$ and $B = \|\mathcal{C}_g\|_{op}^{-1}$. □

6.6 Concluding Remarks

What we have established in this chapter are a set of functional spaces that are tailored for the analysis of time, frequency, and direction. We have seen the motivation for these spaces in the modulation spaces of time-frequency analysis and have shown that they are actually rich spaces which can be shown by their relationship to other spaces.

Finally, we were able to show boundedness of our frame operator on these new spaces along with an extension of the the concept of a frame from functions in $L^1 \cap L^2$ to functions in $G^{p,q,r}$.

Part III

Applications

Chapter 7

Algorithm Development

To begin to study the applications of this theory, we need to look at possible algorithms to be implemented and what type of things need to be accomplished to apply this theory in a completely discrete setting.

This chapter simply shows how algorithms were constructed, although the author admits that there may be better ways to implement this theory on a computer. Pseudocode will be used to present the general ideas of the algorithms used. In all the algorithms we are assuming $n = 2$. Please note the algorithms included here are not complete and they are just to give an idea of how one might implement this theory.

7.1 Breaking Things Down

The first thing we need to do is to break down our theory into different pieces which we would like to generate algorithms for. We will start with the analysis and synthesis operators from the previous chapter. As a reminder, they were defined as

$$\mathcal{C}_g(f) = \langle f, G_{m,t,u} \rangle,$$

$$\mathcal{D}_\psi(\{c_{m,t,u}\}) = \int_{\mathbb{S}^{n-1}} \sum_{m\in\mathbb{Z}} \sum_{t\in\mathbb{Z}} c_{m,t,u}\Psi_{m,t,u}du.$$

Together, they form the general frame operator $S_{g,\psi}$.

$$S_{g,\psi} = \mathcal{D}_\psi(\mathcal{C}_g(f)) = \int_{\mathbb{S}^{n-1}} \sum_{m\in\mathbb{Z}} \sum_{t\in\mathbb{Z}} \langle f, G_{m,t,u}\rangle \Psi_{m,t,u}du.$$

The applications involving manipulations of the coefficients come in between the analysis and synthesis process and we will also look at those topics in the later chapters.

7.2 Analysis Operator $\mathcal{C}_g$

To create an algorithm for the analysis operator, it is helpful to remember what type of analysis we are doing. The best way to view the analysis of $\mathcal{C}_g$ is as time-frequency analysis on the Radon transform of the function. Recall that

$$\mathcal{C}_g(f) = \langle f, G_{m,t,u}\rangle = \langle D_{\frac{n-1}{2}}(R_u f), g^{m,t}\rangle.$$

So, we continue with the presentation of our algorithm with comments and explanations where necessary. We will start with an algorithm for computing $D_{\frac{n-1}{2}}(R_u f)$.

The first thing we calculate is the discrete Radon transform for a specified set of angles. In other words, we calculate

$$R_{u_j} f(s_i) = \int_{u_j \cdot x = s_i} f(x)dx.$$

A simple example of the Radon transform algorithm is given below. This algorithm simply approximates line integrals by summing over a discrete matrix of values (image) that is iteratively rotated to consider line integrals from different directions.

```
1   ************* RADON TRANSFORM ******************
    PROGRAM NAME: radon
    % INPUTS: theta - vector of angular directions
    %         data  - 2d array of data
5   %
    % OUTPUT: proj  - radon projections
    ************************************************

    % First the initial data should be zero padded so
10  % that data isn't lost in the rotations. This is
    % a simple procedure.

    n = length(theta)
    for i = 1 to n
15     tmp = rotateimage(data, 90-theta(i))
       proj(:,i) = columnsum(tmp)
    end

    ENDPROGRAM
```

In the last algorithm we are using an image rotating subroutine which will be left out for the purpose of clarity, but this subroutine is important in that it generates a new matrix of values corresponding to a rotated version of the original. Obviously,

some interpolation must be utilized in this process.

Now that we have the Radon transform of a function, we need to apply an appropriate weight ω. The general weight (for $n = 2$) from the definition of $\mathcal{C}_g$ is the following weight (along with its Fourier transform):

$$\widehat{\omega}(\sigma) = |\sigma|^{\frac{1}{2}}.$$

The filter that we will actually apply will be an apodized one corresponding to Table 1.3.2 and the apodized reconstruction of chapter five Definition 5.2.2. Our actual filter will have the following form:

$$\widehat{\omega}(\sigma) = |\sigma|^{\frac{1}{2}} \widehat{A}(\sigma).$$

To apply this filter we will create an algorithm to compute $(\widehat{R_u f}\widehat{\omega})^{\vee}$ since there are already fast algorithms for the Fourier transform. We begin with a algorithm that designs the filter for later use.

```
1   ************* FILTER DESIGN ********************
    PROGRAM NAME: filter
    % INPUTS: type - type of filter to be used
    %         num  - number of filter values
5   %         d    - fraction of nyquist rate
    %
    % OUTPUT: filter - the filter that will be used
    ***********************************************
```

```
10   size = 2^nexthighestpowerof2(2*num)
     % Start with a ramp filter
     filter = 2*[0:(size/2)]/size
     l = 2*pi*[0:len(filter,2)-1)]/size %frequency axis


15   if type = 'ram-lak'
             % already done
     else if type = 'shepp-logan'
             filter = filter * (sin(l)/(2*d)) / (l/(2*d))
     else if type = 'hamming'
20           filter = filter * (.54 + .46 * cos(l/d))
     else if type = 'hann'
             filter = filter  * (1+cos(l/d))/2
     end


25   ENDPROGRAM
```

Now, given that we have our filter, we calculate the (discrete) convolution of $R_{u_j} f *^d \omega$ by multiplication in the frequency domain. That is, we calculate the following:

$$IFFT(FFT(R_{u_j} f) FFT(\omega)) = R_{u_j} f *^d \omega$$

where FFT and $IFFT$ stand for the *fast Fourier transfrom* and *inverse fast Fourier transform* respectively. There are already many good algorithms currently available

for these operations (Cooley-Tukey, [16]).

```
1   ************* WEIGHT CONVOLVE ******************
    PROGRAM NAME: weight
    % INPUTS: data  - input data to be weighted
    %         filter- filter used as weight
5   %
    % OUTPUT: wdata - weighted data
    ************************************************


    % Zero pad radon data
10  data(length(filter))=0


    fproj = fft(data)
    ffilter = fft(filter)
    newproj = fproj*ffilter
15  wdata = real(ifft(newproj))


    %Truncate the data
    wdata(length(data)+1:end) = [empty]


20  ENDPROGRAM
```

The previous algorithms generate a discrete filter and implements it using mul-

tiplication in the frequency domain. We now need to consider an algorithm for a discrete time-frequency (Gabor) analysis.

```
1   *************** GABOR FRAME ********************
    PROGRAM NAME: gabor
    % INPUTS: g - window function
    %         f - function data (discrete signal)
5   %         a - time spacing
    %         b - frequency spacing
    %
    % OUTPUT: gabor(:,:) - gabor (TF) coefficients
    ************************************************
10
    % This program really just calculates the STFT
    % of a function, which coincides with a gabor
    % frame expansion.

15  % Check that length of f is divisible by a
    if (a divides length(x))
            continue
    else
            ERROR, end
20  end
```

```
    for j = 0 to length(x)/b-1
            tmp = f*shift(g,j)
            gabor(j+1,:) = fft(tmp)
    end

    ENDPROGRAM
```

Applying all of these alogrithms together will generate a set of time frequency coefficients for $R_{u_i} f *^d \omega$ for a discrete range of $u_i \in \mathbb{S}^{n-1}$. They are applied in the following order.

General algorithm:

Step 1: Apply discrete Radon transform (radon).

$$R_{u_i} f$$

Step 2: Generate filter and convolve with data (filter, weight).

$$R_{u_i} f *^d \omega$$

Step 3: Calculate time-frequency information for the data (gabor).

$$\langle R_{u_i} f, g^{m,t} \rangle$$

Step 4: Do this for all directions and collecte coefficients.

$$\langle f, G_{m,t,u_i} \rangle$$

7.3 Synthesis Operator $\mathcal{D}_\psi$

To create an algorithm for the synthesis operators we need to look at all the components of it. Recall that

$$\begin{aligned}
\mathcal{D}_\psi(\{c_{m,t,u}\})(x) &= \int_{\mathbb{S}^{n-1}} \sum_{m\in\mathbb{Z}} \sum_{t\in\mathbb{Z}} c_{m,t,u} \Psi_{m,t,u}(x) du \\
&= \int_{\mathbb{S}^{n-1}} \sum_{m\in\mathbb{Z}} \sum_{t\in\mathbb{Z}} c_{m,t,u} D_{\frac{n-1}{2}}(\psi^{m,t})(u\cdot x) du \\
&\approx \sum_{u_j} \sum_{m\in\mathbb{Z}} \sum_{t\in\mathbb{Z}} c_{m,t,u_j} (\psi^{m,t} *^d \omega)(u_j \cdot x).
\end{aligned}$$

Now that we have established the filtering operation and Gabor expansion, our reconstruction from coefficients $C_g f$ only needs one new piece of computation called backprojection. This involves the integral over the sphere in our continous theory and will become a discrete sum in our application now.

```
1   ************* BACKPROJECTION ********************
    PROGRAM NAME: backproject
    % INPUTS: theta - vector of angular directions
    %         data  - direction dependent radon data
5   %
    % OUTPUT: backp - backprojection of data
    ************************************************


    % Before the following code is implemented, x and y
10  % variables should be initialized for the correct
```

```
% coordinates based on radon data.


for i = theta

        newdata=data(:,i)

15      s = x*cos(i) + y*sin(i)

        a = floor(s)

        backp = (s-a)*newdata(a+1) + (s+1-a)*newdata(a)

end


20  ENDPROGRAM
```

The above algorithm is one simple way of calculating a discrete backprojetion based on linear interpolation which works surprisingly well as was shown by Ramachandran and Lakshminarayanan [50].

So to calculate D_ψ we just need to implement the following general algorthithm.

General algorithm:

Step 1: Reconstruct using only time-frequency data (gabor).

$$\sum_{m\in\mathbb{Z}}\sum_{t\in\mathbb{Z}} c_{m,t,u}\psi^{m,t}$$

Step 2: Generate filter and convolve with data (filter, weight).

$$\left(\sum_{m\in\mathbb{Z}}\sum_{t\in\mathbb{Z}} c_{m,t,u}\psi^{m,t}\right) *^d \omega$$

Step 3: Backproject over the discrete set of directions (backproject).

$$\sum_{u_i\in\mathbb{S}^{n-1}}\sum_{m\in\mathbb{Z}}\sum_{t\in\mathbb{Z}} c_{m,t,u_i}\Psi_{m,t,u_i}$$

Our last step is approximately equal to

$$\mathcal{D}_\psi(\{c_{m,t,u}\}) = \int_{\mathbb{S}^{n-1}} \sum_{m\in\mathbb{Z}} \sum_{t\in\mathbb{Z}} c_{m,t,u}\Psi_{m,t,u}du.$$

In step 1, we just need to apply the gabor code as before, but with the "dual" window function ψ which can be calculated from g. There are some very fast and efficient algorithms already developed for this [6].

7.4 Concluding Remarks

What we have seen here are the basic building blocks of the theory as they could be implemented on a digital computer. We have seen how to discretely implement our continuous operators $\mathcal{C}_g$ and $\mathcal{D}_\psi$ which together form our general frame operator $S_{g,\psi}$.

All of the applications take place between the coefficients and synthesis operator. The actual time-frequency-direction coefficients can be used in many ways (to enhance or denoise images, for example). What we will see in the final chapters are some examples of these applications and how the coefficients are altered to produce many different results.

Chapter 8

Image Processing

Applications involving image processing were readily available as the structure of the Gabor ridge function lends itself to directional frequency information. This allows for many different generalized image processing techniques such denoising, filtering, enhancement, etc. The added benefit is being allow to do all of these things in a directionally sensitive manner.

We will start by looking at filtering by direction and then move onto other topics including edge detection, image enhancement, and compression.

8.1 Filtering By Direction

Image processing depends heavily on the idea of filtering either by changing pixel values directly or altering the frequency content of the image. We will use these concepts to introduce filtering by direction in which we have more control over the direction(s) over which our filtering is being done and therefore how it affects the actual image.

First we will see what happens when certain time-frequency-direction information

is altered. In the first example (see Figure 8.1) we see the original head phantom along with its time-frequency-direction coefficients at directions of 45 and 125 degrees.

Now we are interested in working with the time-frequency-direction information to see how the image is affected. Here it should be noted that it is not truly appropriate to call the affine parameter "time," but it should be understood in context. If we, for example threshold the high frequency content, we see that (see Figure 8.2) the end result of the phantom image is blurry, but only on edges which are tangent to the directions we have chosen to threshold. Here we reduced by a sizable factor the time-frequency-direction coefficients which correspond to the angles from 0 to 45 degrees.

We now continue with the same experiment, but this time we amplify high frequency content in the same angular interval. What we see now is that the image is actually sharpened in the angular range and specifically on edges which are tangent to the directions in the range.

8.2 Robust Edge Detection

There is also an application to edge detection. The Radon transform itself has been specifically used to find edges in other image processing algorithms. We are also able to detect edges in images as our time-frequency-direction coefficients are large when the direction is tangent to a certain edge. The added benefit is that we are actually able to detect edges of different thickness. The difference in the thickness of the edges can be detected by the actual coefficients.

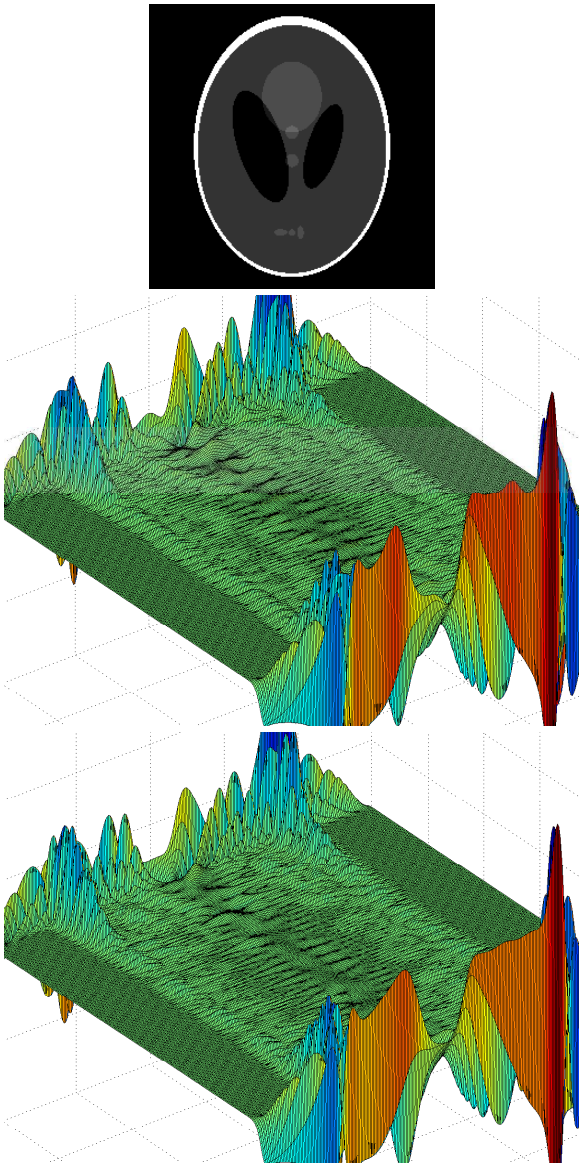

Figure 8.1: Time-frequency-direction coefficients corresponding to 25 and 125 degrees.

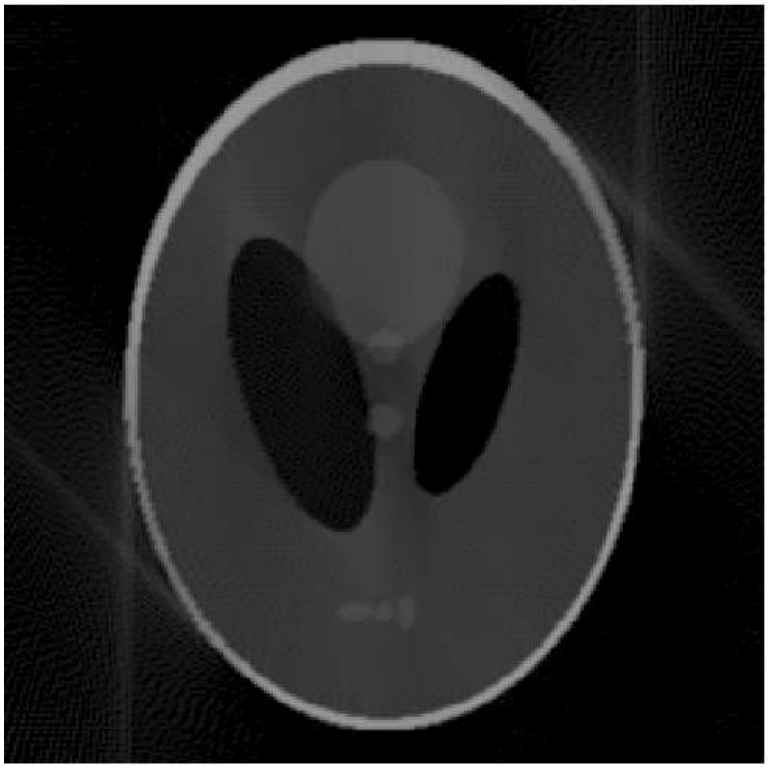

Figure 8.2: Reconstructed Phantom with Thresholding

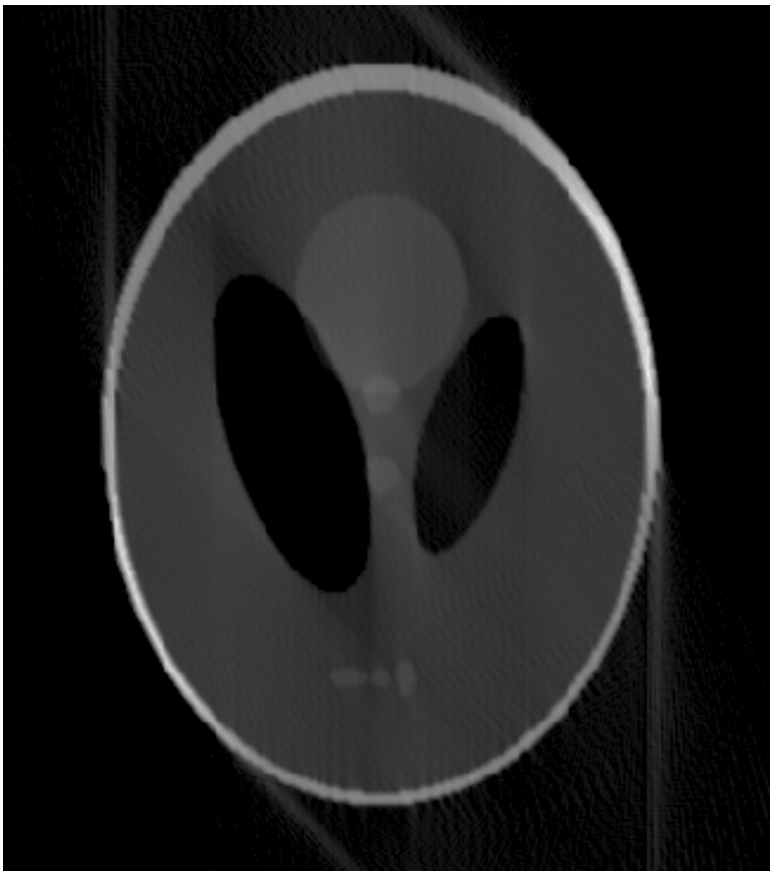

Figure 8.3: Reconstructed Phantom with Sharpening

An added benefit is that edge detection in the presence of noise is also an easy task as the noise (which we will see in a later section) only corresponds to very small coefficients.

We will do two examples of edge detection. By edge detection we mean an analysis of coefficients that allows us to determine where edges of an image might be. In the first example (see Figure 8.4), we see that the coefficients pick out well the lines (edges) of varying thickness in our image. We also see that the thickness of the edge affects the coefficients in that the wider edges have larger coefficients corresponding to lower frequencies that the thinner lines. Notice that the small square made up of a few pixels in the data is visible in the coefficients, but in a very minimal sense, especially in comparison to the edges. Also notice that the horizontal line is not "visible" at all, but would be if we considerd coefficients corresponding to 90 degrees, in which case the others would no longer be visible.

The next example (see Figure 8.5) shows the robustness of the edge detection in displaying the coefficients of the same data with varying leves of noise added. Each example is a higher order of magnitude of noise. One can see how the lines are easy to detect on the coefficients with minimal noise and the difficulty increases with the noise, although a good algorithm should still be able to find these eges. In a later section we will consider the topic of denoising an image.

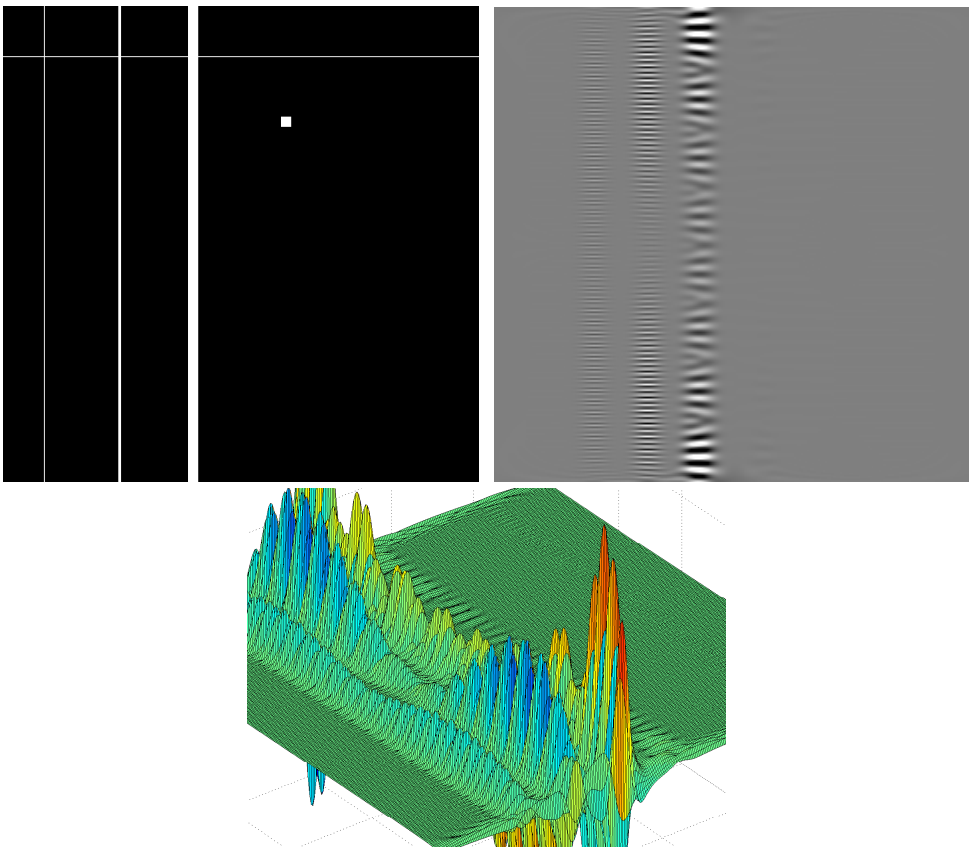

Figure 8.4: We have our *edge phantom* data along with the coefficients corresponing to 0 degrees represented by an intensity image and a three-dimenstional surface.

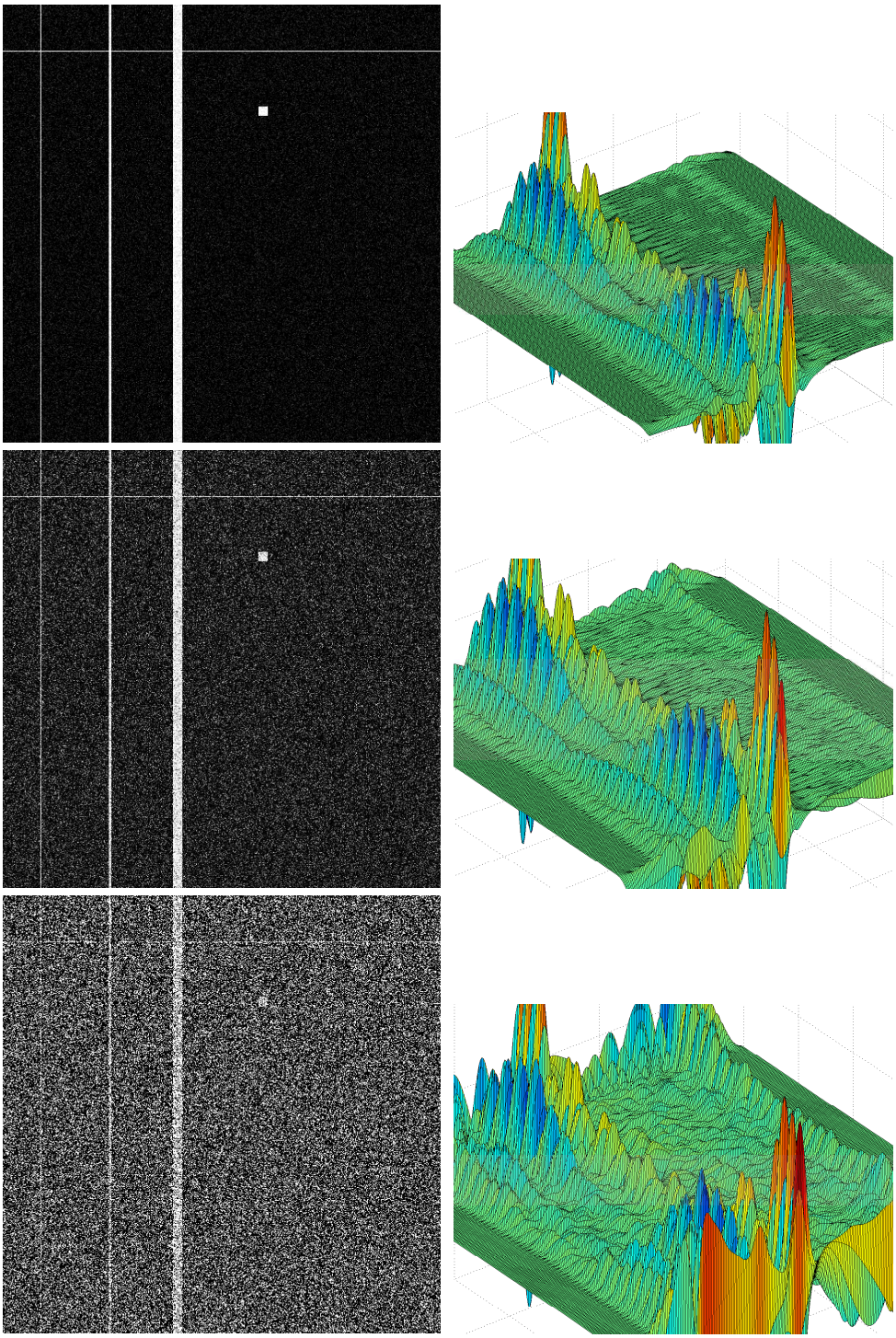

Figure 8.5: We have differing levels of noise added to our data and the corresponding coefficients.

8.3 Image Enhancement

In this section we will apply our new theory to image enhancement. There are many ways to "enhance" an image. One of the most common ways is to actually enhance (make sharper or more defined) the edges or curvilinear singularities of the image. This can be done in a very systematic using our general theory. The time-frequency-direction coefficients are largest when there is an edge in our image. The larger the coefficient, the stronger the edge. A smaller coefficient corresponds to a faint edge. In image enhancement the goal is to enhance the faint edges and not disturb the stronger edges. We do this by multiplying all the coeffcients $c_{m,t,u}$ by $y(c_{m,t,u})$ (as was used in [54]) defined as

$$\begin{cases} \left(\frac{m}{n}\right)^p & \text{if } |c| \leq c_{min} \\ \left(\frac{m}{|c|}\right)^p & \text{if } c_{min} < |c| \leq c_{max} \\ 1 & \text{if } |c| > c_{max} \end{cases}$$

where m, n, c_{min}, and c_{max} are constants to be determined and change depending upon the specific problem.

In our first example (see Figure 8.6), we see our orginal image along with a display of coefficients corresponding to 0 degrees. We then apply the function above to our coefficients and reconstruct the function using new coefficients. In these new coefficients we can that larger coefficients are not affected as much, while the smaller ones are altered producing an image with much more detail. We do a similar example with a more natual image (see Figure 8.7). Although there seems to be no good reason

for enhancing this particular image, it is interesting to see what is actually enhanced. Notice that the areas in the original image corresponding to curvilinear singularities (edges) are dramatically increased in the resulting image. Notice the texture in the closing and the objects in the image background. One can actually make out ridges of texture that were not apparent in the original image.

The next two examples are much more interesting in that it can be seen why certain images might need to be enhanced. The first is an example of a satellite image of the planet Saturn (see Figure 8.8). The second is a similar example using a satellite image of the planet Mars (see Figure 8.9). In both of these, more information of the original image seems to be available in the enhanced reconstructions. In reality, the information was alredy there and we are just emphasizing the fainter edges.

8.4 Image Compression

In this section we will introduce the application to image compression. Image compression can be accomplished whenever one can represent an image with fewer coefficients than the original image required. This can be done with wavelets coefficients (as in current JPEG-2000 technology) and it can also be achieved with our general time-frequency-direction coefficients as we will show in the examples of this section.

In image compression, certain small coefficients are set to zero and not used in the reconstruction of the image. This is not truly a "compression" until one introduces bit allocation and entropy coding which we will not discuss in the work. The general idea is that setting most of the coefficients to zero guarantees nice compression as these

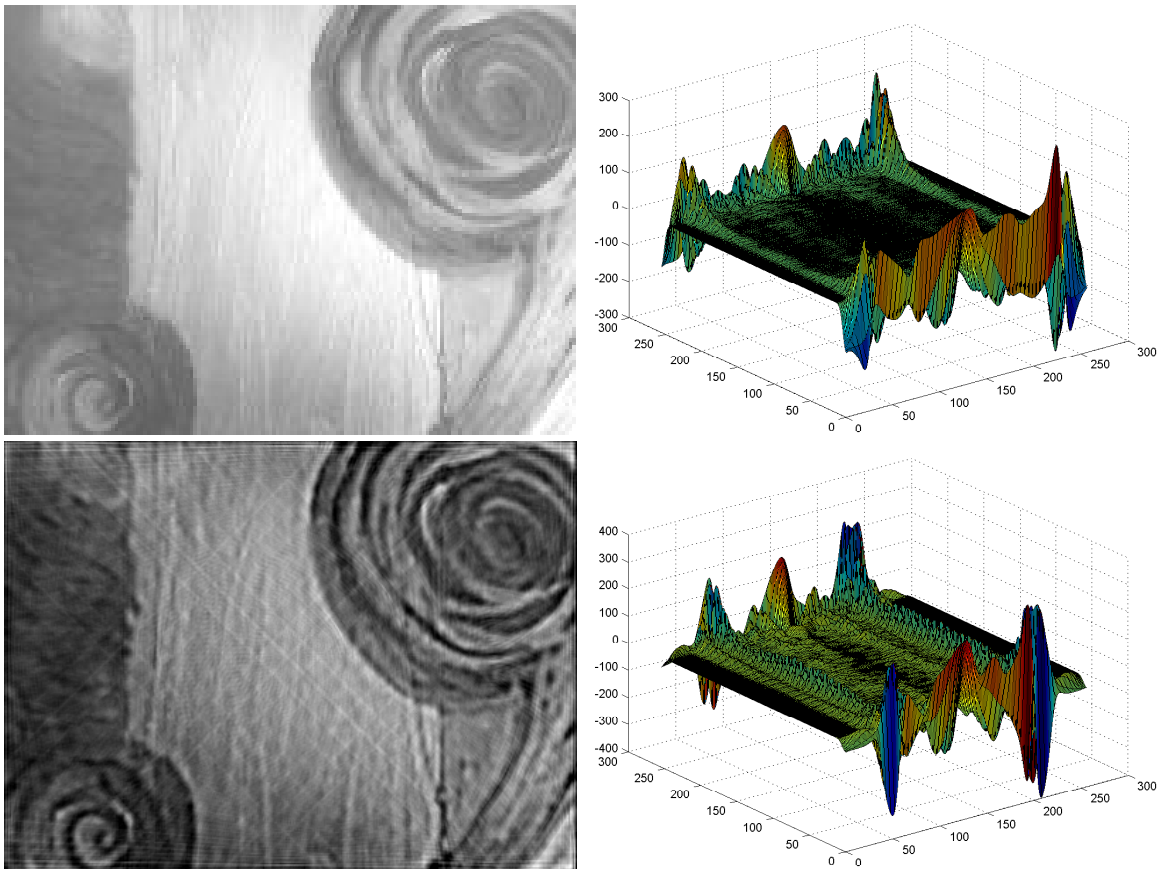

Figure 8.6: The top is the the original image along with its coefficients correspoding to 0 degrees. The image on the bottoms is the enhanced version along with it coefficients corresponding to 0 degrees.

Figure 8.7: Another example of image enhancement.

Figure 8.8: An enhance picture of Saturn.

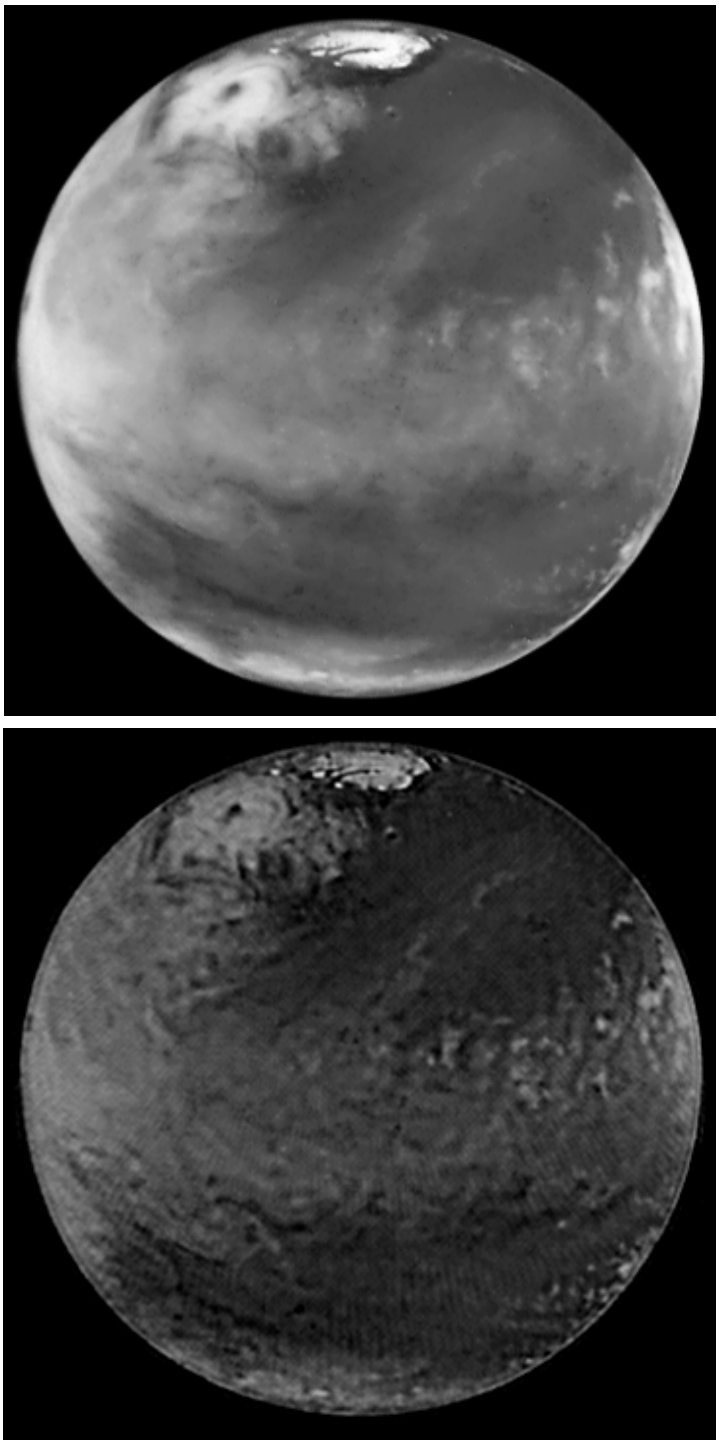

Figure 8.9: An enhanced picture of Mars.

algorithms are already developed and in use. The zero coefficients are compressed using entropy coding and this greatly reduces the size of the file.

With this brief introduction in mind, we will introduce examples of images reconstructed using only a certain percentage of the original coefficients and calculate the mean square error (MSE)

$$MSE = \sum_{j \in J} |f_j - g_j|^2$$

of the original and reconstructed version. These example will show the application to image compression very well.

8.4.1 Examples

In our first example (see Figure 8.10), we take an artwork image and represent it with varying levels of coefficients and consider the MSE for each reconstruction. Please note what we are actually calculating is the MSE between the reconstructions with fewer coefficients versus the "full" amount of coefficients as that is what would usually be included in a digital file.

It is interesting to note that even with 10 percent of the coefficients, the reconstructed image is very visually close to the original image. The places where there is obvious blurryness or error is away from edges, where time-frequency-direction coefficients would be smaller and therefore set to zero.

Also, the explanation for apparent smoothing out of the reconstruction is that the original image was 120×160 pixels and the algorithms are developed to produce a 512×512 image.

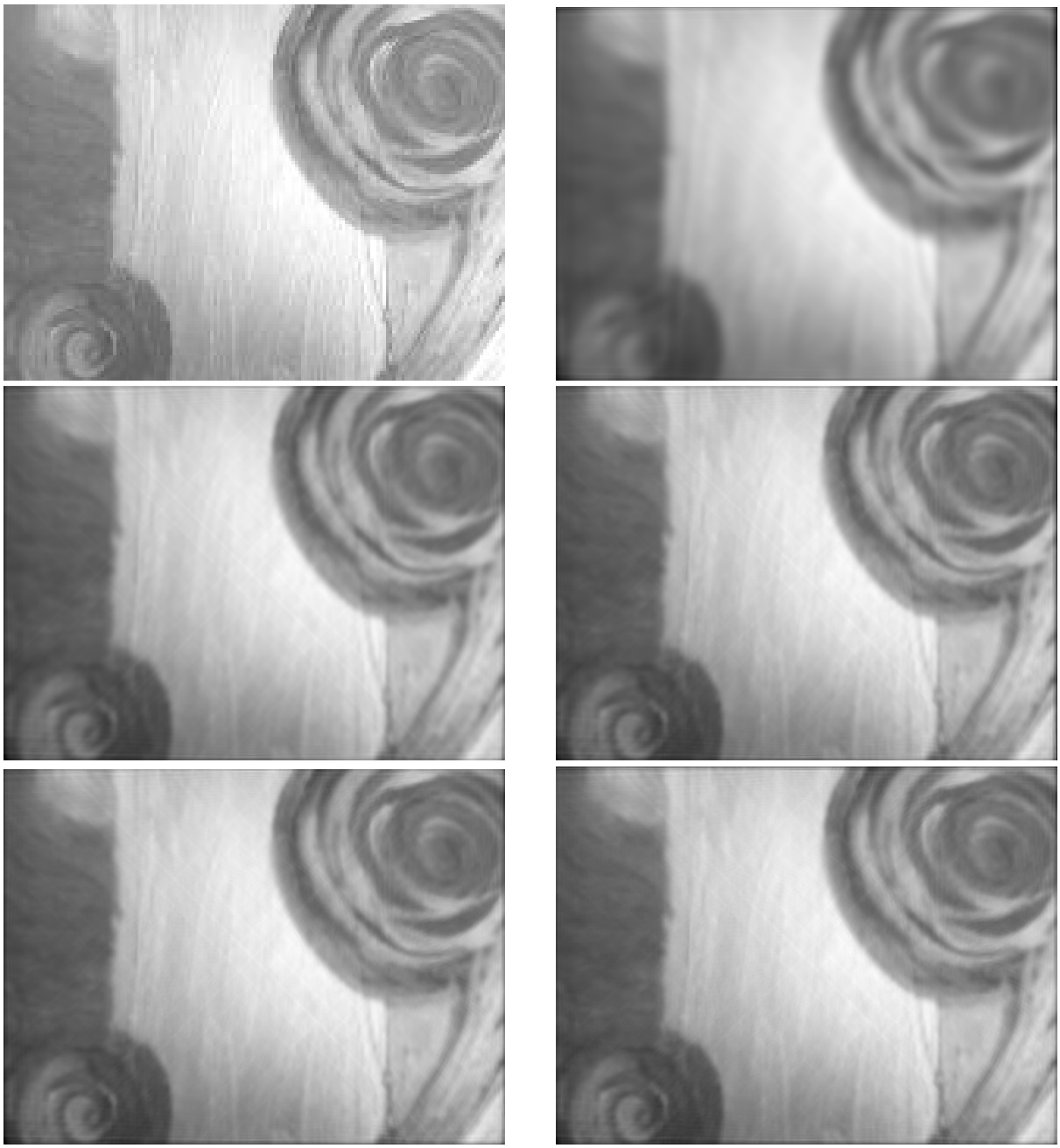

Figure 8.10: Going left to right, top to bottom, we have have the original picture, along with reconstructions using 10% (MSE=0.2184), 20% (MSE=0.0367), 30% (MSE=0.0136), 50% (MSE=0.0022), and 100% (MSE=0) of the available coefficients.

As another example (see Figure 8.11) we will use another picture with more contrast in it than the previous. Again we see the images quality is very high even using only 20% of the available coefficients.

8.4.2 Why Does This Work?

The compression results look promising, but why do they work so well? The answer is a culmination of all the previous sections. We saw that the edges of an image are represented well with the largest of the coefficients. When we compress an image by throwing out a certain percentage of ceofficients, we are throwing out the smallest of the coefficients which, as we have seen, either correspond to noise or some insignificant part of the image. When we reconstruct the image with a small percentage of the largest coefficients, we are able to still preserve our most contrasting edges giving us a good representation of the original image.

Figure 8.11: Going left to right, top to bottom, we have have the original picture, along with reconstructions using 10%, 20%, 30%, 50%, and 100% of the available coefficients.

Chapter 9

Medical Imaging

As we have already seen, the Radon transform plays an integral role in most current medical imaging modalities. With this in mind, we can begin to explore the different avenues in medical imaging where this time-frequency-direction analysis can play a role. One such application is in the area of local tomography (or lambda tomography). The usual process of computerized tomography is global in nature. Local tomography, although slightly less accurate, is local and therefore has some usefulness and advantages above the usual process. In the next few sections, we will look at the use our our theory in computertized tomography along with the setting of local tomography and how the weighted Gabor ridge functions can play a role in reconstruction and denoising of medical images.

9.1 Computerized Tomography

As seen in the first chapter, computerized tomography (CT) is a product of taking the Radon transform of an object (x-rays) and inverting that algorithmically to generate the density image. Our system is tailored specifically for medical imaging because of

its inherent relationship with the Radon transform.

9.1.1 Applications to Computerized Tomography

Our system actually simulates the reconstruction done in a CT machine except for the extra time-frequency elements. This could be duplicated commercially by programming the CT machine to compute Gabor frame coefficients for a certain weighted Radon transform as it is obtained from the x-ray detectors. Analysis can then be done of these coefficients and the images can be processed after that. What we will see in this section is an example of a reconstructed CT image (using a standard phantom image) and then a denoising application by using the extra properties of the time-frequency-direction coefficients.

First let us simply use our system to reconstruct a standard phantom image. In this example (see Figure 9.1), we have the original image and the reconstructed image using directions from 0 to 180 degrees.

What is reconstructed in the algorithm is essentially the following:

$$CT = \sum_{u=1}^{180} \sum_{m=1}^{256} \sum_{t=1}^{256} \langle original, G_{m,t,u} \rangle \Psi_{m,t,u}$$

9.1.2 Denoising in Computerized Tomography

Denoising is possible using our general theory by setting to zero some of the coefficients which correspond to noise (small coefficients) versus those which correspond to the actual image. As we have seen large coefficients correspond to edges or curvilinear singuarities of our image. Small coefficients correspond point singularties such as noise.

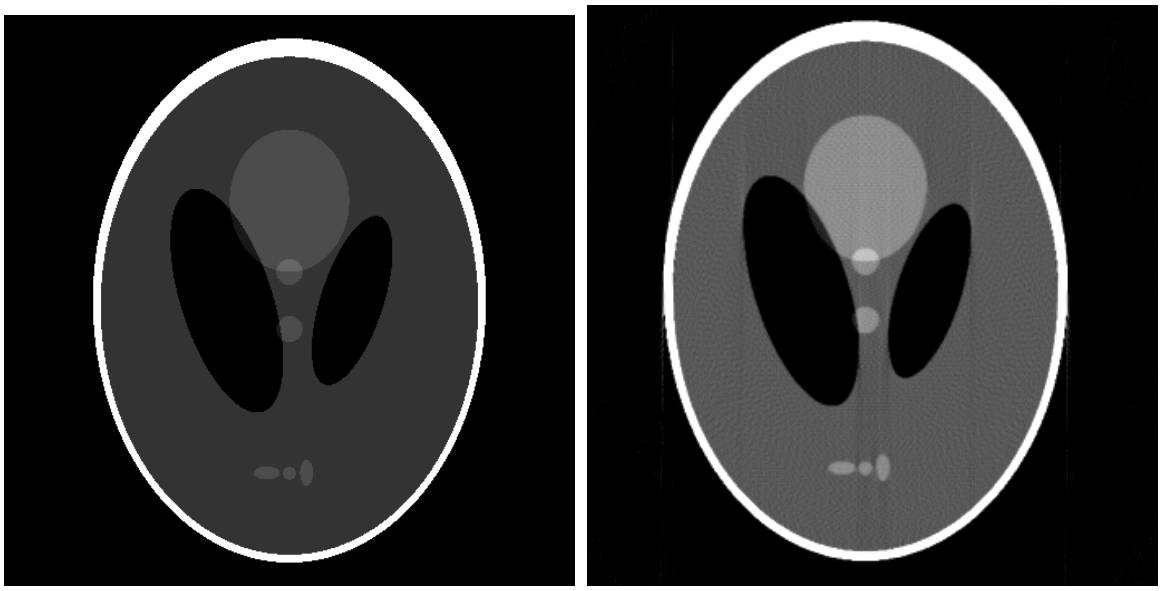

Figure 9.1: The first image is the original head phantom and the second is the simulated CT reconstruction using our system.

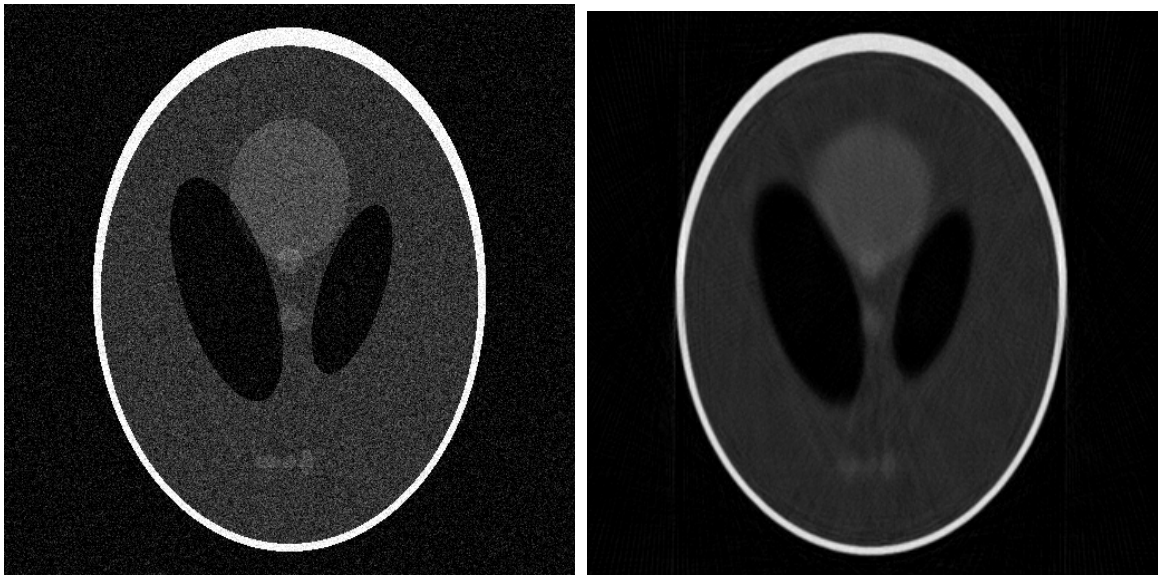

Figure 9.2: Here we have an image of a head phantom with Gaussian noise and the denoised image.

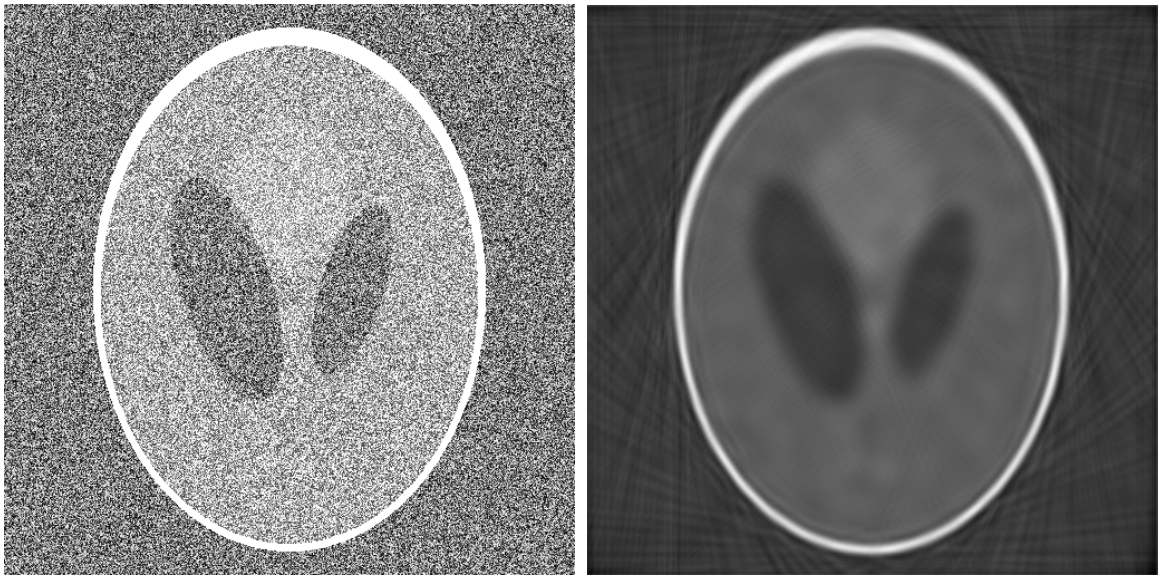

Figure 9.3: Here we have an image of a head phantom with uniform noise and the denoised image.

9.2 Local Tomography

Local tomography (also called lambda tomography) involves reconstructing a function related to f instead of f itself [51]. In local tomography we are constructing the function $Lf = \Lambda f + \mu\Lambda^{-1}f$, where $\Lambda = \sqrt{-\Delta}$ (square root of the positive Laplacian) and μ is some constant which may depend upon f. This is a strictly local reconstruction and it has been shown that Lf produces an image that still "looks like" f. By this we mean that certain aspects of the function f are preserved. For example, since Λf is an invertible elliptic operator, f and Λf have precisely the same singularities. Λf is "cupped," however, within regions of constant density. The extra term $\mu\Lambda^{-1}f$ is an attempt to neutralize this cupping.

Both Λ and its inverse can be defined in terms of their Fourier transform by

$$(\Lambda f)\widehat{\ }(\xi) = |\xi|\widehat{f}(\xi)$$

$$(\Lambda^{-1} f)\widehat{\ }(\xi) = |\xi|^{-1}\widehat{f}(\xi).$$

Notice that Λ^{-1} is just the non-filtered backprojection (for $n = 2$) that we have seen before. This is what produced the blurry image instead of reconstructing f. It will now serve as a useful tool in local tomography. It is a local operation as it only backprojects the lines that intersect a point x. This is why we got a blurry picture before because we actually need all the line integrals to reconstruct $f(x)$.

9.2.1 Applications to Local Tomography

We can implement a local tomographic reconstruction process using our weighted Gabor ridge functions. The system, however, has to be altered to account for a construction of Lf instead of a reconstruction of f.

Definition 9.2.1 (Gabor ridge functions with altered weights) *We will define new Lambda Gabor ridge functions with a special weight in the following way:*

$$G^{\Lambda}_{\beta m,\alpha t,u} = \left(D_{\frac{n}{2}}(g^{\beta m,\alpha t})\right)(u \cdot x).$$

For our current example ($n = 2$), that corresponds to

$$G^{\Lambda}_{\beta m,\alpha t,u} = \left(D_1(g^{\beta m,\alpha t})\right)(u \cdot x).$$

This allows us to be able to create a new representation which allows for analysis of time, frequency, and direction for local tomography. A reconstruction for Lf is

now simply given by:

$$Lf = \int_{\mathbb{S}^{n-1}} \sum_{m\in\mathbb{Z}} \sum_{t\in\mathbb{Z}} \langle f, G^{\Lambda}_{\beta m,\alpha t,u}\rangle \Psi^{\Lambda}_{\beta m,\alpha t,u} du +$$

$$+\mu \int_{\mathbb{S}^{n-1}} \sum_{m\in\mathbb{Z}} \sum_{t\in\mathbb{Z}} \langle f, g_{\beta m,\alpha t,u}\rangle \psi_{\beta m,\alpha t,u} du.$$

Notice in the above reconstruction formula that the second term is the formula from chapter 3 concerning our first attempt at a reconstruction for f. It turns out to be a useful addition to the application for local tomography.

Lets look at an example of reconstruction using our method in this section. We will take the original head phantom and, using our method, construct the image of Lf (see Figure 9.4).

9.2.2 Denoising in Local Tomography

Given that our system is well suited for local tomography, we can also apply our denoising algorithm in a local tomographic setting. What you will will see in the next example (see Figure 9.5) is the local tomographic reconstruction of Lf that has been denoised in the same way we denoised in the CT example (setting to zero coefficients below a certain threshold).

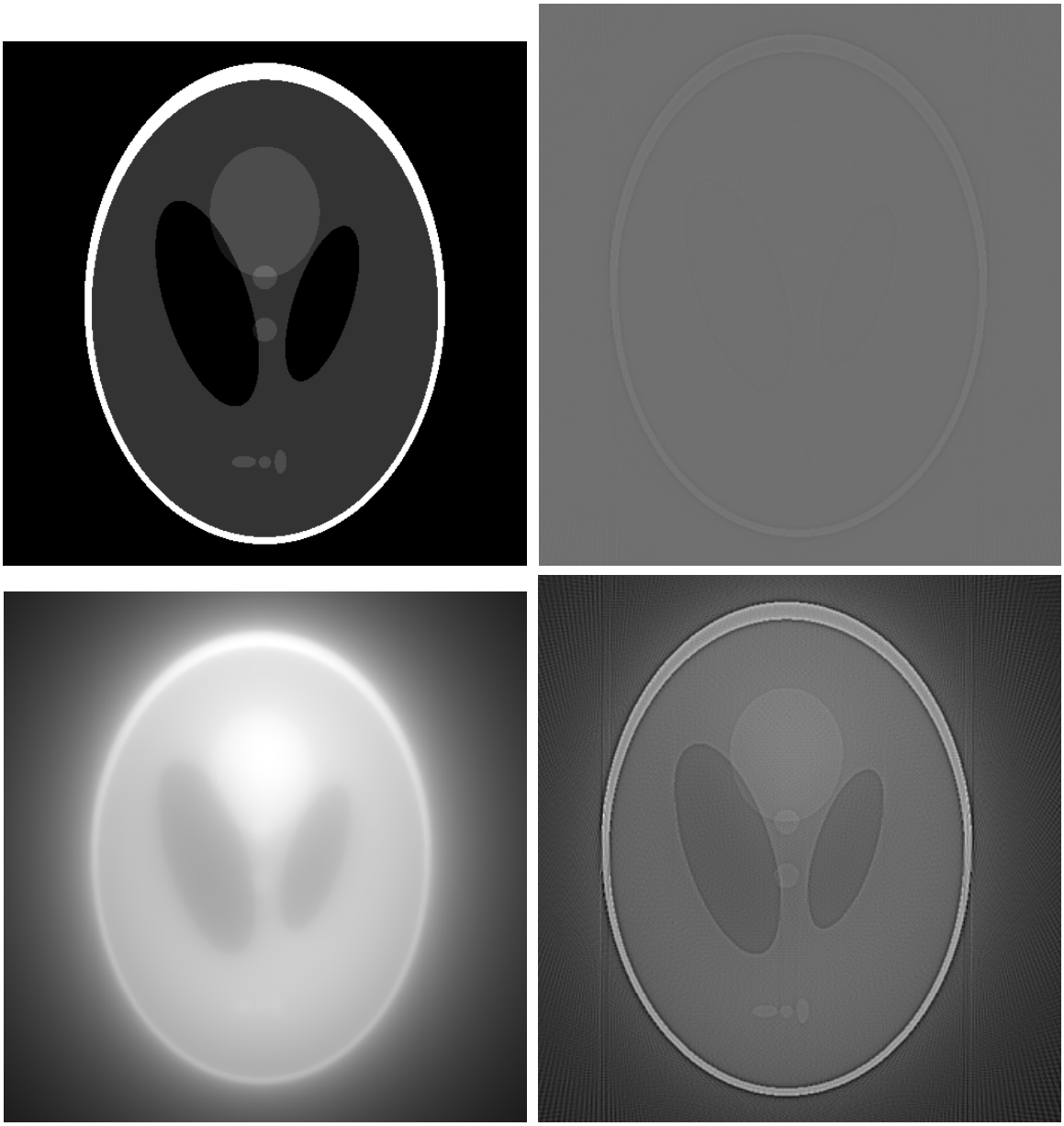

Figure 9.4: From left to right, top to bottom, we have the original head phantom, Λf, $\Lambda^{-1} f$, and the local reconstruction $Lf = \Lambda f + \Lambda^{-1} f$.

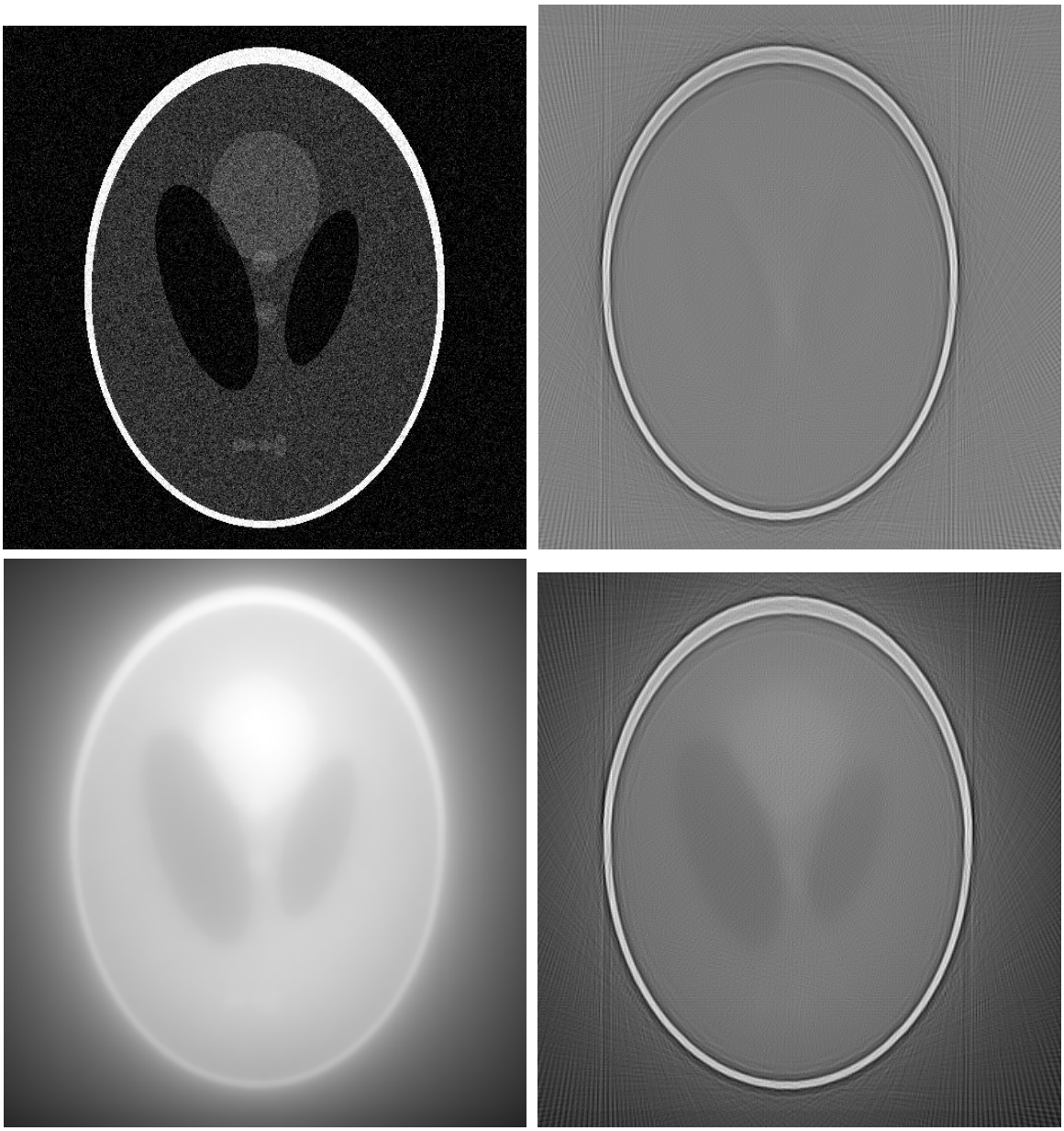

Figure 9.5: From left to right, top to bottom, we have the original head phantom with gaussian noise, Λf, $\Lambda^{-1} f$, and the local reconstruction $Lf = \Lambda f + \Lambda^{-1} f$.

Appendix A

Tools from Fourier Analysis

We briefly mention in a little more detail some of the tools used in this dissertation. For an excellent reference on harmonic analysis, one may consult [30] which has many basic properties and advanced analysis along with justifications.

A.1 The Fourier Transform on the Schwartz Class

A.1.1 The Schwartz Class $\mathcal{S}(\mathbb{R}^n)$

The Schwartz space is a natural space on which to consider the Fourier transform initially because of inversion begin well-defined. It can be extended, however, to much more general classes of functions. For functions in L^1, Fourier inversion makes sense only if $\widehat{f}$ is also in L^1, which is not always the case. In what follows, C^∞ will represent the class on infinitely differentiable functions and a multiindex *alpha* is an n-tuple of nonnegative integers $(\alpha_1, \alpha_2, \ldots, \alpha_n)$ where $\partial^\alpha f = \partial_1^{\alpha_1} \ldots \partial_n^{\alpha_n}$ and $|\alpha| = \alpha_1 + \cdots + \alpha_n$.

Definition A.1.1 (The Schwartz Class $\mathcal{S}(\mathbb{R}^n)$) *A function $f \in C^\infty$ is said to be in the Schwartz class $\mathcal{S}(\mathbb{R}^n)$ if for all multiindices α, β, there exist positive constants*

$C_{\alpha,\beta}$ such that

$$\rho_{\alpha,\beta} = \sup_{x\in\mathbb{R}^n} |x^\alpha \partial^\beta f(x)| = C_{\alpha,\beta} < \infty.$$

In other words, the function f along with all of its partial dervative decay faster than the reciprocal of any polynomial.

As an example, $g(x) = e^{-|x|^2}$ is in the Schwartz class, but $h(x) = (1 + |x|^{100})^{-a}$ for $a > 0$ is not in Schwartz since it decays like the reciprocal of a fixed polynomial function.

A.1.2 The Fourier Transform

Given a function $f \in \mathcal{S}(\mathbb{R}^n)$, we call the following the Fourier transform of f:

$$\widehat{f}(\xi) = \int_{\mathbb{R}^n} f(x) e^{-2\pi i x\cdot\xi} dx,$$

where $x, \xi \in \mathbb{R}^n$. We may also find the inverse Fourier transform of a function $f \in \mathcal{S}(\mathbb{R}^n)$ by

$$f^\vee(x) = \widehat{f}(\xi) e^{2\pi i x\cdot\xi} d\xi.$$

Theorem A.1.2 (Properties of the Fourier transform) *For functions $f, g \in \mathcal{S}(\mathbb{R}^n)$, we have*

1. $$\int_{\mathbb{R}^n} f(x)\widehat{g}(x)dx = \int_{\mathbb{R}^n} \widehat{f}(x) g(x) dx,$$

2. *Fourier Inversion*

$$(\widehat{f})^\vee = \widehat{(f^\vee)} = f,$$

3. Plancherel's Identity

$$\int_{\mathbb{R}^n} f(x)\overline{g}(x)dx = \int_{\mathbb{R}^n} \widehat{f}(\xi)\overline{\widehat{g}(\xi)}d\xi,$$

4. Parseval's Identity

$$\|f\|_{L^2} = \|\widehat{f}\|_{L^2} = \|f^\vee\|_{L^2},$$

5.

$$\int_{\mathbb{R}^n} f(x)g(x)dx = \int_{\mathbb{R}^n} \widehat{f}(x)g^\vee(x)dx.$$

A lot of other very useful properties follow from the definition of the Fourier transform. We will now introduce some notation and view some of these properties in the form of a proposition.

For a function f defined on $\mathbb{R}^n$, $x \in \mathbb{R}^n$, and $a > 0$, we can define translation, dilation, and reflection by

$$T_y(f)(x) = f(x - y)$$

$$\delta^a(f)(x) = f(ax)$$

$$\tilde{f}(x) = f(-x).$$

Also, for $f, g \in L^1(\mathbb{R}^n)$ we define the *convolution* $f * g$ by

$$(f * g)(x) = \int_{\mathbb{R}^n} f(y)g(x - y)dy.$$

Proposition A.1.3 *For $f, g \in \mathcal{S}(\mathbb{R}^n)$, $y \in \mathbb{R}^n$, $b \in \mathbb{C}$, α a multiindex, and $a > 0$ we have*

1. $\|\widehat{f}\|_{L^\infty} \leq \|f\|_{L^1}$.

2. $\widehat{f+g} = \widehat{f} + \widehat{g}$.

3. $\widehat{bf} = b\widehat{f}$.

4. $\widehat{\widetilde{f}} = \widetilde{\widehat{f}}$.

5. $\overline{\widehat{f}} = \widehat{\overline{f}}$.

6. $\widehat{T_y(f)} = M_{-y}\widehat{f}$.

7. $(M_y f(x))\widehat{\ } = T_y\widehat{f}$.

8. $\widehat{\delta^a(f)} = a^{-n}\delta^{a-1}(\widehat{f}\ )$.

9. $(\delta^\alpha f)\widehat{\ }(\xi) = (2\pi i\xi)^\alpha \widehat{f}(\xi)$.

10. $(\delta^\alpha \widehat{f}\ )(\xi) = ((-2\pi i\xi)^\alpha f(x))\widehat{\ }(\xi)$.

11. $\widehat{f} \in \mathcal{S}(\mathbb{R}^n)$.

12. $\widehat{f * g} = \widehat{f}\,\widehat{g}$.

A.2 Distributions

Certain functions may not be easy to work with directly and it may be useful to look at how they act on spaces of "test" fuctions. In some cases, we may want to consider an object that is not a function at all, but is well-defined as an action on a class on "nice" functions.

A.2.1 Definition of a Distribution

We will call the class on infinitely differentiable functions with compact support $C_0^\infty(\mathbb{R}^n)$. This will be our space of test functions.

We can now view a distribution as a linear functional acting on our set of test functions. We will view a distribution u acting on a test function f with the following notation:

$$\langle u, f \rangle.$$

Proposition A.2.1 *A linear functional u acting on $C_0^\infty(\mathbb{R}^n)$ is a distribution if and only if for every compact $K \subseteq \mathbb{R}^n$, there exist a $C > 0$ and an integer m such that*

$$|\langle u, f \rangle| \leq C \sum_{\alpha \leq m} \|\partial^\alpha f\|_{L^\infty},$$

for all $f \in C^\infty$ with support in K.

An example used in this dissertation was the Dirac delta function

$$\langle \delta, f \rangle = f(0).$$

We can also extend functions which are locally integrable to distributions since they act well on test functions.

A.2.2 The distribution $|x|^\alpha$

We begin with a definition for the distribution $|x|^\alpha$.

Definition A.2.2 (The distribution $|x|^\alpha$) *The distribution $|x|^\alpha$ acts on test functions $f \in \mathcal{S}(\mathbb{R}^n)$ in the following way:*

$$\langle |x|^\alpha, f\rangle = \int_{\mathbb{R}^n} \frac{\pi^{\frac{\alpha+n}{2}}}{\Gamma\left(\frac{\alpha+n}{2}\right)} |x|^\alpha f(x)dx. \tag{A.1}$$

These distribution coincide with the locally integrable functions

$$\pi^{\frac{\alpha+n}{2}} \Gamma\left(\frac{\alpha+n}{2}\right)^{-1} |x|^\alpha$$

when $\Re(z) > -n$, the definition only making sense for that range of $z's$.

The definition of this distribution can be extended to all $z \in \mathbb{C}$ in the following way.

Theorem A.2.3 (Fourier transform of $|x|^\alpha$) *The fourier transform of $|x|^\alpha$, for $x \in \mathbb{R}^n$ only exists in a distributional sense and is given by the following formula:*

$$\left(\frac{\pi^{-\frac{\alpha}{2}}}{\Gamma\left(-\frac{\alpha}{2}\right)} |x|^\alpha\right)^\frown = \frac{\Gamma\left(\frac{\alpha+n}{2}\right)}{\pi^{\frac{\alpha+n}{2}}} |\xi|^{-n-\alpha}.$$

Bibliography

[1] A. Aldroubi and K. Gröchenig, *Nonuniform sampling and reconstruction in shift-invariant spaces*, SIAM Rev. **43** (2001), 585–620.

[2] G. Bal and P. Moireau, *Fast numerical inversion of the attenuated Radon transform with full and partial measurements*, Inverse Problems **20** (2004), 1137–1164.

[3] J. J. Benedetto, *Gabor representations and wavelets*, AMS Contemporary Math. Series **91** (1989), 9–27.

[4] A. Benyi, K. Grochenig, C. Heil, and K. Okoudjou, *Modulation spaces and a class of bounded multilinear pseudodifferential operators*, J. Operator Theory **54** (2005), 389–401.

[5] G. Beylkin, *Generalized Radon transform and its applications*, (1982), Ph.D. thesis, NYU.

[6] H. Bölcskei, H. G. Feichtinger, and F. Hlawatsch, *Diagonalizing the gabor frame operator*, In TFTS'95 - Symposium on Applications of Time-Frequency and Time-Scale Methods University of Warwick, Coventry, UK, Warwick (1995).

[7] E. J. Candes, *Harmonic analysis of neural networks*, Applied and Computational Harmonic Analysis **6** (1999), 197–218.

[8] E. J. Candes and D. L. Donoho, *New tight frames of curvelets and optimal representations of objects with piesewise-C^2 singularities*, Comm. on Pure and Appl. Math. **57** (2004), 219–266.

[9] R. Carmona, W. L. Hwang, and B. Torrésani, *Practical time-frequency analysis: continuous wavelet and gabor transforms, with an implementation in S*, Wavelet Analysis and its Applications, vol. 9, Academic Press, San Diego, 1998.

[10] P. Casazza, *The art of frame theory*, Taiwanese J. of Math. **4** (2000), 129–201.

[11] P. Casazza, O. Christensen, and A. J. E. M. Janssen, *Classifying tight weyl-heisenberg frames*, The Functional and Harmonic Analysis of Wavelets and Frames: AMS Special Session on the Functional and Harmonic Analysis of Wavelets, January 13-14, 1999, San Antonio, Texas (2000).

[12] P. Casazza; O. Christensen; and A. J. E. M. Janssen, *Weyl-Heisenberg frames, translation invariant systems and the Walnut representation*, J. Funct. Anal. **180** (2001), 85–147.

[13] L. Cohen, *Time-frequency distributions: a review*, Proc. of IEEE **77** (1989), 941–979.

[14] L. Cohen, *Time-frequency analysis*, Prentice Hall, New York, 1994.

[15] R. R. Coifman, *Wavelet analysis and signal processing*, Signal Processing, Part I: Signal Processing Theory (Louis Auslander, Tom Kailath, and Sanjoy K. Mitter, eds.), Springer-Verlag, New York, NY, 1990, pp. 59–68.

[16] J. Cooley and J. Tukey, *An algorithm for the machine calculation of complex Fourier series*, Math. Comput. **19** (1965), 297–301.

[17] I. Daubechies, *Ten lectures on wavelets*, SIAM, Philadelphia, PA, 1992.

[18] S. R. Deans, *The Radon Transform and some of its Applications (revised reprint of the 1983 original)*, Robert E. Krieger Publishing Co. Inc., Malabar, FL, 1993.

[19] D. L. Donoho and P. B. Stark, *Uncertainty principles and signal recovery*, SIAM Journal of Applied Mathematics **49** (1989), 906–931.

[20] C. Epstein, *Mathematics of medical imaging*, Prentice Hall, New Jersey, 2003.

[21] H. Feichtinger, *Atomic characterizations of modulation spaces through Gabor-type representations*, Rocky Mountain J. Math. **19** (1989), 113–125, Constructive Function Theory—86 Conference (Edmonton, AB, 1986).

[22] H. Feichtinger and K. Gröchenig, *Gabor frames and time-frequency analysis of distributions*, J. Funct. Anal. **146** (1997), 464–495.

[23] H. Feichtinger and T. Strohmer (eds.), *Gabor analysis and algorithms*, Applied and Numerical Harmonic Analysis, Birkhäuser Boston Inc., Boston, MA, 1998, Theory and applications.

[24] P. Flandrin, *Time-frequency/time-scale analysis*, Wavelet Analysis and its Applications, vol. 10, Academic Press Inc., San Diego, CA, 1999, With a preface by Yves Meyer, Translated from the French by Joachim Stöckler.

[25] G. Folland, *Harmonic analysis in phase space*, Princeton University Press, Princeton, NJ, 1989.

[26] ———, *Real analysis: Modern techniques and their applications*, John Wiley & Sons, Inc., New York, NY, 1999.

[27] P. Fränti, E. Ageenko, S. Kukkonen, and H. Kälviäinen, *On the use of hough transform for context-based image compression in hybrid raster/vector applications*, Proc. Indian Conf. on Computer Vision, Graphics and Image Processing (ICVGIP'00) (2000), 364–372.

[28] M. Frazier and B. Jawerth, *Decomposition of Besov spaces*, Indiana. Univ. Math. J. **34** (1985), 777–799.

[29] R. Gardner, A. Koldobsky, and T. Schlumprecht, *An analytic solution to the Busemann-Petty problem on sections of convex bodies*, 1999, pp. 691–703.

[30] L. Grafakos, *Classical and modern Fourier analysis*, Prentice Hall, New Jersey, 2004.

[31] L. Grafakos and C. Lennard, *Characterization of $L^p(\mathbb{R}^n)$ using Gabor frames*, J. Fourier Anal. Appl. **7** (2001), 101–126.

[32] K. Gröchenig, *Foundations of time-frequency analysis*, Applied and Numerical Harmonic Analysis, Birkhäuser Boston Inc., Boston, MA, 2001.

[33] K. Gröchenig and C. Heil, *Gabor meets Littlewood-Paley: Gabor expansions in $L^p(\mathbb{R}^d)$*, Studia Math. **146** (2001), 15–33.

[34] C. Heil and D. Walnut, *Continuous and discrete wavelet transforms*, SIAM Review **31** (1989), 628–666.

[35] W. Heisenberg, *Über den anschaulichen inhalt der quantentheoretischen kinematik und mechanik*, Z. für Phys. **43** (1927), 172–198.

[36] S. Helgason, *The Radon transform, second edition*, Birkhäuser, Boston, 1999.

[37] M. L. Hilton, Bjorn D. Jawerth, and A. Sengupta, *Compressing still and moving images with wavelets*, Multimedia Systems **2** (1994), 218–227.

[38] A. J. E. M. Janssen, *From continuous to discrete Weyl-Heisenberg frames through sampling*, J. Fourier Anal. Appl. **3** (1997), 583–596, Dedicated to the memory of Richard J. Duffin.

[39] ———, *Representations of Gabor frame operators*, Twentieth century harmonic analysis—a celebration (Il Ciocco, 2000), NATO Sci. Ser. II Math. Phys. Chem., vol. 33, Kluwer Acad. Publ., Dordrecht, 2001, pp. 73–101.

[40] W. R. Madych, *Radon's inversion formulas*, Trans. Amer. Math. Soc. **356** (2004), 4475–4491.

[41] F. Matús and J. Flusser, *Image representation via a finite Radon transform*, IEEE Trans. Pattern Anal. Mach. Intell. **15** (1993), 996–1006.

[42] Taneli Mielikäinen and Janne Ravantti, *Sinogram denoising of cryo-electron microscopy images.*, ICCSA (4), 2005, pp. 1251–1261.

[43] F. Natterer, *Algorithms in tomography*, 1997.

[44] ———, *The mathematics of computerized tomography*, Society for Industrial and Applied Mathematics, Philadelphia, PA, USA, 2001.

[45] F. Noo and J.-M. Wagner, *Image reconstruction in 2D SPECT with 180-degrees acquisition*, Inverse Problems **17** (2001), 1357–1371.

[46] E. Quinto, *An introduction to X-ray tomography and Radon transforms*, Proceedings of Symposia in Applied Mathematics **67** (2006).

[47] W. Hwang R. Carmona and B. Torrésani, *Practical time-frequency analysis*, Wavelet Analysis and its Applications, vol. 9, Academic Press Inc., San Diego, CA, 1998, Gabor and wavelet transforms with an implementation in S, With a preface by Ingrid Daubechies.

[48] M. Swamy A. Fenster R. R. Galigekere, D. W. Holdsworth, *Moment patterns in the Radon space*, Optical Engineering **39** (2000), 1088–1097.

[49] J. Radon, *Über die bestimmung von funktionen durch ihre integralwerte längs gewisser mannigfaltigkeiten*, Berichte Sächsische Akadamie der Wissenschaften, Leipzig,Math.-Phys. Kl. **69** (1917), 262–267.

[50] G. N. Ramachandran and A. V. Lakshminarayanan, *Three dimensional reconstructions from radiographs and electron micrographs: Application of convolution instead of Fourier transform*, Proc. Nat. Acad. Sci. **68** (1971), 2236–2240.

[51] A. G. Ramm and A. I. Katsevich, *The Radon transform and local tomography*, CRC Press, Boca Raton, Florida, 1996.

[52] M. A. Schonewille and A. J. W. Duijndam, *Mixed Fourier-Radon reconstruction of irregularly and sparsely sampled seismic data*, International workshop on Sampling Theory and Application, 1997, pp. 115–120.

[53] E. Stein, *Harmonic analysis : real-variable methods, orthogonality, and oscillatory integrals*, Princeton University Press, Princton, NJ., 1993.

[54] K. V. Velde, *Multi-scale color image enhancement*, Proc. Int. Conf. Image Processing **3** (1999), 584–587.

[55] J.-M. Wagner and F. Noo, *Three-dimensional image reconstruction from exponential parallel-beam projections*, IEEE Transactions on Nuclear Science **48** (2001), 743–749.

[56] D. Walnut, *Applications of Gabor and wavelet expansions to the Radon transform*, Probabilistic and Stochastic Methods in Analysis, with Applications (1992), 187–205.

[57] D. F. Walnut, *Continuity properties of the Gabor frame operator.*, J. Math. Anal. Appl. **165** (1992), 479–504.

[58] D.F. Walnut, *Weyl-Heisenberg wavelet expansions: existence and stability in weighted spaces*, Ph.D. thesis, Univ. Maryland, College Park, 1989.

[59] P. Wojdyllo, *Gabor and wavelet frames. geometry and applications.*, Ph.D. thesis, Department of Mathematics, Computer Science and Mechanics, Warsaw University, 2001.

Index

VITA

Christopher Michael Sansing was born December 22, 1979 in Columbus, Mississippi. He completed his early education through high school at Immanuel Center for Christian Education, a private school in Columbus. He then attended the Mississippi University for Women (accepting men since 1982) in Columbus where he obtained a Bachelor of Science degree in mathematics with honors in May of 2001. During and after his undergraduate education, Chris participated in very rewarding internships at the Engineering Research Center in Starkville, Mississippi and the NASA Glenn Research Center in Cleveland, Ohio. After completing his undergraduate education, Chris attended the University of Missouri where he worked with Dr. Loukas Grafakos in the area of computational and applied harmonic analysis. He recieved his Masters of Science degree in applied mathematics in December of 2003 after completing a project on the mathematics of medical imaging and is expected to receive his Doctor of Philosophy degree in mathematics in May of 2006.